Fraunhofer
ICT

Fraunhofer-Institut für Chemische Technologie ICT

Enhancing carbon nanotubes dispersion in thermoplastics for the development of multifunctional composites

Shyam Sundar Sathyanarayana

Wissenschaftliche Schriftenreihe
des Fraunhofer ICT
Band 56

FRAUNHOFER VERLAG

Fraunhofer-Institut
für Chemische Technologie ICT

Shyam Sundar Sathyanarayana

Enhancing carbon nanotubes dispersion in thermoplastics for the development of multifunctional composites

Wissenschaftliche Schriftenreihe
des Fraunhofer ICT
Band 56

FRAUNHOFER VERLAG

Herausgeber:
Fraunhofer-Institut für Chemische Technologie ICT
Joseph-von-Fraunhofer-Straße 7
76327 Pfinztal (Berghausen)
Telefon 0721 4640-0
Fax 0721 4640-111

Bibliografische Information der Deutschen Nationalbibliothek
Die Deutsche Nationalbibliothek verzeichnet diese Publikation in der Deutschen Nationalbibliografie; detaillierte bibliografische Daten sind im Internet über http://dnb.d-nb.de abrufbar.
ISBN: 978-3-8396-0603-2

D 90

Zugl.: Karlsruhe, Univ., Diss., 2013

Druck: Mediendienstleistungen des
Fraunhofer-Informationszentrum Raum und Bau IRB, Stuttgart

Für den Druck des Buches wurde chlor- und säurefreies Papier verwendet.

FRAUNHOFER VERLAG
Fraunhofer-Informationszentrum Raum und Bau IRB
Postfach 80 04 69, 70504 Stuttgart
Nobelstraße 12, 70569 Stuttgart
Telefon 07 11 9 70-25 00
Telefax 07 11 9 70-25 08
E-Mail verlag@fraunhofer.de
URL http://verlag.fraunhofer.de

Enhancing Carbon Nanotubes Dispersion in Thermoplastics for the Development of Multi-functional Composites

Submitted to the Faculty of Mechanical Engineering
of the Karlsruhe Institute of Technology
for the award of Ph.D. (Dr.-Ing.)

Dissertation

by
M.Sc., Diplôme d'Ingénieur. **Shyam Sundar Sathyanarayana**

Supervisor:	Prof. Dr.-Ing. Frank Henning
Co-supervisor:	Prof. Dr.-Ing. Christian Bonten
Date of Submission:	14.05.2013
Date of Examination:	20.06.2013

DECLARATION

The work presented in this project is to the best of my knowledge and belief, original and my own piece of work, except as otherwise acknowledged in the text. I have not submitted this material, either as a whole or in part for a degree elsewhere.

- Shyam Sundar Sathyanarayana

Dedicated to my dear wife & parents

Acknowledgements

I have been fortunate enough throughout the duration of my dissertation to have had the support and guidance of many people without whose assistance my individual inquiry would have been much more difficult, and the experience much less rewarding.

I express my heartfelt gratitude to Prof. Dr.-Ing. Frank Henning for having accepted me to be a doctoral candidate in his faculty *Lehrstuhl für Leichtbautechnologie - Institut für Fahrzeugsystemtechnik (FAST)* at the Karlsruher Institut für Technologie (KIT). My sincere thanks to him for his time, constant support, guidance, and motivation. whenever I was in need of it. My gratitude is also due to Prof. Dr.-Ing. Christian Bonten (*Direktor, Institut für Kunstofftechnik, Universität Stuttgart*) for agreeing to be the second reviewer for the work, for his constructive comments on the manuscript and valuable time for discussion. I would also like to thank the members of the dissertation jury for their valuable time.

Loads of appreciations are due to my mentor Dr.-Ing. Christof Hübner for his invaluable support, constant encouragement and enormous time for discussion and assistance both in the academic work and with the administrative aspects without which this work would have remained only as a dream instead of indiscernible reality. Special mention to Mr. Patrick Weiss for educating me on the twin-screw extruder and assisting me with the compounding trials. My thanks are also due to my co-workers Mr. Ganiu Olowojoba, Ms. Irma Mikonsaari, Ms. Carolyn Fisher & Mr. Burak Caglar for all that they have done for me. I would also like to appreciate the efforts of all my colleagues at *Fraunhofer Institüt für Chemische Technologie (ICT), Pfinztal* for their friendship and invaluable support for making my stay very fruitful.

I would also like to thank Prof. Enrique Giménez Torres (Instituto de Tecnología de Materiales, Universidad Politécnica de Valencia, Spain) and Mr. Marcin Wegrzyn (Instituto Tecnológico del Plástico (AIMPLAS), Spain) for their assistance during my visiting research tenure at AIMPLAS. I would also like to appreciate the efforts of Dr. Petra Pötschke (Abt. Funktionale Nanokomposite und Blends, Leibniz-Institut für Polymerforschung Dresden e. V., Germany) for her review of a couple of my chapters and for co-authoring a couple of published manuscripts with me.

My gratitude to the European Commission for my Marie Curie Fellowship through European Community's 7th Framework Programme (FP7-PEOPLE-ITN-2008) under grant agreement number 238363. I would also like to appreciate all the partners of the CONTACT project consortium for the continuous exchange of ideas throughout the course of the project.

Finally, I would like to thank my wife, my parents, my brother, my in-laws and extended family for all their love, affection and indefatigable support.

Abstract

This work aims to develop a polypropylene-based multifunctional composite with excellent electrical, thermal, and mechanical characteristics; taking advantage of the excellent electrical conductivity of carbon nanotubes as conductive fillers and to overcome their major drawback to substantially enhance the mechanical properties by the use of glass fibers as structural reinforcement.

The extremely high electrical conductivity of carbon nanotubes makes them an attractive choice as conductive filler. However, the intrinsic tendency of carbon nanotubes to exist as agglomerates due to van der Waals forces of attraction limits their theoretical potential. Achieving good nanotube dispersion in polypropylene is a pre-requisite for good electrical properties prior to the addition of glass fibers. This however is a significant challenge owing to the non-polar nature of polypropylene, high interfacial energy difference with commercially available carbon nanotubes, and the intrinsically inert chemical nature of the nanotubes.

The mechanism of carbon nanotube dispersion in a thermoplastic and the lack of relevant literature on large scale processing of polyolefins with carbon nanotubes mandate proper understanding of the process factors contributing towards improved filler dispersion. Hence, for a start the influence of twin-screw compounding parameters on the quality of carbon nanotube dispersion was investigated with the Design of Experiments approach. Excellent electrical characteristics were achieved on a composite containing 2 wt.% carbon nanotubes at higher screw speeds and lower material throughputs owing to better filler dispersion at these conditions, facilitated by higher specific mechanical energy of processing. Variation in screw configuration had an influence on lowering the resistivity of the composites processed at increased throughputs at lower nanotube loadings. Feeding of carbon nanotubes in the polymer melt resulted in improved electrical and mechanical properties compared to feeding them along with the polymer in the main feed of the extruder.

Peroxides were incorporated as a processing additive to reduce the melt viscosity to facilitate better melt infiltration into the nanotube agglomerates and improve hydrophilicity of polypropylene for better wetting of the agglomerates. Substantially enhanced carbon nanotube dispersion in polypropylene was possible at 50% lower processing energy by using peroxides. In situ functionalization of carbon nanotubes by peroxides confirmed by a novel approach of online Raman spectroscopy observations could have contributed positively in enhancing the dispersion, but also led to structural defects on the carbon nanotubes.

Electrical percolation occurred around 0.4 wt.% carbon nanotube loading on the composites with peroxides. Compression molding parameters had a strong influence on the magnitude of observed resistivities of the composites. Higher melt temperatures and longer holding times were found to be beneficial for improved electrical conductivity. Though carbon nanotube addition slightly enhanced the mechanical properties of polypropylene, the addition of peroxides had a negative effect on the modulus and impact properties of the composites. The structural defects created on the nanotube on functionalization by peroxides could have

been a reason for the aforementioned. The composites presented enhanced thermal stability due to the excellent free radical accepting capacities of nanotubes.

The addition of short glass fibers as secondary fillers resulted in substantially enhanced tensile and impact properties of the composites accompanied by a loss in ductility. The combined reinforcing effect of carbon nanotubes and glass in the bi-filler composite outperforms the mechanical properties achieved with the additive effect of their individual counterparts. The electrical resistivity of the composites resulting from the formation of the conductive percolative pathway by the carbon nanotubes was only minimally altered by the addition of glass fibers. The thermal stability of the bi-filler composite was also considerably high. The bi-filler composite thus shows all the traits of an excellent multi-functional composite.

Optimization of process parameters for achieving good carbon nanotube dispersion in a polypropylene resin, significant savings in both raw-material and energy costs by employing peroxide as a reactive functional additive, and the addition of economic short glass fibers as secondary fillers augurs well for the development of a multi-functional composite with excellent electrical, mechanical and thermal properties, and also tremendous potential for product development.

Table of Contents

List of Figures

List of Tables

List of Abbreviations

CNT	Carbon nanotube
SWCNT	Single-walled carbon nanotube
MWCNT	Multi-walled carbon nanotube
DWCNT	Double-walled carbon nanotube
vdW	van der Waals
CVD	Chemical vapour deposition
DC	Direct current
CEFIC	European chemical industrial council
CKNMT	Centre for knowledge management of nanoscience and technology
CAGR	Compounded annual growth rate
CFRP	Carbon fiber reinforced plastic
EMI	Electromagnetic interference
ESD	Electrostatic dissipation
SEM	Scanning electron microscopy
MFR	Melt flow rate
PP	Polypropylene
PP-Px	Peroxide modified polypropylene
PS	Polystyrene
PMMA	Poly(methyl methacrylate)
PE	Polyethylene
PC	Polycarbonate
PA	Polyamide
PVC	Polyvinyl chloride
SBR	Styrene-butadiene rubber
HIPS	High impact polystyrene

DMA	Dynamic mechanical analysis
DSC	Differential scanning calorimetry
TGA	Thermogravimetric analysis
L/D	Aspect ratio of the twin-screw compounder
MF	Mainfeed position for filler (position of polymer feed)
SF	Sidefeed position for filler (located at the L/D = 16 of the extruder)
DoE	Design of experiments
SE	Screening experiment
ME	Mainstream experiment
Sxy	Sample nomenclature for SE (where: xy are numerals)
Eab	Sample nomenclature for ME (where: ab are numerals)
R2	Measure of how well the DoE model fits data
Q2	Measure of how well the DoE model predicts new data
D peak	CNT peak in the Raman spectra activated by the presence of disorders
G peak	Graphitic peak in the Raman spectra resulting from in-plane C-C vibration
G* peak	Secondary overtone of D peak in the Raman spectra
δ-CH_2 peak	Bending vibration peak of PP in the Raman spectra
FWHM	Full width at half maximum
I_D/I_G	Intensity ratio of the CNT D peak to the CNT G peak (Measure of CNT defect concentration)

List of Symbols

σ_a	Inherent agglomerate strength	MPa
F	Fragmentation number	Dimensionless
η	Viscosity	Pa.s
$\dot{\gamma}_r$	Shear rate	s^{-1}
σ_{am}	Maximum agglomerate strength	MPa
A_f	Undispersed CNT area fraction	%
SME	Specific mechanical energy	kWh/kg
η_e	Gear drive efficiency	%
M_{max}	Maximum torque for one screw shaft	N/m
I	Motor current	%
N	Screw speed	rpm
M	Material throughput	kg/h
T	Barrel temperature	°C
W	Weight fraction of CNT	wt.%
T_o	Temperature of onset of degradation	°C
T_{max}	Maximum temperature of degradation	°C
T_g	Glass transition temperature	°C
X_c	Crystallinity	%
ΔH_m	Enthalpy of melting	J/g
ΔH_{mp}	Enthalpy of fusion of 100% crystalline PP	J/g
T_c	Crystallization temperature	°C
T_m	Melting temperature	°C
G’	Storage modulus	Pa
η^*	Complex viscosity	Pa.s
Tan δ	Tangent delta/ Loss tangent	Dimensionless

E	Elastic Modulus	MPa (or) GPa
I_{notch}	Notched impact strength	kJ/m^2
σ_{max}	Maximum tensile strength	MPa
ε_{break}	Failure strain	%
Strain at σ_{max}	Elongation at maximum tensile strength	%

1. Introduction and Scope of Study

Ever since the discovery of single-walled carbon nanotubes (SWCNTs) by Iljima early in 1991 [1], carbon nanotube (CNT) based polymer composites have found enormous interest among the academic and industrial community. To tap the extraordinary potential that CNTs bring in the form of thermal, mechanical and electrical properties, they have to be effectively dispersed into polymeric matrices. Though carbon black is an automatic choice for making conductive polymer composites owing to its economics, electrical percolation occurs at around 10 wt.% carbon black loading. This also comes with a tradeoff of reduction in the mechanical properties of the composites. In a drastic contrast, CNT based composites show much lower conductive percolation filler thresholds with additionally enhancing or without significantly disturbing the mechanical characteristics [2]. From a broader perspective very high costs associated with the CNT raw material and technical issues associated with dispersing CNTs have so far prevented broad commercialization of these materials.

Commercially available CNTs especially multi-walled carbon nanotubes (MWCNTs) exist as severely entangled agglomerates due to their intrinsic van der Waals (vdW) forces of attraction. These forces have to be overcome by shear forces during composite processing or by approaches like ultrasonication prior to processing. The shear forces generated from the viscous flow during the twin-screw compounding process (for example) has to be of a significant magnitude to overcome the vdW forces of the agglomerated CNTs to achieve good filler dispersion in the matrix. Also, from existing literatures on secondary processing (after extrusion) of these composites by compression molding (nanoscale re-agglomeration of dispersed CNTs under the influence of reduced viscosity with minimal shear) [3,4], and injection molding (re-agglomeration and CNT orientation with secondary shear) [5,6], it is understood that re-agglomeration of the previously dispersed CNTs on the nanoscale is critical for the formation of conducting pathways for good electrical properties. However, this process of creation of secondary agglomeration is inherently dependant on the dispersion of CNTs which evolves from the extrusion step. In spite of several investigations over the past 20 years it is rather unclear as to what levels of dispersion are expected out of each of these processing steps for the composite to show the desired properties. Even when such information is available, the primary processing source is either a laboratory mixer [3,4], or an extruder [7,8], on which the combined influence of all the principle process variables have not been considered.

A review of the mechanical properties of polymer-CNT composites by Coleman et al. in 2006 point a significant step forward in the enhancement of structural characteristics of these composites [9], but unfortunately majority of the published literatures do not address this aspect. Schaefer and Justice with their small-angle X-ray scattering, light scattering, and electron imaging of polymer-nanocomposites conclude that the pervasive large scale morphology of the fillers in the composites irrespective of the quality of dispersion lead to substantial reduction in the theoretical potential of reinforcement [10]. Also, the inability to achieve a strong polymer-CNT interface to facilitate load transfer has been a major concern.

From the type and the quality of the CNTs, the nature of the host matrix, processing conditions and equipments, and techniques for suitable characterization; all limit the development and understanding of a polymer-CNT composite. Tuning the surface of the CNTs by functionalization both by chemical and physical means has shown promise, but findings do not support strong and consistent evidences of good mechanical reinforcements in polymer-CNT composites [11,12]. Even in situations where good mechanical property enhancements are reported, it comes with a shortcoming of reduced electrical properties [13-15]. Research findings till date has led to a situation which makes one wonder if CNTs are worthy polymer reinforcements for structural characteristics.

From the theory of dispersion of CNTs in polymers, low viscosity thermosets present a favorable condition for CNT dispersion due to better melt infiltration of the CNT agglomerates (elaborated in Section 2.3.1). Hence, the enhancements in the macroscopic properties of CNT filled thermosets are reported in plenty. Ultra low CNT percolation thresholds of the order of 0.0025 wt.% CNT in epoxy was reported by et Sandler al. [16]. This however does not seem to be the case in most thermoplastics where at least a minimum of 0.5-1 wt.% CNT are generally desired for property enhancements. Thermoplastics especially polyolefins reinforced with CNTs form one of the least reported categories due to associated difficulties in achieving better CNT dispersion in those matrices.

Motivation

Polypropylene (PP), an olefin is one of the widely employed commodity thermoplastics, and any economical effort to enhance its characteristics with a view of developing a multi-functional composite would certainly be a worthy challenge. Excellent electrical, thermal and mechanical properties of these composites are sought after with a bi-filler system of CNTs and glass fibers.

Prior to taking advantage of glass fibers as structural reinforcements, it is critical to achieve a very good CNT dispersion in PP for high electrical properties at low filler loadings. However, incompatible surface energies between PP and CNT, the hydrophobic characteristics of PP, and the inert chemical surface of CNTs together present the biggest challenge to achieve good CNT dispersion morphologies in PP. A considerable magnitude of viscosity of the PP melt (compared to those of the thermosetting matrices) during processing also hinders the prospects of a good CNT dispersion.

This study is primarily driven by the need to enhance CNT dispersion in PP by processing them on large scale equipment and the development of economic strategies to achieve good dispersions with largely available industrial grades of CNTs. Thereon, it becomes important to investigate the addition of glass fibers into the PP-MWCNT composite for its influence on the macroscopic properties towards the development of multi-functional characteristics.

2. State of the Art

2.1 Carbon Nanotubes

The interest in the special allotrope of carbon called CNTs was greatly stimulated by the observation of tubular forms of carbon with nanometric dimensions by Iljima [1], and succeeding reports on the capabilities to synthesize these nanoparticles in large quantities [17,18]. CNTs belonging to the fullerene family are geometrically idealized to be a cylinder formed by concentrically rolled graphene sheets with at least one end of the cylindrical structure capped with a hemispherical fullerene structure. They are typically of a few nanometers in diameter and microns in length.

2.1.1 Structure of CNT

Similar to the structure of graphite, the sp^2 hybridized CNT has each of its atoms bonded to three neighboring atoms in an hexagonal array. As the cylindrical structure of the CNT is brought about by the rolling up of the graphene sheets, the type of CNT would depend upon the number of concentric cylinders. CNTs principally exist as SWCNTs, double-walled carbon nanotubes (DWCNTs) or as MWCNTs (Figure 1).

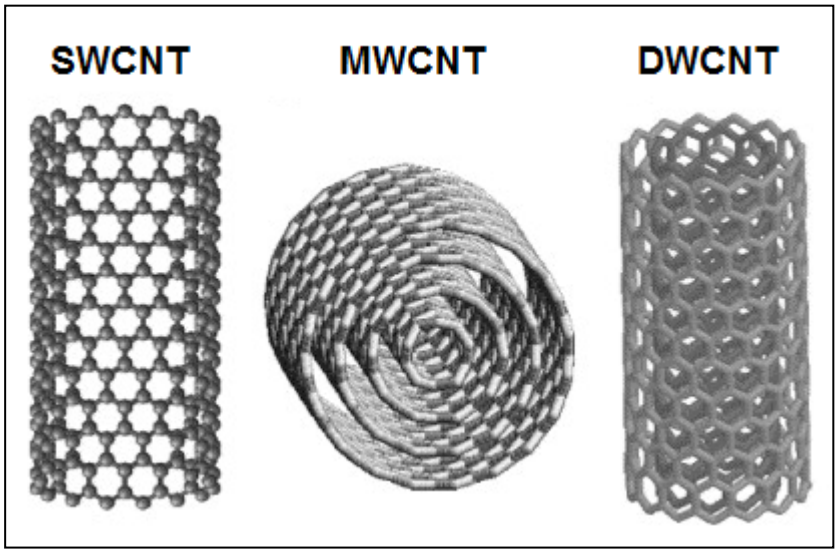

Figure 1. Different types of CNTs - Based on the number of tube walls [19]

The intrinsic properties of the CNTs would stem from the atomic arrangement (or in other terms the way their graphene sheets are rolled), the type of the CNT and their individual geometric dimensions. The rolling up of the graphene sheets and hence the atomic structure of the CNTs is well defined by the tube chirality. The chirality is given by the chiral vector $C_h = n\overrightarrow{a_1} + n\overrightarrow{a_2}$ where $(\overrightarrow{a_1}, \overrightarrow{a_2})$ are the unit vectors and (n,m) are the number of steps along the unit vector of the hexagonal lattice [20]. This gives rise to three possible orientation forms for the carbon atoms of the CNTs. If n=m, it leads to the “armchair” structure while the “zigzag” structure results when m = 0. Any other orientation leads to “chiral” structure. The electronic conduction of the CNTs is dependent on the chirality. CNTs with “armchair” chirality are metallic, semi-metallic when (n – m) / 3 = i and n ≠ m, where i is an integer and

semi-conducting otherwise [21]. The chirality of a MWCNT as used in this work is extremely complex as each of the concentric nanotube walls could carry different chiralities. Figure 2 shows the nomenclature system of CNTs and the different chiral forms of SWCNTs [(a) arm chair, (b) zigzag, (c) chiral].

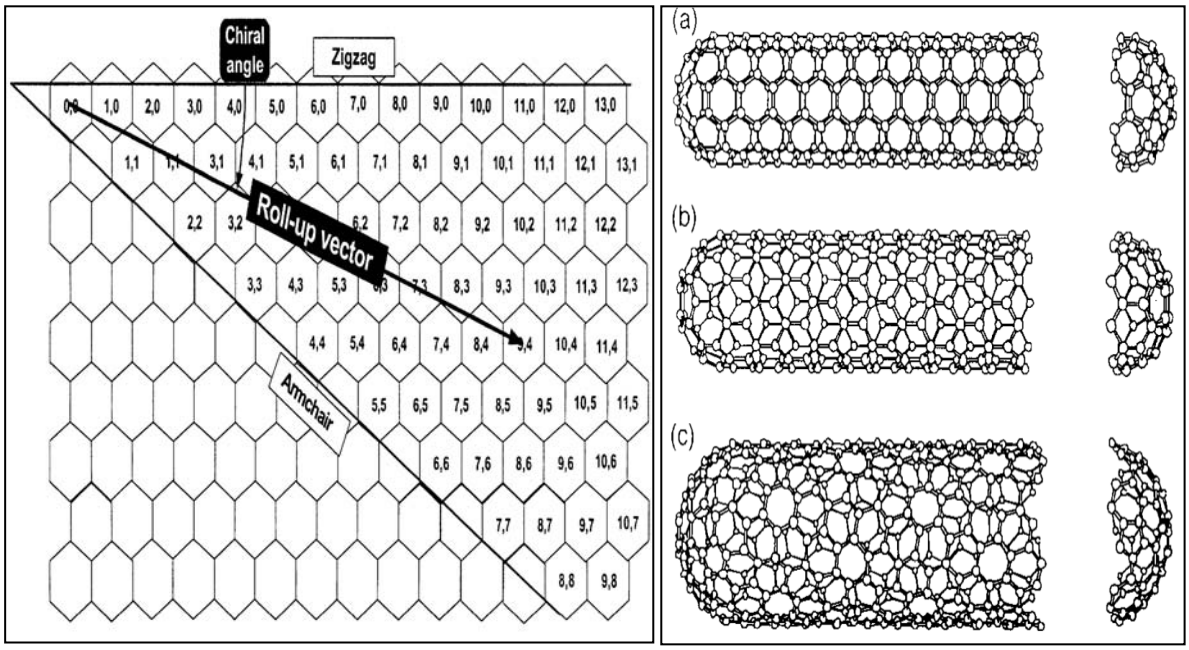

Figure 2. System of CNT nomenclature [22] (Left); Chiral forms of SWCNTs [23] (Right)

2.1.2 Synthesis of CNTs

Arc discharge, laser ablation and chemical vapor deposition (CVD) are three principal techniques by which CNTs are synthesized. They are briefly described below. The schematic of the different techniques are shown in Figure 3.

The **arc discharge** approach is probably the easiest to synthesize MWCNTs, however the quality of the resulting CNTs and their pattern of growth is not the best compared to production by other techniques [24]. In the arc discharge approach, two graphite electrodes are placed 1 mm apart in an inert atmosphere and a direct current (DC) of about 50-100 A at a voltage of 20 V is applied across them. The vaporization of carbon at these conditions lead to a high temperature discharge (also termed as plasma) resulting in the consumption of the anode and the formation of deposits on the surface of the cathode from where the CNT grows. The typical yield of this process is around 30-90 % and the principal advantage of this process is the economic production of MWCNTs without a catalyst. The doping of the anode with a metal catalyst would result in the formation of SWCNTs [21]. The principal drawback of the arc discharge approach is the production of shorter and impure CNTs which mandates a purification step to generate high quality CNTs.

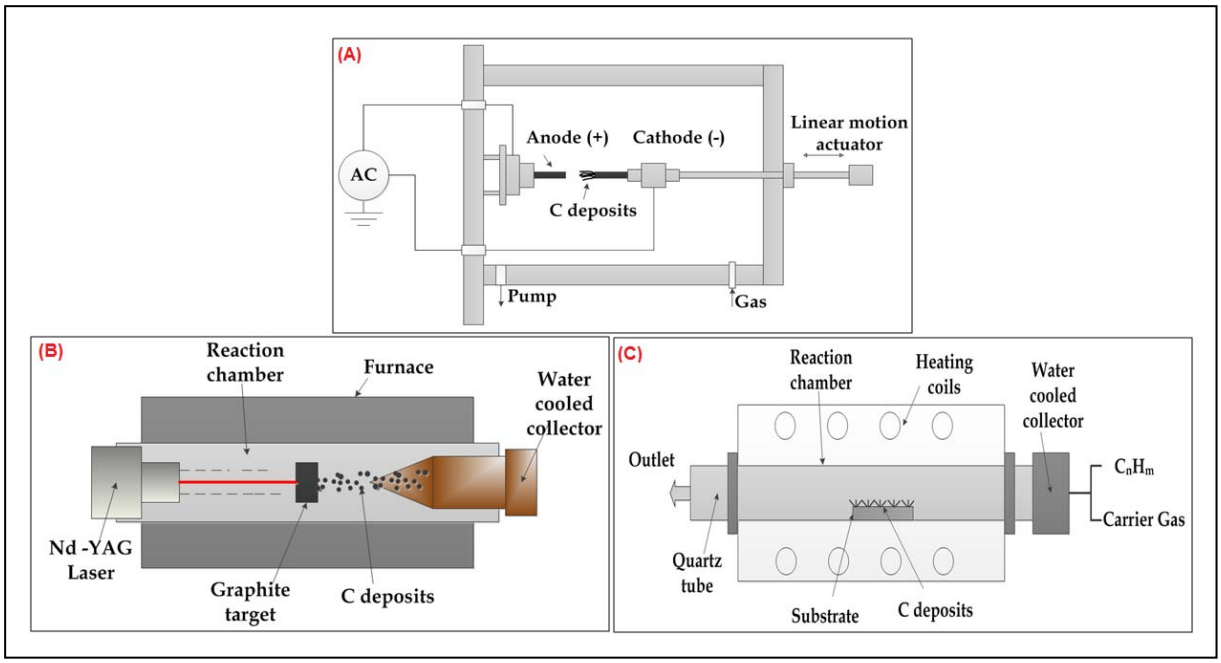

Figure 3. Techniques for CNT synthesis [25]. (A) Arc discharge, (B) Laser ablation, (C) CVD

The **laser ablation** technique uses a high power laser to form the discharge product unlike the DC generated electricity in the arc discharge approach. Laser is shot on a graphite source that is placed in an oven under inert atmosphere at temperatures of around 1100-1200 °C. The carbon vapors formed under these conditions expands and cools resulting in the formation of CNTs and other members of the fullerene family depending upon the set process conditions. MWCNTs are the principal product and are shorter in length compared to arc-discharge process [21,26], but the addition of a metal catalyst to graphite would result in SWCNTs. The typical yield of this process is around 70-80% and the purity of the produced tubes is significantly higher. Good product control is possible; however this comes with the trade-off of high production cost due to higher power requirements for operating the laser.

CVD is the widely adopted industrial approach for producing CNTs owing to its scalability. When a carbon containing gaseous source like acetylene, methane etc. is passed over a metal catalyst at temperatures ranging from 550-1200 °C it results in the freeing up of carbon atoms on the decomposition of the gas, which recombines in the form of CNTs on the metallic substrate. This method is widely adopted for flexibility in controlling the quality and exercising good control over the dimensions of the formed product. The yield varies from 20-100 % with minimal need for purification of the synthesized CNTs due to the negligible traces of amorphous carbon. Very long CNTs can be produced by this approach. The production of extremely pure SWCNTs is possible with controllable diameters, but the MWCNTs that are formed with the CVD process have more structural defects [27], and are highly entangled compared to the arc discharge and laser ablation approach.

2.1.3 Properties of CNTs

CNTs are known for their intrinsically high mechanical, thermal and electrical properties. The sigma bonds which make up the C-C bonding in CNTs attribute to their excellent mechanical characteristics. Elastic modulus of 1.2 TPa and tensile strength of about 50-200 GPa have been reported for CNTs [28]. However, there does not seem to be a consensus on the reported mechanical behaviour among published literatures. Their high axial and low lateral thermal conductivity also add to their significance. Although theory predicts a room temperature thermal conductivity of 6000 W/mK [29], Kim et al. estimate the thermal conductivity of MWCNTs to be 3000 W/mK [30], and Pop et al. report 3500 W/mK for SWCNTs [31]. This is significantly higher than the thermal conductivity of diamond (1000-2200 W/mK) which is reported to be one of the best known thermal conductors [32].The oxidative thermal stability for both MWCNTs and SWCNTs are greater than 600 °C which compares strongly with that of 450-650 °C for graphite. The co-efficient of thermal expansion is very minimal which supports the excellent thermal conductivity of these materials. SWCNTs show electrical conductivities of the order of 10^2-10^6 S/cm, while it ranges between 10^3-10^5 for MWCNTs. The lower scales are very similar to the reported in-plane electrical conductivity of graphite of about 200-2500 S/cm [33], indicating the dominative electrical properties of CNTs compared to one of the best reported electrical conductors in graphite. They also boast of extremely high intrinsic electron mobility of greater than 10^5 cm^2/Vs [34], which is very similar or even higher than graphite.

The extraordinary multi-faceted properties of CNT confer to these materials a significant potential to be used in a wide-variety of applications. The intrinsic tendencies of the CNTs to exist as agglomerates due to their vdW forces of attraction (0.5 eV/nm) [35], by large limits the realization of the complete potential of these materials as nanoscale reinforcements in different host matrices.

2.1.4 Applications of CNTs

The intriguing properties of CNTs have led to many research efforts leading to uncovering the potential prospects of employing CNTs in practical applications. Although it has been very complex to translate the theoretical potential of CNTs till date into potential applications, efforts are still ongoing towards understanding the intrinsic properties of CNT and ways to implement them in real life. The benefits of CNTs are expected to be significantly realized from an economical perspective when they are used as reinforcements for materials like plastics, ceramics etc., however their potential to be used as such (especially SWCNTs in flexible electronics applications) is also being widely worked on. This is supported from the finding that 69 % of the global CNT market share of $472.9 million in 2010 was the contribution of the plastics and composites industry [36].

Although a wide variety of applications could result owing to superior CNT properties, they can principally be classified into three main categories of mechanical (structural composites for aerospace and automotive industries, textiles, sport goods, etc.), thermal (flame retardant additives, coatings, electronic circuitry etc.) and electrical & electronics (semi-conducting

materials, electronic circuitry, fuel supply systems of automobiles, navigation systems etc.). The multi-functional derivatives that stems out by a combination of these properties on the final part application adds significant value to the applications of CNTs.

The European Chemical Industrial Council (CEFIC) classifies the potential applications of CNT on the basis of time into short term – those products based on CNT already available or will shortly be available (e.g. conductive composites, sensors, electromagnetic shielding, sport goods etc.), mid-term (e.g. coatings, lithium-ion battery, fuel cells, semiconducting materials, petrochemical catalysts etc.) and long term – those currently under the scope of research & development (e.g. drug delivery, microwave antennas, medical implants etc.) [37].

Some of the existing commercial applications of the CNTs include the long range vessel LRV-17 from *Zyvex Marine* made of a carbon fiber-nanocomposite system consisting of carbon fiber reinforced plastic (CFRP) and CNTs which enables reduction in structural weight, efficient fuel usage and increased range [38], and a 25 times stronger tennis racket by *Völkl* made of CNT compared to carbon fibers (at same weight) which would eventually result in more kinetic energy returned to the ball [39]. *Aldila* have also reported to have used CNT based epoxy composites for golf shafts for vibration damping [40].

2.1.5 CNTs – A Market Outlook

The production capacity of CNTs is expected to grow globally from 3141 metric tons to 12806 metric tons in 2016 at a Compound Annual Growth Rate (CAGR) of 10.5% according to Centre for Knowledge Management of Nanoscience and Technology (CKMNT), India [36]. As per their 2011 forecast the total CNT market is to yield around $1.1 billion by 2016 at a CAGR of 10.5 %.

A Frost & Sullivan report published in 2011 forecasts a $35.52 million market for CNT in the automotive composites market by 2015, indicative of a market share of 3.6 % at 1 % CNT loading [41]. The report also predicts a 10 % penetration of CNT in the construction industry, 15 % in the fibers and textile domain, and about 25 % in the intumescent coating market. From the standpoint of an electronics industry, the largest share for CNT is expected for the displays (1->5 %) and flexible displays (1-10 %) while only 1% penetration in the sensor market is foreseen. Significantly CNTs are also expected to gain a 1-5 % share in the total authentication market. With recent developments in research, it is expected that these numbers will continue to rise in spite of a foreseen potential threat by graphene which is expected to gain a significant market share especially in the electronics industry.

2.2 Polymer-Carbon Nanotube Composites

CNT based polymer composites have been an area of profound interest owing to the high aspect ratios of CNTs with nanometric dimensions, low mass density and intrinsically superior electrical [42,43], mechanical [43,44], and thermal properties [43,45]. Continuously lowering costs of CNTs with increase in demand and production capabilities augment

favorably for a huge CNT/polymer nanocomposite market. Interesting observations on MWCNT based composites have been plenty starting from different ways of MWCNT synthesis to its application in electromagnetic shielding (EMI) [46,47], sensors [48,49], electrostatic charge dissipation (ESD) [50], flame retardancy [51], wind turbine blades [52], photovoltaic packaging [53], electrically conducting cables [54] etc.

On the other hand, it has so far been unable to achieve macroscopic properties for CNT reinforced polymer composites anywhere close to what theory would predict. In addition to being severely entangled, the relatively high interfacial energy difference between CNTs and most polymers present a challenge to achieve optimum CNT dispersion in polymer matrices for improved macroscopic properties of the nanocomposites. Individualized CNTs on processing would present an ideal scenario to translate the intrinsic characteristics of the CNT to its composite; however this is limited by the agglomerate strength of the CNT. Commercially available MWCNTs are highly agglomerated which mandates high shear stresses during processing to achieve good filler dispersion. But, processing with enhanced shear could result in structural damage to the CNTs [55], negatively affecting the efficiency of property improvements.

Highly conductive and structurally performing characteristics of the CNT reinforced polymer composites are of significant interest in addition to their thermal properties, EMI shielding behaviour etc. The ability of the dispersed CNTs to form a conductive network in the host matrix gives rise to a conductive composite. These conductive networks could be formed at lower CNT loading fractions due to the very high aspect ratio of CNTs compared to materials like carbon fibers, signifying the importance of CNT as conductive filler for polymers. Electrical properties of CNT reinforced polymer composites are widely reported in literature with extremely low filler percolation thresholds, for example 0.0025 wt.% in CNT filled epoxy composites [16].

Large surface area owing to nanometric dimensions of the CNT would theoretically be expected to result in a larger area for polymer-filler interaction facilitating load transfer from the host matrix to the CNT; however results on mechanical reinforcements of polymers with CNT have been a disappointment thus far. The inability to develop a strong interface owing to the agglomerative tendency and the chemically inert surfaces of CNT could be attributed as principal reasons for the aforementioned. Functionalization both by chemical and physical means has been largely reported as strategies to reduce intra-filler vdW forces and render the surface of the CNT suitable for interactions with the polymer, both leading to enhanced CNT dispersion in the polymer.

Chemical functionalization is done either on the side walls or by creating defects on CNT surfaces by acid treatments resulting in very strong matrix-CNT interaction with a trade off on the structural characteristics of CNTs. The sp^2 hybridization of carbon is transformed to sp^3 to create active sites for effective interaction with polymer accompanied with the loss of π conjugation bonds on the outer walls. Covalent functionalization of CNTs could modify CNT stacking morphologies by altering hydrogen bonds resulting in improved CNT solubility in

solvents [56]. But, covalent functionalization tends to negatively affect the physical and chemical integrity of CNTs. Strong acid treatments affects the geometry of the CNTs, and thus the reduced CNT aspect ratio results in increased filler percolation thresholds [57]. Covalent treatments could also result in loss of intrinsic electrical properties of the CNTs and also affect their metallic characteristics [58]. Enhanced reactivity between CNT and the polymer could result in wrapping or encapsulation of CNT surfaces by the polymer due to coupling or grafting, lowering the bulk conductivity of the composite [59]. The phonon scattering length is also expected to be lowered resulting in lower thermal conductivities [60]. Covalent treatments are mainly aimed at improving polymer-CNT compatibility and CNT dispersion. Effective achievement of this could lead to improved structural characteristics accompanied with losses in electrical and thermal conductivity of the composite.

Physical functionalization is done by polymer wrapping (vdW forces and π-π stacking), surfactant adsorption on CNT surface (physical adsorption) and endohedral techniques (capillary principle). Although this technique would not damage CNTs, only a weak CNT-polymer interaction could be expected out of these approaches. Non-covalent or physical treatment of CNTs result in the outer tube walls subjected to more treatment than the inner tubes [61]. This could result in the CNTs being bundled even after treatment. Hence mechanical treatments like milling, ultrasonication etc should precede physical functionalization. Since physical methods do not result in significant structural damage of CNT, their composites could be expected to show enhanced electrical conductivity as the π-conjugation of the CNTs and their electron transfer paths could maintain their identities. Polymer wrapping of CNT surfaces cannot be completely ruled out resulting in lower electrical conduction. Mechanical property enhancements cannot be expected to be on a larger scale because the chance for the interfacial strength to improve is minimal owing of lack of chemistry.

The techniques of chemical and physical modifications are however relatively expensive which limits modification of the CNT for large scale applications. A review by Bose et al. [62], discusses the positives and the drawbacks of both physical and chemical functionalization in detail on the properties of CNT based polymer composites.

Processing of Polymer-Carbon Nanotube Composites

The level of CNT dispersion visible on the composite morphology is a direct function of the type of polymer and CNT employed, the processing approach and the process factors. The morphology and therein the macroscopic properties of the composite are dictated by the thermo-mechanical history during processing. Several processing methodologies such as solution casting [63-65], melt mixing [4,66,67], solution mixing [63,64,68], different methods of in situ polymerization of the monomer in the presence of CNTs [69,70], coagulation spinning [71], mechano-chemical pulverization [72], solid-state shear pulverization [73], electro spinning [74] etc. have been adopted for the synthesis of polymer-MWCNT composites. In this section only the widely employed approaches namely solution processing, melt mixing and in situ polymerization would be discussed in brief.

Solution processing is one of the widely utilized approaches owing to its simplicity. It involves dispersion of the CNT in a suitable solvent by sonication and/or stirring followed by mixing with a solution of the polymer host, evaporation of the solvent and drying with or without vacuum. Ultrasonication is commonly used to break the CNT agglomerates as the shear in the solution mixing process is significantly low. The type of ultrasonication (ultrasonic bath or horn), bath temperature, rate of sonication (frequency and time) and the nature of the solvent could have a strong influence on the properties of the final product. Although this method can be successful with the right choice of solvent and complete removal of the solvent during the drying stage, it is not easily scalable. It is widely adopted for preparing thermoset based composites where a significant magnitude of shear is not required as the low viscosity of the polymer host would result in good infiltration of the CNT agglomerates facilitating dispersion.

Owing to its simplicity and adaptability for a commercial scale up, melt mixing/compounding seems to be the most commonly employed processing approach for thermoplastic polymer/MWCNT nanocomposites. This method is most suitable for polymers that cannot be processed with the solution processing approach owing to its inability to dissolve in commonly used solvents. The higher magnitude of shear during the melt mixing process facilitates the breakup of the CNT agglomerates followed by simultaneous dispersion and distribution in the polymer melt. For a melt mixing process to give optimum dispersion quality optimization of all the process parameters like the screw configuration, screw speed, throughput/residence time, barrel temperatures, filler feeding position etc. is imperative. A detailed insight is presented in Section 2.3.3.

In situ polymerization of monomers in the presence of CNTs is another widely used technique for composite preparation. This technique is proposed to form a very good chemical affinity between the polymer chains and the CNTs in most cases, but depending on the nature of the reactants a non-covalent interaction is a definite probability. The polymerization of the monomer in the presence of an initiator is carried out with CNTs in the vicinity enabling the production of composites with high CNT loadings. A mix of polymer grafted CNTs and free polymer chains are obtained which creates a favorable environment for the development of a highly compatible polymer-CNT interface. The low viscosity of the starting monomer facilitates better infiltration into the CNTs. CNT based composites of polystyrene (PS), poly (methyl methacrylate) (PMMA), and vinyl monomers are commonly produced using this approach. Yuan et al. show significant enhancement in the mechanical properties of PS-MWCNT composites prepared by a combination of in situ polymerization followed by melt mixing owing to strong interfacial adhesion between the CNT grafted PS and the PS matrix [75].

2.3 Dispersion of Carbon Nanotubes in Thermoplastics

Commercially available CNTs that primarily results out of the CVD process have a highly agglomerated morphology with a significant agglomerate strength. These cohesive or the vdW forces of attraction that result in the agglomerated morphology of CNTs have to be

overcome or minimized in order to gain a competitive advantage with CNTs as polymeric fillers. The initial or the primary CNT agglomerates have to be broken down theoretically into individual CNTs or in other terms dispersed well into the polymer host to translate the intrinsic characteristics of the CNTs to their composites. This has remained a significant challenge over the years and any effort to maximize the quality of dispersion on industrial scale could result in taking these nanocomposites close to application.

Due to its economics and availability in bulk, MWCNTs would be the ideal choice for high volume industrial applications; hence attention would be focused on MWCNT dispersion in thermoplastics in this dissertation. Scanning electron micrographs (SEM) images of two of the most widely used MWCNTs in literature namely *Baytubes® C 150 P* (*Bayer Material Science, Germany*) and *Nanocyl™ NC 7000* (*Nanocyl S.A., Belgium*) are shown in Figure 4.

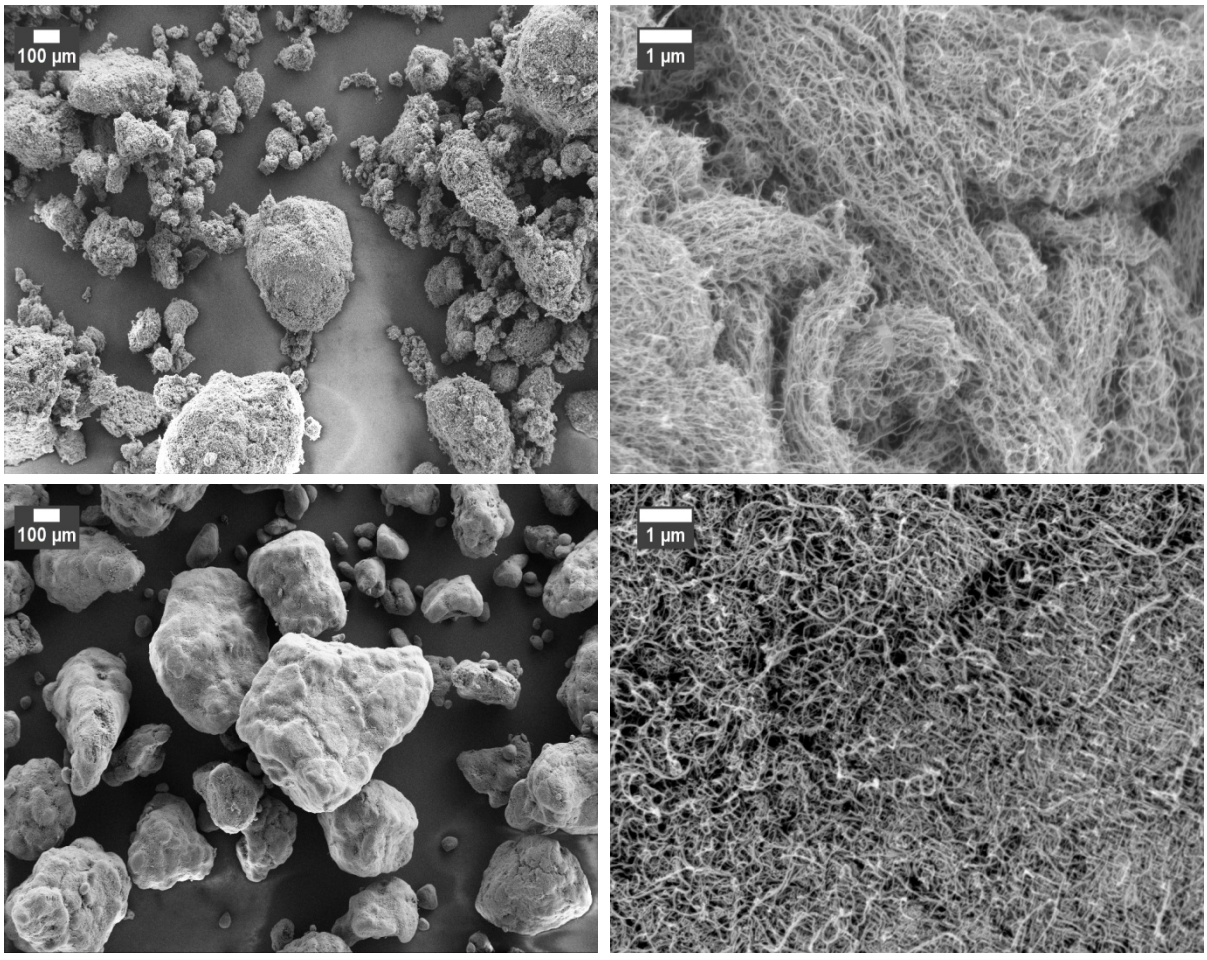

Figure 4. Low and high magnification images of NC 7000 (Top), C 150 P (Bottom)

These pictures indicate a highly entangled network of MWCNTs with sizes ranging upto a few microns, unusual for a material described as nanofiller. Alig et al. describe the structure of loosely packed larger agglomerated NC 7000 as a “combed yarn” structure while that of C 150 P as a “birds nest” with smaller tightly held primary agglomerates [76]. Although the geometries of these MWCNTs do not differ significantly, the average deformation stress (at 25 % strain) of C 150 P with a bulk density of 120-170 kg/m^3 [77], is 0.64 MPa [78], while that of NC 7000 with a bulk density of 60 kg/m^3 [79], is 0.39 MPa [78]. This difference in the

deformation stresses of the MWCNTs will be a critical factor in determining the magnitude of processing parameters and consequently the extent of processing shear required to create equivalent dispersion qualities with these two different CNT types.

2.3.1 Mechanism of CNT Dispersion in Thermoplastics

Dispersion of CNT in thermoplastics is a simultaneous sequential process starting with the wetting of the CNT agglomerates by the polymer melt, infiltration of the polymer melt into the CNT agglomerates, disintegration of agglomerate fractions weakened by the infiltration process and shear forces into small fractals by mechanisms of erosion and/or rupture followed by their distribution in the polymer host (Figure 5). This mechanism of filler dispersion is strongly influenced by the processing approach, associated process parameters and the nature of the polymer and the CNTs.

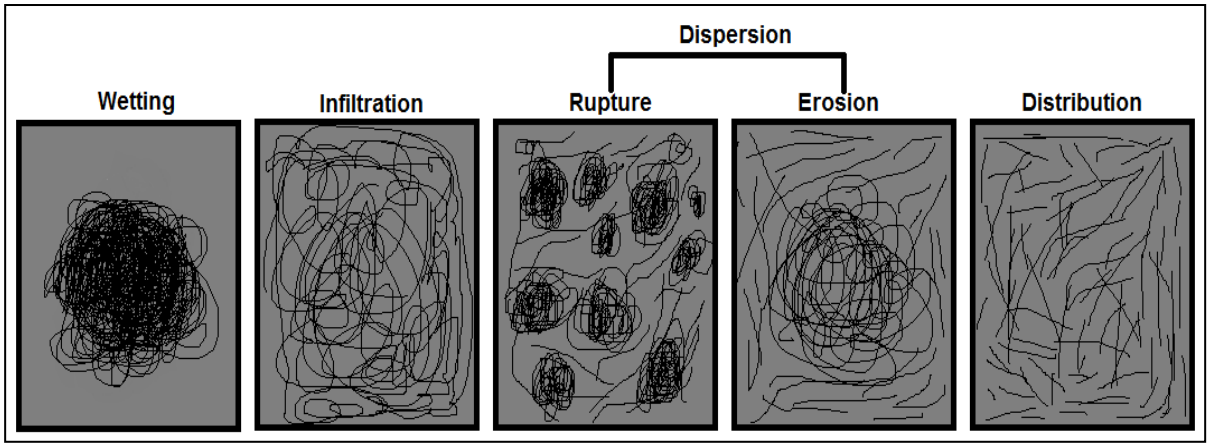

Figure 5. Mechanism of CNT dispersion

For effective wetting of the primary CNT agglomerates by the polymer melt, the interfacial energy difference between the polymer and the CNT should be at its minimum. As the interfacial energy difference between polar thermoplastics like polycarbonate (PC), polyvinyl chloride (PVC) etc, with CNTs is significantly low, excellent CNT dispersion is achievable with these matrices resulting in extremely low filler percolation thresholds for the final macroscopic properties [3,80-82]. On the other hand, polyolefins exhibit a very high interfacial energy difference with the CNT limiting the level of CNT dispersion in the composite [66,83]. Incorporation of surface functionalities to the CNT is a solution to render compatibility with the polymer; however this is an expensive approach as detailed earlier.

Infiltration of the polymer melt is principally governed by the mobility of the polymer chains (dependent on viscosity), the available pore radius or the agglomerate density of the CNTs, the strength and size of the CNT agglomerates and interfacial energy difference between the polymer and the CNTs. Lower polymer viscosity or high melt temperatures and low agglomerate density would aid faster infiltration, while minimal interfacial energy difference between the polymer and the CNT would enhance the efficiency of infiltration. The infiltration process can be manipulated by the choice of the raw-materials and the process parameters which will be discussed in detail later in Sections 2.3.2 & 2.3.3.

The magnitude of applied shear stresses arising due to the viscous flow to the CNT agglomerates during processing must be above the inherent strength of the agglomerates (σ_a) for dispersion to occur. The dispersion of the weakened primary agglomerates by the preceeding wetting and infiltration steps would take place by mechanisms of rupture and/or erosion governed by a dimensionless fragmentation number (F) which is directly proportional to the product of the melt viscosity (η) and the shear rate ($\dot{\gamma}_r$) and inversely proportional to the inherent maximum agglomerate strength (σ_{am}). The magnitude of contribution of the infiltration step towards the reduction in σ_a could play a role in regulating the maximum shear stress that has to be exerted on the agglomerates. It is to be remembered that enhanced shear stress could result in tube breakage and also could lead to possible polymer degradation. Though rupture and erosion would co-occur, a significantly larger magnitude of F ($F >> 1$) would result in a situation where rupture would dominate while lower F ($F << 1$) would result in dispersion dominated by erosion [84]. The mechanism of rupture is comparatively faster than erosion owing to the instantaneous breakage of primary agglomerates into smaller fractals in the former, while a slowly peeling of individualized CNTs occurs from the outer surface of the primary agglomerate fraction in the latter. Distribution of the dispersed agglomerate fractals takes place simultaneously with the disintegration or rupture of remaining agglomerates over the course of the process. Idealizing this in the context of twin-screw extrusion, residence time of the melt would determine the extent of filler dispersion for a given set of process parameters and material combination.

2.3.2 Influence of Raw Materials

The selection of a suitable polymer host and the intrinsic characteristics of that polymer host is one of the critical factors affecting the quality of filler dispersion in the final composite. An increased affinity between the polymer and the CNT would result in better wetting of the CNT agglomerates which is the preliminary step in the mechanism of dispersion. Polymers like PC and PA which has lower interfacial energy difference with the CNTs could result in better wetting of the CNT agglomerates and hence result in better CNT dispersion, while the quality of dispersion in polyolefins is poor owing to its hydrophobic nature and higher interfacial energy difference with CNT. Exceptionally polystyrene (PS) presenting a polar characteristic shows poor CNT dispersion owing to the high chain stiffness due to its phenyl groups [55].

The viscosity of the polymer melt governs the extent of melt infiltration into the agglomerates and the dominating mechanism of filler dispersion via rupture or erosion. Lower polymer viscosity would result in better melt infiltration, but could result in lower magnitude of shear stresses arising out of viscous flow during processing. Higher polymer viscosity would hinder easier and faster melt infiltration, but can result in increased shear stresses for agglomerate breakage. Magnitude of the shear stresses required for dispersion of CNT is also dictated by the intrinsic characteristics of the CNT. Kasaliwal et al. discuss the influence of PC melt viscosity and molecular weight on the level of MWCNT dispersion and conclude that lower matrix viscosity resulted in better melt infiltration leading to better MWCNT dispersion and hence lower electrical resistivities in the composite [85].

The type of CNT especially its number of walls, length, aspect ratio, agglomerate strength and morphology, and the nature of surface functionalization are factors to be considered while designing the process and the associated parameters for its dispersion in a polymer matrix. A CNT with higher agglomerate strength would present increased difficulties to melt infiltration compared to a CNT type with more loosely packed agglomerates even if larger agglomerate size fractions are present in the latter. High aspect ratio of CNTs is beneficial for efficient load transfer and hence improved mechanical properties at low percolation thresholds. However, it could complicate dispersion owing to the enhanced available surface area for intra-CNT interactions compared to employing CNTs with low aspect ratios. A balance between the level of dispersion and the aspect ratios of the CNT is quite critical for the end properties as elucidated by Castillo et al. on their work on PC incorporated with different types of CNTs [81]. The enhancement in the compatibility of the CNT with the polymer by functionalization techniques also plays a role in dictating the level of MWCNT dispersion in the polymer host. Menzer et al. found that the altering of the CNT lengths by ball milling resulted in compact agglomerate morphologies and reduction in CNT lengths contributing to higher electrical and rheological percolation thresholds in the composite [66]. Idealizing this to the reduction in the CNT lengths as a function of processing, it is worthwhile to prefer CNTs with longer average lengths.

2.3.3 Influence of Process Parameters

The typical melt mixing or compounding parameters namely screw speed, barrel temperature, material throughput, screw configuration and the position of filler feed would have to be tailored to a specific thermoplastic polymer-CNT system in order to achieve the desired CNT dispersion quality for maximum composite performance [55,82,86]. As dispersion is a continuous mechanism influenced by the shear stresses generated by the viscous flow governed by these parameters, addressing their individual contribution is complicated. This section briefly outlines the individual effects and complementary influences these factors could have on the level of CNT dispersion from a processing perspective.

A higher screw speed would lead to increased specific mechanical energy (SME) of the process resulting in enhanced shear stresses and thereby dominant dispersion mechanism by rupture. A higher screw speed also would result in a decreased level of screw fill and a lower residence time for the melt in the extruder at a condition where the other parameters are kept constant. Higher screw speeds could also result in lower polymer viscosity aiding faster melt infiltration, but at the same time can result in polymer degradation and also negatively affect the aspect ratio of the CNTs [86]. Lower speeds on the other hand would act opposite to what has been detailed with significant limitation on the level of generated shear stresses. A higher screw speed was found to be helpful when employing matrices that are not known to be compatible with the CNTs like PS, PE, PP and while using CNTs with a high agglomerate strength in a wide scope of this dissertation.

Melt or barrel temperatures influence the melt viscosity of the polymer and thereby the level of infiltration and the magnitude of generated shear stresses for agglomerate

dispersion. Lower melt viscosities are highly recommended for faster and better infiltration of the CNT agglomerates while higher melt viscosities are important for enhanced shear stresses. The desired level of dispersion would determine the domination of the melt infiltration step or the creation of enhanced shear stresses for higher fragmentation numbers.

Low material throughputs would result in higher SMEs, lower screw fill, and higher local melt residence time compared to higher throughputs leading to improved filler dispersion quality with a trade-off on production volume. Throughput levels are also regulated by the feeding capacity of the nanomaterial feeder owing to very low bulk density of the CNT along with a very low volume fraction of filler feed.

An optimum screw design must be able to provide the desired level of SME for the pre-set extrusion parameters and is generally a combination of mixing, kneading and transportation elements. The magnitude of SME, the nature of the CNT agglomerates and the desired residence time of the melt in the extruder would dictate the screw configuration. The screw configuration should be designed keeping in mind of the other process factors. When a high speed is required for processing composites containing high agglomerate strength CNT, the screw design must be able to accommodate this process with a sufficient residence time to allow for other dispersion steps like wetting and infiltration. An enhanced residence time is bound to result in polymer degradation while shorter residence times may not provide the desired level of dispersion.

The position of filler feeding becomes important when dealing with CNTs. CNTs with enhanced intrinsic agglomerate strength like the Baytubes® C 150 P are recommended to be fed along with the polymer in the principle feeding port in order to allow for increased residence time for agglomerate dispersion. Side feeding of the filler Nanocyl^{TM} NC 7000 which has a lower agglomerate strength is recommended owing to its loosely packed agglomerate structure with better dispersion envisioned by a dominant melt infiltration [87].

The influence of the twin-screw process parameters on MWCNT dispersion in PP is presented in Chapter 4 while results in PS and PC also obtained in the wider scope of this work have been published elsewhere [55,82].

Though good primary filler dispersion is a pre-requisite for good macroscopic characteristics of the composite, widely employed secondary processing or finishing operations for nanocomposites like injection or compression molding also have a major role in regulating final composite properties. The thermo-mechanical history generated on the composites due to these operations has an effect on the level of primary CNT dispersion (created with the extrusion process). Compression molding results in the re-agglomeration of the previously dispersed CNTs facilitated by the reduction in the viscosity of the matrix at a specific process temperature, pressure and holding time. A network of re-agglomerated CNTs forms multiple conductive pathways in the polymer leading to good composite electrical properties, though theoretically one such pathway is sufficient for achieving conductive properties. Higher melt temperatures and longer holding times have been reported to result in lower electrical

percolation threshold and better composite conductivity [3]. It must however be remembered that the re-agglomeration of the dispersed CNTs could negatively affect the mechanical characteristics. Injection molding on the other hand is associated with a significant magnitude of secondary shear compared to the compression molding process resulting in filler orientation [5]. The temperature gradient existing between the low temperature mold wall and the high temperature melt results in the freezing of the outer core lowering the bulk conductivity of the composite [5]. Injection molding is widely preferred from an industrial perspective being a high volume manufacturing process and hence the tailoring of the process parameters to achieve good macroscopic characteristics of the composite becomes important. Villmow et al. recommend lower injection velocities to limit orientation effects and higher melt temperatures for good electrical conductivity of the composites [5]. Mold temperature and holding pressure had a minimal influence in their work. Elevated mold temperatures could minimize the effect of temperature gradient. Some variations in injection molding and compression molding parameters were also considered in the scope of this dissertation and will be discussed in Chapter 5.

2.4 Hypothesis

The excellent potential of CNTs as fillers for conductive composites, the complexities and the reasons preventing the achievement of good mechanical properties with CNT filled polymer matrices is outlined in the state of the art. Hence, the development of multifunctional composite with excellent electrical and mechanical properties with a bi-filler system of CNT and glass fibers respectively is sought after in this work. CNTs are expected to impart desirable electrical characteristics to the composite, while the proven ability of the glass fibers as fillers for mechanical reinforcements would be taken advantage of to give rise to enhanced mechanical properties of the composite.

As discussed earlier, CNT dispersion in thermoplastics is a challenge and even more challenging when a composite has to be produced from a polyolefin like PP which has a poor compatibility with CNTs. The unavailability of literature in understanding of the influence of twin-screw compounding parameters on the CNT dispersion morphology in polyolefins has to be addressed. Also, the quantifying relation on the effect of varying process parameters on CNT dispersion has to be established.

The issues relating to the poor compatibility between CNTs and PP would have to be addressed for enhanced CNT dispersion. Physical or chemical functionalization of the CNTs is predominantly employed in literature to adapt the surface properties of the CNTs to those of the polymer matrix, but inconclusive and contradicting reports from literature on the macroscopic properties of the CNT filled polymer composites adds to the complexity. In situ polymerization of polyolefins is a possibility, but is highly complicated as these reactions are carried out at very high pressures. Reducing the hydrophilicity of CNTs by graphitization to render it compatible with PP would facilitate better dispersion, but to carry out this process on large volumes of CNTs at very high temperatures does not make it economically viable.

Hence, any effort to tailor dispersion should come from simple strategies like enhancing the functionality of the polymer matrix, reducing the viscosity of the polymer melt etc. by the usage of dispersing and stabilizing additives preferably during processing.

With due consideration to what has been reported in literature, the first effort to enhance CNT dispersion in PP would have to evolve from understanding the mechanism of dispersion and the process parameters associated with a specific process that could result in optimum dispersion. Imparting high shear stresses during processing through higher screw speeds would contribute to agglomerate breakage and improve CNT dispersion in PP, but this could also negatively affect the aspect ratio of the CNTs. Lower melt viscosity would lead to better melt infiltration of the agglomerates, a pre-requisite for good filler dispersion and this could be influenced by employing higher extruder barrel temperatures. Alternatively, lower viscosity would reduce the magnitude of the applied shear stress on the agglomerates. Due to these contradicting effects and the fact that dispersion cannot be controlled by tailoring a single process variable, the process factors affecting the quality of MWCNT dispersion in a twin-screw compounding process have to be identified for its level of influence in CNT dispersion in PP. As each of the process variables have an individual effect on the level of CNT dispersion, the combined influence of all parameters derived from the SME input during processing will have to be correlated to the achieved filler dispersion morphologies.

The usage of peroxides as processing additives would lower the polymer's melt viscosity ensuring better melt infiltration. It would also enhance the polarity and lower the surface tension of PP, leading to improved melt wetting of the agglomerates. The conditions of improved melt wetting and melt infiltration which are pre-requisites for a good CNT dispersion in polymer matrices would be sufficiently satisfied with peroxide addition. Although the ability of peroxides to act as surface functionalizing agents for SWCNT is available in literature, it could create functional groups on the CNT surface. This is to be understood by carrying out in situ Raman measurements. CNT functionalization would present enhanced sites for polymer-CNT interaction, but peroxides could also negatively affect the mechanical characteristics of the composite. How possible enhancement in CNT dispersion and functionalization on peroxide addition could affect the mechanical, electrical and thermal properties of the composites have to be investigated. Certainly better CNT dispersion could lead to better electrical properties at extremely low filler contents as have been observed with thermosetting matrices, but mechanical property enhancements would still be sceptical owing to possible structural defects created on the CNTs due to functionalization.

Once, a PP-MWCNT composite with good MWCNT dispersion is achieved, glass fibers would be incorporated as secondary filler to these composites to enhance the mechanical properties of the composites. Their provenability to create substantially enhanced structural properties whilst rendering themselves suitable for conventional composite processing techniques would augur well in the development of a multifunctional composite.

3. Experiments & Characterization

3.1 Materials

As polymer matrix, *R352-08R*, a random co-polymer PP resin purchased from *Dow Chemicals* was used. It had a density of 0.9 g/cm^3 (ISO 1833) and a melt flow index of 8 g/10min (ISO 1133).

Nanocyl^{TM} NC 7000 (*Nanocyl S.A., Belgium*) was used as the source of MWCNTs. These MWCNTs had a carbon purity of > 90%, average length and diameter of 1.5 µm and 9.5 nm respectively, and a bulk density of 60 kg/m^3 according to the manufacturer [79]. Refer to Figure 4 for their morphologies.

PEROXAN BEC (*PERGAN GmbH, Germany*) is an organic peroxide. t-butyl peroxy-2-ethylhexylcarbonate is a liquid with a decomposition temperature of +60 °C.

Chopped glass fiber OCV 968/968A from *OCV reinforcements* were used as short fibers. The fibers had a compatible sizing for PP with a nominal diameter of 13 µm and an average length of 4.5 mm.

3.2 Processing

3.2.1 Compounding – Twin-screw Extrusion

PP and MWCNT were compounded on a *Leistritz ZSE 27HP – 52D* (*Leistritz GmbH, Germany*) extruder (Figure 6) with 13 barrels, screw diameter D of 27 mm and an L/D ratio of 52 to form PP-MWCNT composites. Two different feeding positions for MWCNTs were employed namely main feed (MF) where they were fed along with the polymer in the main hopper and the side feed (SF) where they were fed into the polymer melt at the L/D=16 position (Figure 7). In Chapters 5 and 7, the peroxide was premixed with PP in a rotating batch mixer and the mixture was fed into the main polymer feed. Chapter 7 deals with the addition of short glass fibers as secondary fillers for PP. Herein, the glass fibers were fed to the previously compounded PP-MWCNT masterbatch at the downstream (L/D=40 position) of the extruder to limit their potential aspect ratio damage.

Screw configuration, screw speed, material throughput and barrel temperatures were taken to be the process variables along with the feeding position of the MWCNT. The details of parameter variations employed in the experiments are indicated in the respective chapters. SME is an important parameter in extrusion given by the units of kWh/kg. It is a resulting measure of the energy going into the compounder per unit mass of the melt from the motor. According to *Leistritz*, it is calculated as:

$$SME = \frac{2\ x\ M_{max}\ x\ I\ x\ N}{9550\ x\ \eta_e\ x\ M} \quad (1)$$

Where M_{max}, I, N, η_e and M are maximum torque for one screw shaft (in Nm), motor current (in %), screw speed (in rpm), gear drive efficiency, and throughput (kg/h) respectively.

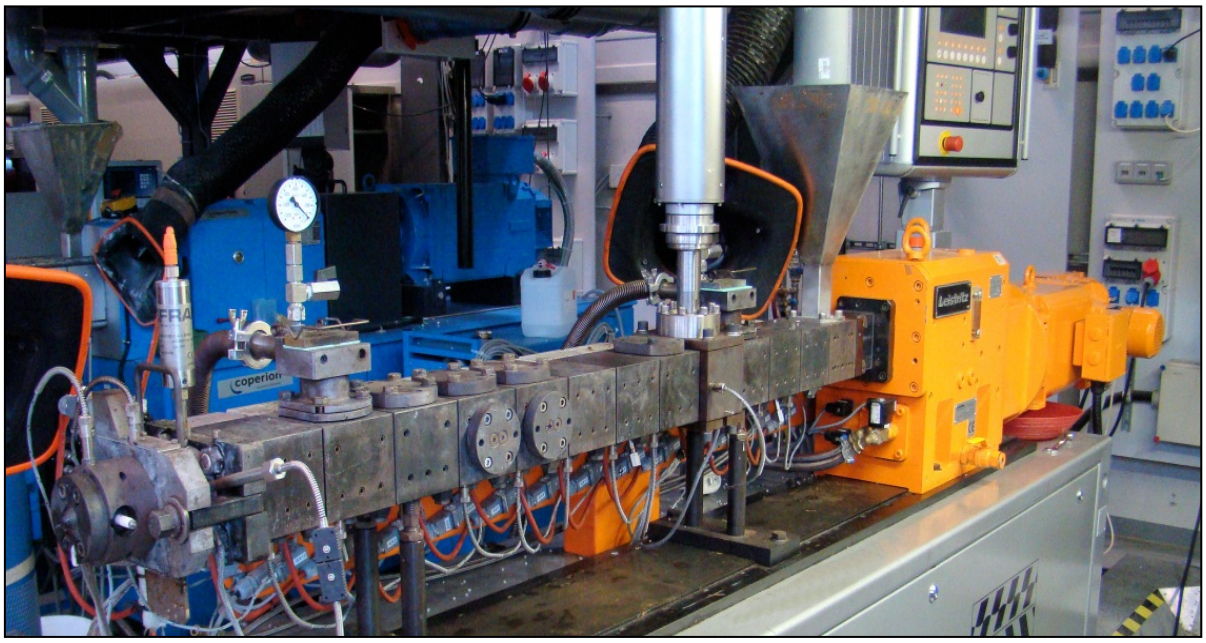

Figure 6. Twin-screw extruder

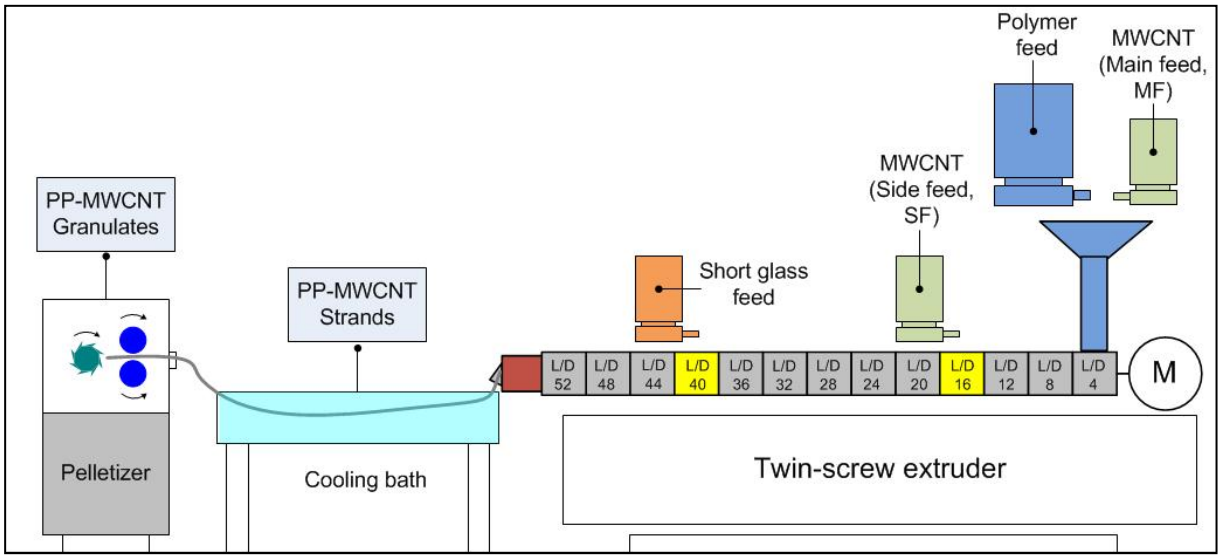

Figure 7. Illustration of different feeding positions in the twin-screw extruder

3.2.2 Compression Molding

Compression molding of extruded granulates was carried out on a *Collin P 200/M* (*Dr. Collin GmbH, Germany*) compression molding machine. Part geometry of 60 x 10 x 1 mm^3 was produced with optimized conditions listed in Table 1. The electrical conductivity of the composites processed by cooling of the sample in the mold at rates of 10 K/min and 30 K/min in Stage 5 of compression did not show any differences in comparison to samples cooled by quenching in water (molding stopped with Stage 4); thus the latter approach was adopted to minimize the cycle time.

Table 1. Compression molding parameters

Stage	1	2	3	4
Temperature (°C)	220	220	220	220
Pressure (bar)	1	15	25	100
Holding Time (min)	5	1	1	4

In Chapter 5, to study the variation of compression molding parameters on the electrical properties of PP-MWCNT composites, a mold temperature of 240 °C in all the four stages and a holding time of 2 min in the last stage were additionally employed.

3.2.3 Injection Molding

Extruded granules were injection molded into specimens for tensile testing (according to ISO 527-1), impact testing (ISO 179-1/1eA) and electrical measurements on an *Engel ES 200/60 HL ST I* (*ENGEL, Austria*) injection molding machine. The specimens for electrical measurements were cut out from the gauge length of the tensile bars and had dimensions of 50 x 10 x 4 mm^3. The reference samples and the composites were dried at 80 °C for 4 hours before injection molding. Optimized injection molding parameters employed for producing the composites in Chapter 5 is given in Table 2. In Chapter 7, the back pressure was increased to 60 bar and the mold temperature was set at 45 °C to accommodate the effective processing of glass as secondary filler.

Table 2. Injection molding parameters

Parameters	
Holding Pressure (bar)	80
Holding Time (sec)	30
Injection Pressure (bar)	150
Injection speed (mm/s)	3x25,2x20,5x15
Cooling Time (sec)	20
Back Pressure (bar)	14-20
Screw Speed (rpm)	150
Mold Temperature (°C)	30
Melt Temperature (°C)	225

3.2.4 Small Scale Melt Mixing

In order to be able to study the MWCNT concentration at which the composites exhibit their electrical percolation threshold, extruded composites in Chapter 5 were subjected to melt mixing using a small scale melt mixer *MiniLab Haake Rheomex CTW5* (*Thermo Scientific, Germany*) to dilute them to lower MWCNT concentrations. This mixer had a chamber volume of 7 cm^3 and the composites were diluted at 220 °C and 100 rpm.

3.3 Characterization of the Composites

An overview of the characterizations that have been carried out on the composite samples in various forms arising from different processing steps is depicted in Figure 8.

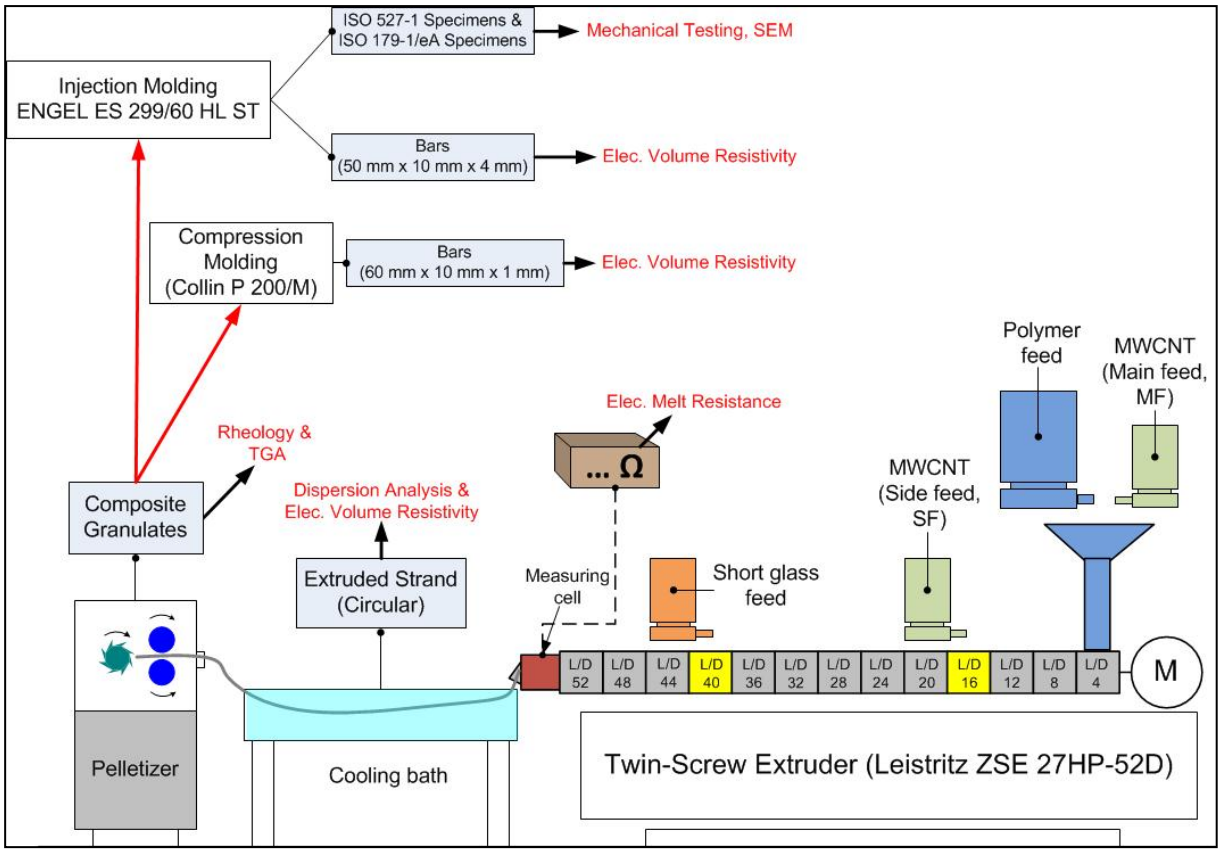

Figure 8. Overview of characterizations and the nature of the tested composite forms

3.3.1 Morphological Investigations

The morphology of the extruded strands was investigated using optical microscopy. Thin slices of 5 µm thickness were cut perpendicular to the direction of extrusion on at least 6 different strands at room temperature on a microtome (*R. Jung, Germany*) with a diamond knife. Imaging was done using 10x magnification objective lens of a *BRESSER Science TRM-301 Transmission microscope* (*Meade Instruments Europe GmBH & Co.KG, Germany*) fitted with a *BRESSER Microcam*. A minimum of 6 mm^2 micrograph area was investigated for every sample. Image analysis was performed using macros developed in-house with *Image J* software version 1.44o. The area fraction of undispersed MWCNT agglomerates (A_f) defined as the area of the undispersed MWCNTs to the overall micrograph area was quantified.

Agglomerates having an area < 20 μm^2 or circle equivalent diameter < 5 µm were ignored according to ISO 18553:2002 (*Method for the assessment of the degree of pigment or carbon black dispersion in polyolefin pipes, fittings and compounds*).

Scanning Electron Microscopy (SEM) were carried out on cryofractured injection molded bars (Chapter 7) using *Zeiss SUPRA 55 VP* microscope (*Carl Zeiss GmbH*, *Germany)*. Samples were sputter coated with Gold-Palladium for 120 s at 0.05 mbar and 40 mA on a *Cressington 208HR Sputter Coater* (*Cressington Scientific Instruments Ltd*., *United Kingdom*). As-received MWCNTs without any sputter coating were examined additionally.

3.3.2 Measurement of Electrical Properties

As there was a limitation of the measuring equipment to measure the entire range of electrical volume resistivities, two different measuring sources were employed. Low resistivity measurements (< 10^6 Ωcm) were carried out as a 4-probe measurement on a *FLUKE 8846A Digital Multimeter* (*FLUKE*, *Germany*) while higher volume resistivities (> 10^6 Ωcm) were measured using *4339B High Resistance Meter* (*Agilent Technologies*, *Germany*) as 2-probe measurements.

Measurements were made on at least five injection molded bars (50 x 10 x 4 mm^3) or on at least three compression molded bars (60 x 10 x 1 mm^3) without any sample surface tuning. Contact points were created using silver conductive paint (*RS Components Ltd., United Kingdom*). Samples were conditioned for 24 hours at 23 °C and 50 % relative humidity before measurements.

The electrical properties of extruded strands were measured as 4-probe measurements similar to those employed on injection molded and compression molded composites. Extruded strands were approximated to have a circular cross section.

Melt resistance measurements during processing are recorded with the *FLUKE 8846A Digital Multimeter* as a continuous function of time. This also served to assure the quality of the composites produced. The approach is detailed in Appendix A.

3.3.3 Measurement of Mechanical Properties

The notched impact strength of the injection molded specimens was evaluated using ISO 179-1/1eA norm on 10 samples with the help of a *CEAST Resil Impactor* while tensile properties were evaluated with ISO 527-1 standard on at least 5 samples on a *Universal testing machine Inspekt Table 50KN* (*Hegewald & Peschke, Germany*). The samples were conditioned at 23 °C and 50 % RH for 24 hours before testing.

3.3.4 Determination of Thermal Stability

Thermo Gravimetric Analysis (TGA) was performed in air atmosphere (25 ml/min) on *TGA Q5000* (*TA Instruments, USA*). 10-12 mg of the extruded granulates were placed in a platinum pan and heated from room temperature to 120 °C at 20 °C/min, kept under isothermal conditions for 10 minutes and thereafter heated at 10 °C/min to 700 °C. The onset

of decomposition (T_o) (temperature at 5 % weight loss) and temperature of maximum weight loss (T_{max}) (temperature from the inflexion point of dw/dT) were obtained.

3.3.5 Rheological Characterization

Melt rheology measurements were carried out under nitrogen atmosphere on *Rheometer MCR 501* (*Anton Paar, Austria*) equipped with a conventional temperature device CTD 450 in a parallel plate configuration on extruded granulates. The upper measuring plate had a 10 mm diameter and the measuring gap was maintained between 1-2 mm. Increasing frequency sweeps from 0.1 to 100 rad/s were carried out at 220 °C after equilibration. The strains were always checked to be within the linear viscoelastic limit.

3.3.6 Contact Angle Measurements

Contact angles for PP and peroxide modified PP (PP-Px) were evaluated using water (hydrophilic) and diiodo-methane (hydrophobic) as solvents on a *Drop Shape Analysis (DSA)* system (*KRÜSS GmbH, Germany*). Owens-Wendt-Rabel-Kaelble (OWRK) approach was used to calculate the surface tension from the contact angle values and the known solvent parameters from the data of at least 3 measurements.

3.3.7 Differential Scanning Calorimetry

Differential Scanning Calorimetry (DSC) measurements were carried out on 8-10 mg samples in nitrogen atmosphere (50 ml/min) on *DSC Q1000* (*TA Instruments, USA*). Samples were placed in hermetic aluminum pans. First heating cycle involved heating of the sample from room temperature to 200 °C and holding it at isothermal conditions for 5 minutes to remove any thermal history due to processing. The sample was cooled down to room temperature after which second heating was carried out similar to the first heating regime. Heating and cooling rates were 10 °C/min. The melting temperature (T_m) and the enthalpy of melting (ΔH_m) were measured. The crystallinity (X_c) is given by:

$$X_c\ (in\ \%) = \frac{\Delta H_m}{\Delta H_{mp}} * \frac{100}{(1 - W)} \qquad (2)$$

Where ΔH_{mp} is the enthalpy of fusion of 100% crystalline PP and is taken to be 209 J/g [88] and W is the weight fraction of the filler.

3.3.8 Raman Spectroscopy

The effects of peroxide addition on PP-MWCNT composites were studied in detail with the help of Raman spectroscopy in Chapter 6. This characterization was applied both in situ during small scale melt mixing and on the extruded composites. In situ monitoring of the melt mixing reaction using Raman spectroscopy has been reported for first time in the scope of this work. Raman spectroscopy probe *Dispersive Raman RXN1* (*Kaiser Optical Systems Inc*., *USA*) was placed in the back flow channel of the melt mixer. A 785 nm laser source was used and data for 5 accumulations were gathered for a 10 second exposure time with a laser power of 150 mW every second minute of mixing. The experiments were repeated at least 3 times to check the reproducibility of the spectra. The spectroscopy probe was calibrated

before every measurement. As-received MWCNT powder and extruded composite strands were also measured with identical parameters. Baseline corrections of the spectra were made with *RAMalyze software* (*LabCognition Analytical Software GmbH & Co. KG, Germany*) and the averaged and normalized spectra (to the D peak of the MWCNT) are presented. The schematic of the melt mixer and the position of the Raman probe are shown in Figure 9.

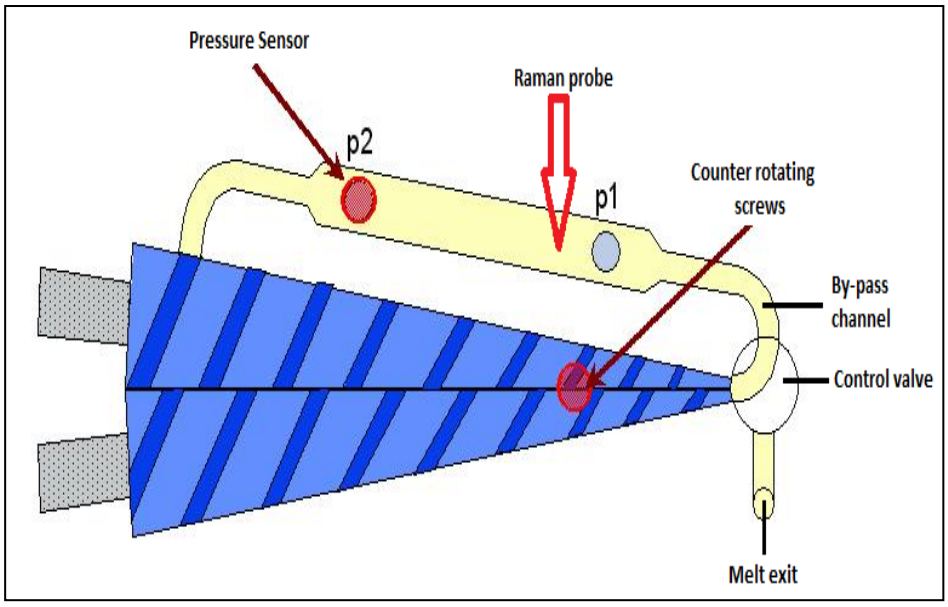

Figure 9. Online Raman spectroscopic investigation – Experimental setup

3.3.9 Dynamic Mechanical Analysis

Dynamic mechanical analysis (DMA) of the nanocomposites was measured on a *Rheometric Scientific ARES* (*TA Instruments, New Castle, USA*) in tension mode on at least four injection molded bars (50 x 10 x 4 mm^3). Vibration frequencies of 1, 10 and 100 Hz were employed for a temperature sweep from -80 to 100 °C with a heating rate of 1 °C/min. The glass transition temperature (T_g) was determined from the point of inflexion of the Tan Delta curve.

4. Optimization of Compounding Parameters for Enhanced MWCNT Dispersion in PP

When employing MWCNTs without any surface functionalization due to economic considerations it becomes important to optimize the composite production approach by understanding the processing parameters to achieve good filler dispersion in the polymer. This would eventually lead to improved macroscopic properties at much lower filler loadings or in other words at a lower CNT percolation threshold. Considering the fact that twin-screw compounding is one of the most commonly employed approaches for large scale processing of thermoplastic composites, optimization of a large number of process variables are required to establish an optimum working regime.

This chapter is primarily dedicated to understand the influence of process parameters on a twin-screw extruder on the dispersion of MWCNTs in PP by employing a design of experiments (DoE) approach. An initial screening was performed for determining the best processing conditions for optimum MWCNT dispersion by varying the processing speed, throughput and extruder barrel temperature for a fixed screw design at varying MWCNT concentrations. The analysis of the process is reported in terms of relative correlations of the area fraction of the undispersed MWCNT agglomerates from the optical micrographs and resulting volume resistivities of the extruded strands with consideration to the SME input. With the means of a novel measurement technique, the resistance of the melt measured online is correlated with the offline measurements in order to get an insight of composite volume resistivities during the processing stage. Projections are drawn from the DoE approach for the values of SME and A_f that would arise by employing a combination of varying operating parameters. Once the optimum working regime was identified with the DoE approach for the principal extruder parameters, the screw configuration was varied to investigate its effect on MWCNT dispersion and electrical properties of the composite. Compression molding was carried out under identical conditions as a secondary processing step in order to study the effect of primary dispersion state on the electrical resistivity of the composites. Finally, the effect of different MWCNT feeding positions on the level of dispersion and the final composite properties were investigated on both the injection molded and compression molded composites processed with optimized process conditions.

The processing conditions were designed by using the DoE software MODDE 8.0 as a four factor and three level experiment. In the Screening Experiment (SE) a “Standard Screw” configuration was used to study the influence of processing speed, temperature and throughput at varying MWCNT contents for responses of SME and A_f. The Mainstream experiment (ME) was carried out with two different screw designs described here as “Soft Screw” and “Aggressive Screw” to study the influence of screw configurations for selected samples from SE. The DoE plan for the screening and the mainstream experiments is presented in Figure 10. Samples from the screening experiments are labeled with a suffix ‘S’ while the ones for mainstream experiments are labeled as ‘E’. Figure 11 shows the screw

configuration adopted for the SE & ME. The incorporated variations in ME from that of the SE are highlighted. The nomenclature for the different screw elements are given in Appendix B.

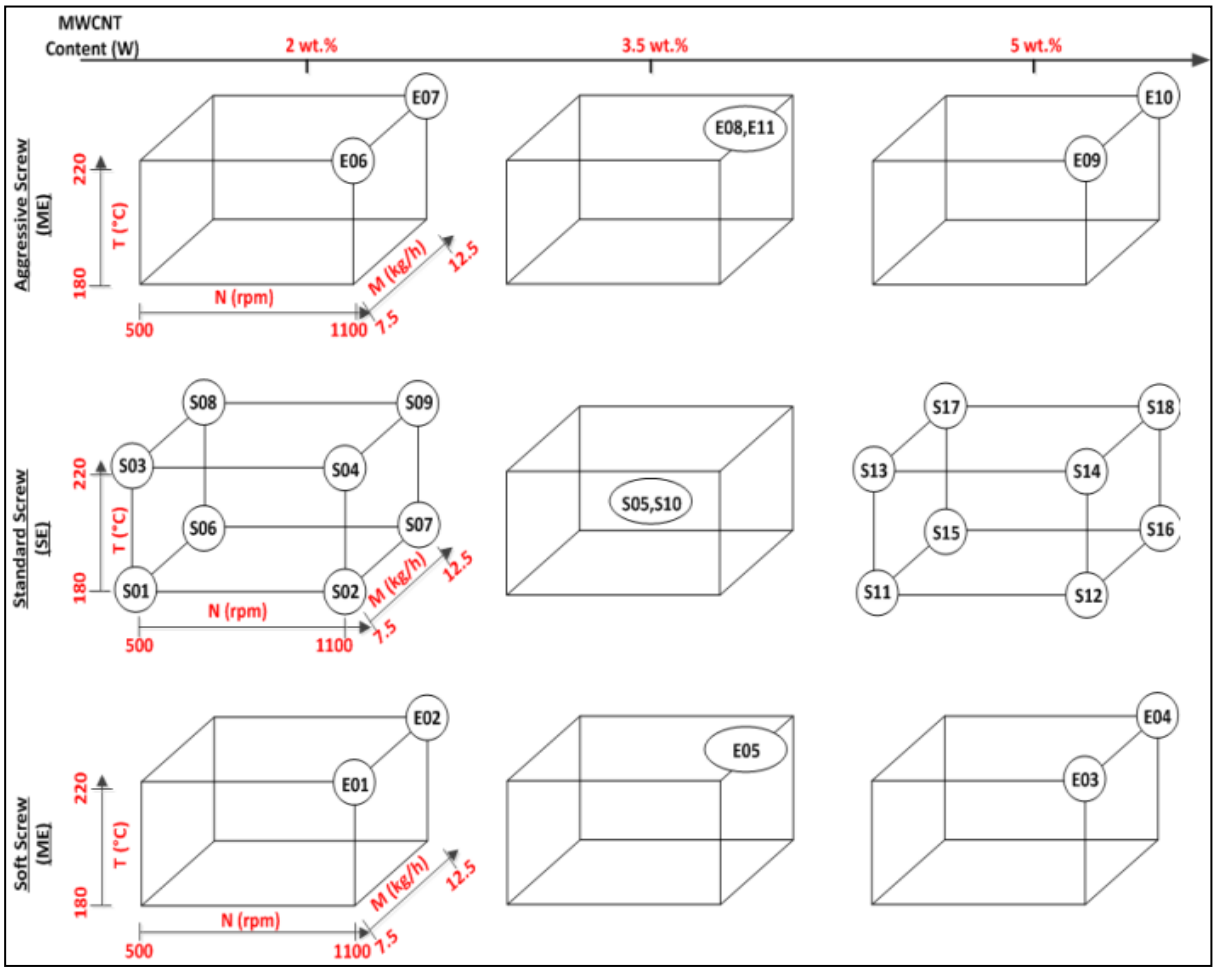

Figure 10. DoE plan for the processed composites

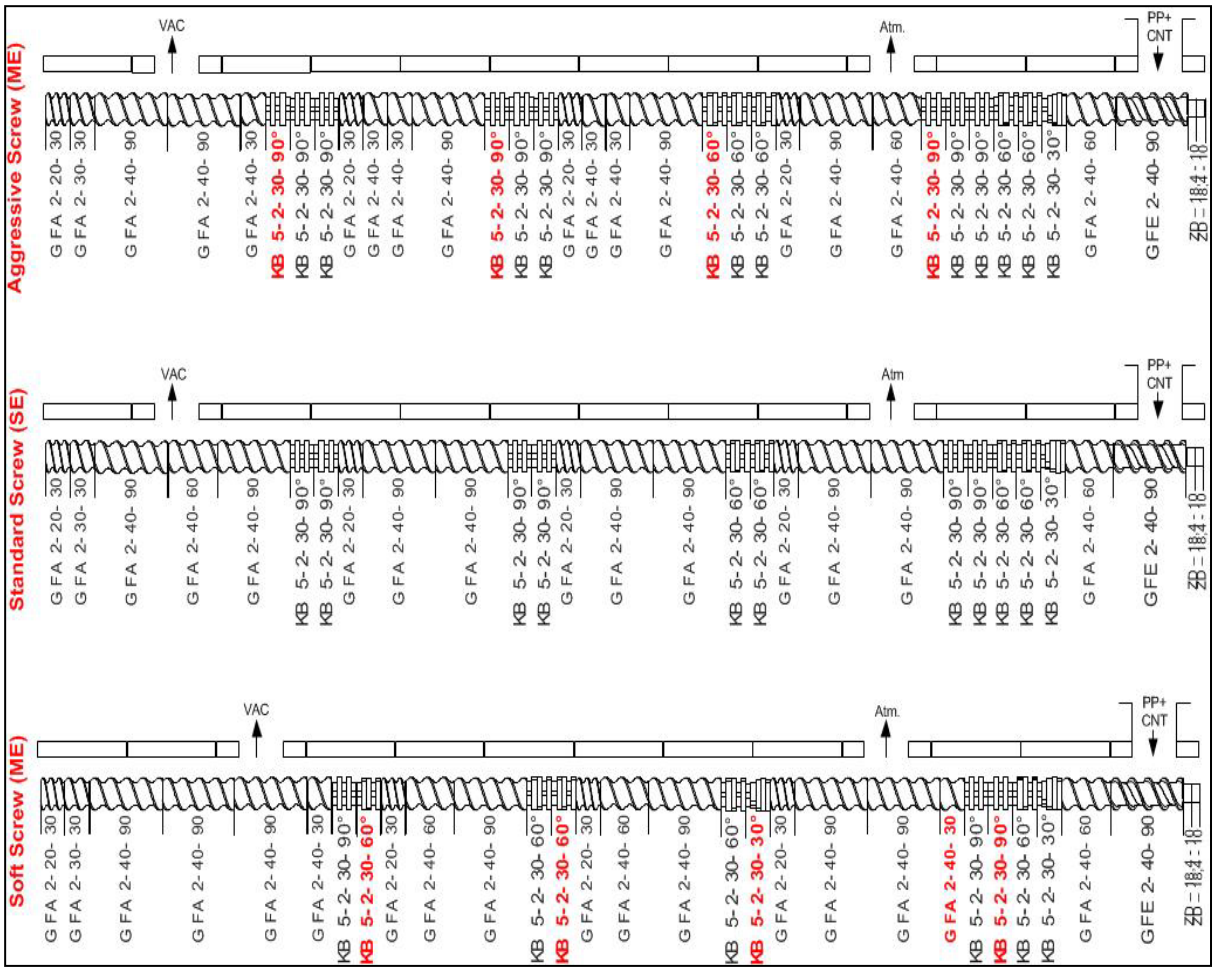

Figure 11. Screw configurations employed for the SE and ME

4.1 Screening Experiment (SE)

4.1.1 Electrical Volume Resistivity of the Extruded Composite Strands

The variation of volume resistivity as a function of process parameters for different MWCNT loadings is presented in Figure 12. Increase in MWCNT content from 2 to 5 wt.% and the screw speed from 500 to 1100 rpm seems to have had the biggest impact on volume resistivity of the composite. Sample S04 (containing 2 wt.% MWCNT and processed at 1100 rpm) shows volume resistivity 12 orders lower than sample S03 (containing 2 wt.% MWCNT and processed at 500 rpm) by virtue of its exposure to a higher processing speed. This holds high significance considering the fact that sample S14 (containing 5 wt.% MWCNT and processed at 1100 rpm) processed similar to S04 exhibits lower resistivity only by a factor of 10. This observation is critical from the perspective of the cost of the final product, as the desired electrical properties can be achieved at 3 wt.% lower MWCNT content.

The dispersion of CNT in a polymer matrix is governed by the mechanism of erosion or rupture/shatter determined by the fragmentation number discussed in Section 2.3.1. Higher processing speeds result in increased local shear forces resulting in enhanced contribution to dispersion by rupture or shattering mechanisms compared to processing at lower screw speeds, at conditions of constant throughput and temperature. Higher shear forces

generated as a result of high speed processing dominates the agglomerate dispersion compared to the slightly longer residence times that would have been on offer at lower processing speeds. Hence, higher screw speed is probably the ideal solution to achieve improved dispersion in cases where there is a poor compatibility between the matrix and the CNT; however with a prospective compromise of reduced MWCNT aspect ratio.

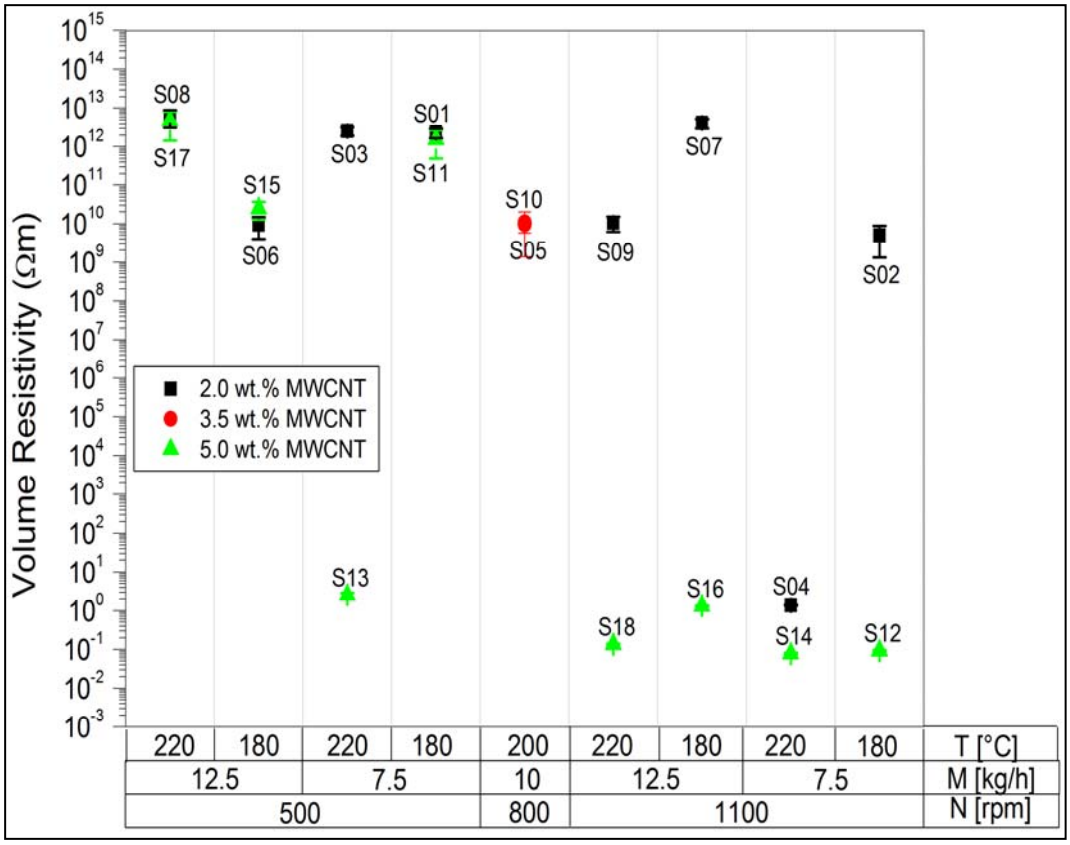

Figure 12. Dependence of electrical volume resistivity on process parameters

At a defined screw speed and material throughput, high melt temperatures (and consequently lower melt viscosity and shear stresses) facilitate better wetting and infiltration of the MWCNT agglomerates by the polymer melt in the initial zones of the extruder which could result in better dispersion dominated by the mechanism of erosion. On the contrary, lower melt temperatures (and higher melt viscosity and shear stresses) would have the trade-off of poor infiltration but a varied dispersion mechanism through agglomerate rupture. Although rupture and erosion co-exist, the domination of one over the other determines the composite morphology on the nanoscale and consequently the electrical properties. The sample S04 (containing 2 wt.% MWCNT and processed at 220 °C) unlike S02 (containing 2 wt.% MWCNT and processed at 180 °C) shows lower resistivity. Lower melt viscosity could have potentially resulted in better melt infiltration with minimal damage to the aspect ratios of the CNT. Considerations on the SME and the quality of dispersion of these composites are discussed in due course. All composites with 5 wt.% MWCNT content and processed at 1100 rpm shows volume resistivities not significantly different from S04 (a composite containing 2 wt.% MWCNT and processed at 1100 rpm).

4.1.2 Morphology of the Composites

SME values which are derived from the effect of varying processing conditions throw significant light on the amount of energy that the composite would have experienced in its melt. It is seen from Figure 13 that the SME values of samples S04 and S02 containing 2 wt.% MWCNT are 0.96 kWh/kg and 1.28 kWh/kg respectively. Correlating these numbers to the volume resistivities discussed previously, higher SME of the S02 sample could have resulted in better dispersion quality than that of the S04 sample. Figure 14 augments this fact by showing S02 and S04 have an A_f of 2.9 % and 3.6 % respectively. This comprehensively explains the fact better dispersions might not suffice in certain cases for good conductivities as enhanced nanotube separation distances leads to increased electron tunneling distance [89], which is destructive to the formation of a conductive pathway. On the other hand high SME input could have resulted in CNT breakage thereby reducing the aspect ratio of the MWCNT and negatively affecting the electrical properties. Although the S13 sample (containing 5 wt.% MWCNT) shows an extremely poor dispersion with an A_f of 11.9 %, it is the only sample presenting a very low volume resistivity value in the regime of 500 rpm processing (Data from Figures 12 & 14). This goes on to indicate that the poorest of dispersions could also result in improved electrical properties because of high probabilities of conductive network formation by co-joined agglomerates. The above discussions lead to a stage which indicates that electrical properties of the composite cannot be quantitatively defined just by assigning numbers to the quality of dispersion. The representative optical micrographs of a few nanocomposites are presented in Figure 15.

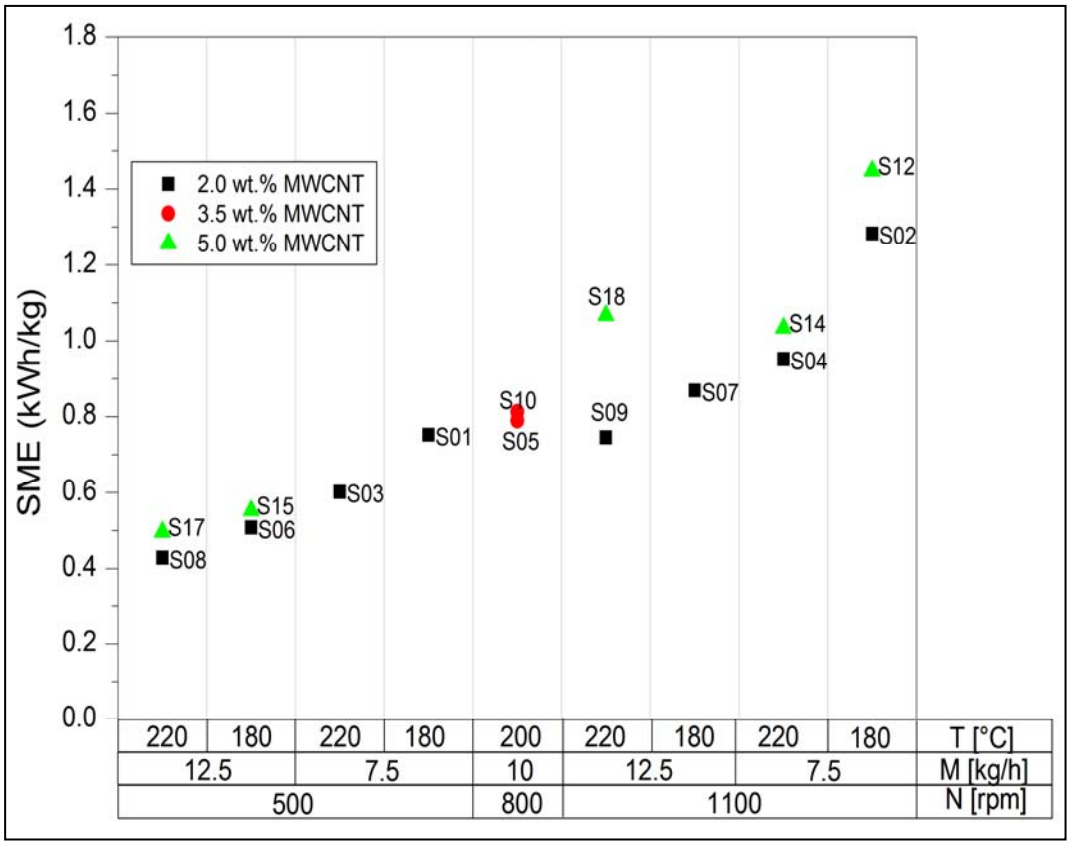

Figure 13. Dependence of SME on process parameters

Observations from Figures 13 and 14 show substantial reductions in MWCNT A_f with higher SME values. The observations from Figures 12-14 indicate that a specific level of dispersion accompanying every processing condition determines the range of conductivities that could be achieved with specific CNT loadings. Henceforth the discussion on MWCNT percolation for conductivities would be appropriate when they are described in terms of principal processing parameters at specified MWCNT contents rather than at different loadings of MWCNT with similar processing conditions. Also, samples S05 and S10 both containing 3.5 wt.% MWCNT and processed with identical conditions on different days are plotted in Figures 12-14 to demonstrate the repeatability of the process and reproducibility of the results.

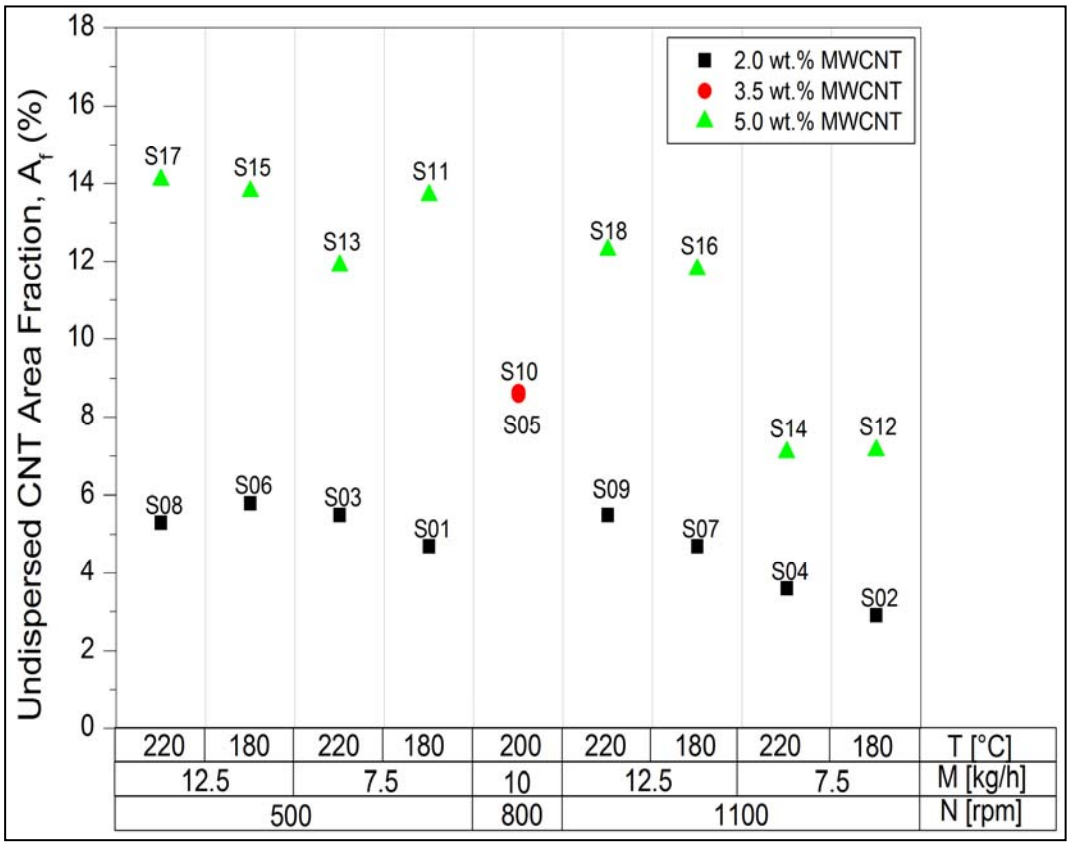

Figure 14. Dependence of A_f on process parameters

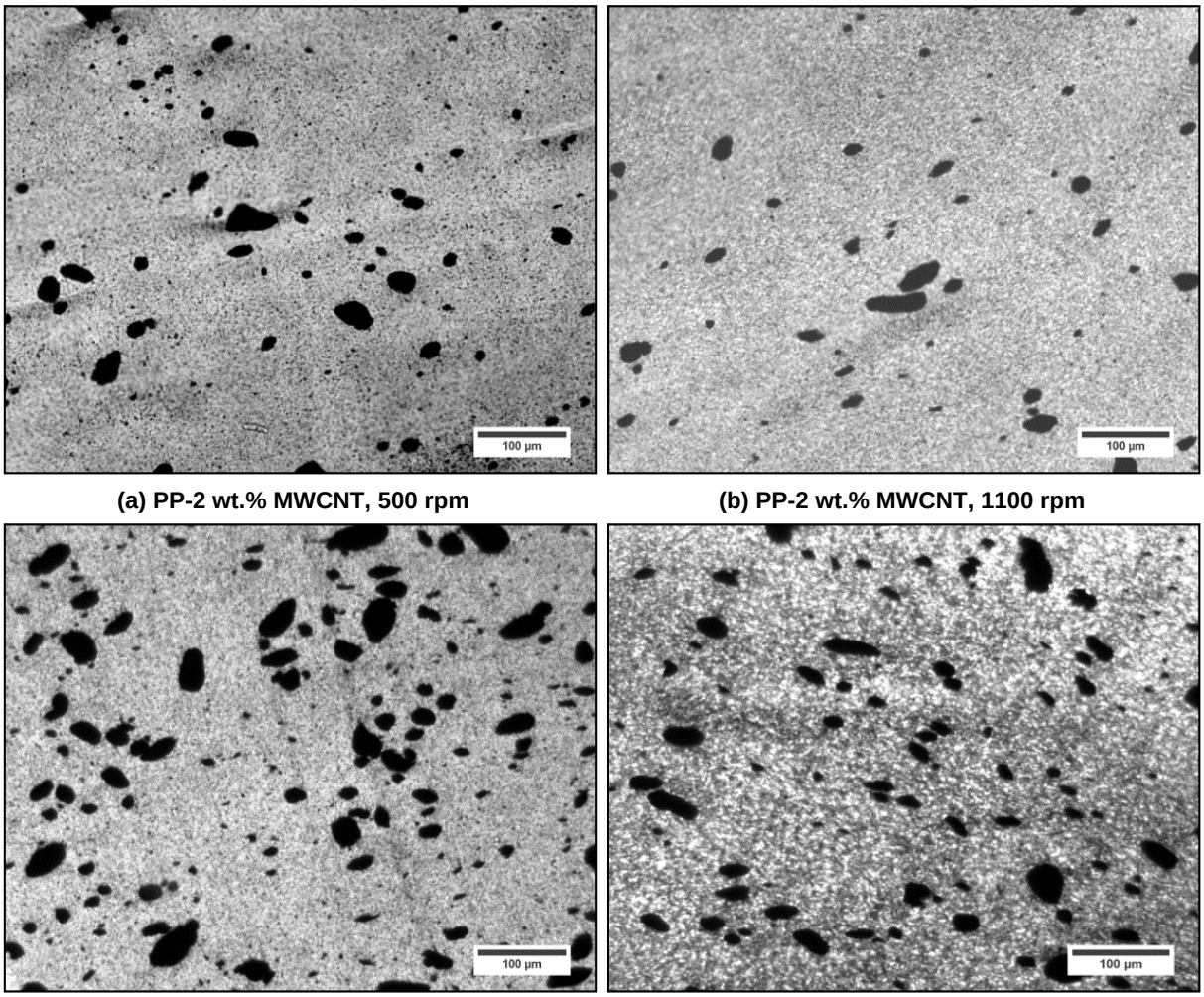

(a) PP-2 wt.% MWCNT, 500 rpm **(b) PP-2 wt.% MWCNT, 1100 rpm**

(c) PP-5 wt.% MWCNT, 500 rpm **(d) PP-5 wt.% MWCNT, 1100 rpm**

Figure 15. Optical micrographs of composites processed at 220 °C and 7.5 kg/h

4.1.3 Correlation between Online and Offline Electrical Measurements

Observations from the melt resistance measurements are plotted in Figure 16. This is significant because it helps to monitor the process and predict prospective conductivities of the composite. As the regime for the conductive composite melt resistances could be tracked, this was quite useful in determining the range of operation for the mainstream experiment. A comparison of the volume resistivity observed on the strands and the resistance of the melt is presented via Figure 17. This is a plot of samples on which melt resistance measurements were possible. The volume resistivity (Ωm) trend observed on the strands correlates well with the observed melt resistance (Ω) on the logarithmic scale and the step variation is more pronounced in the conductive regime (samples having volume resistivity < 10^6 Ωm). Also, the CNT feeder must feed extremely low volume of material over a prolonged period of time and hence fluctuations in the rate of feeding were expected. Hence, these online measurements served as a valuable tool to ensure the quality of the produced composites.

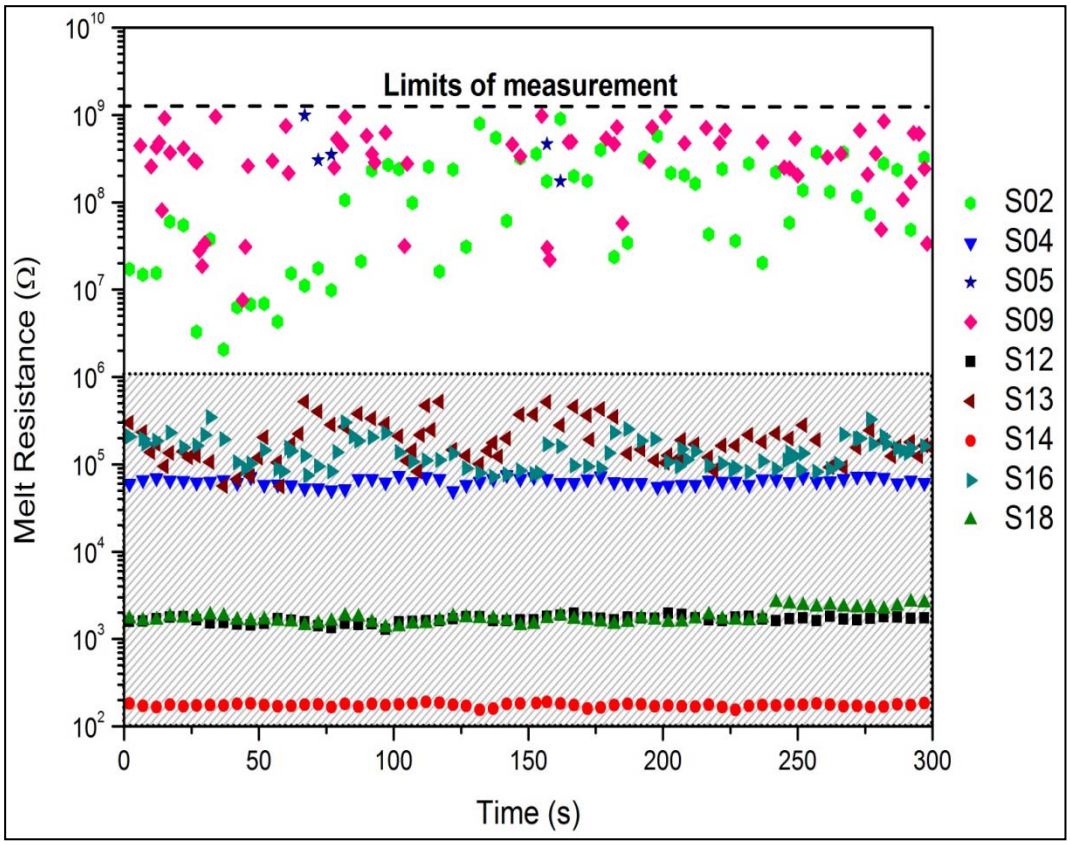

Figure 16. Observations of melt resistance for composites processed in SE

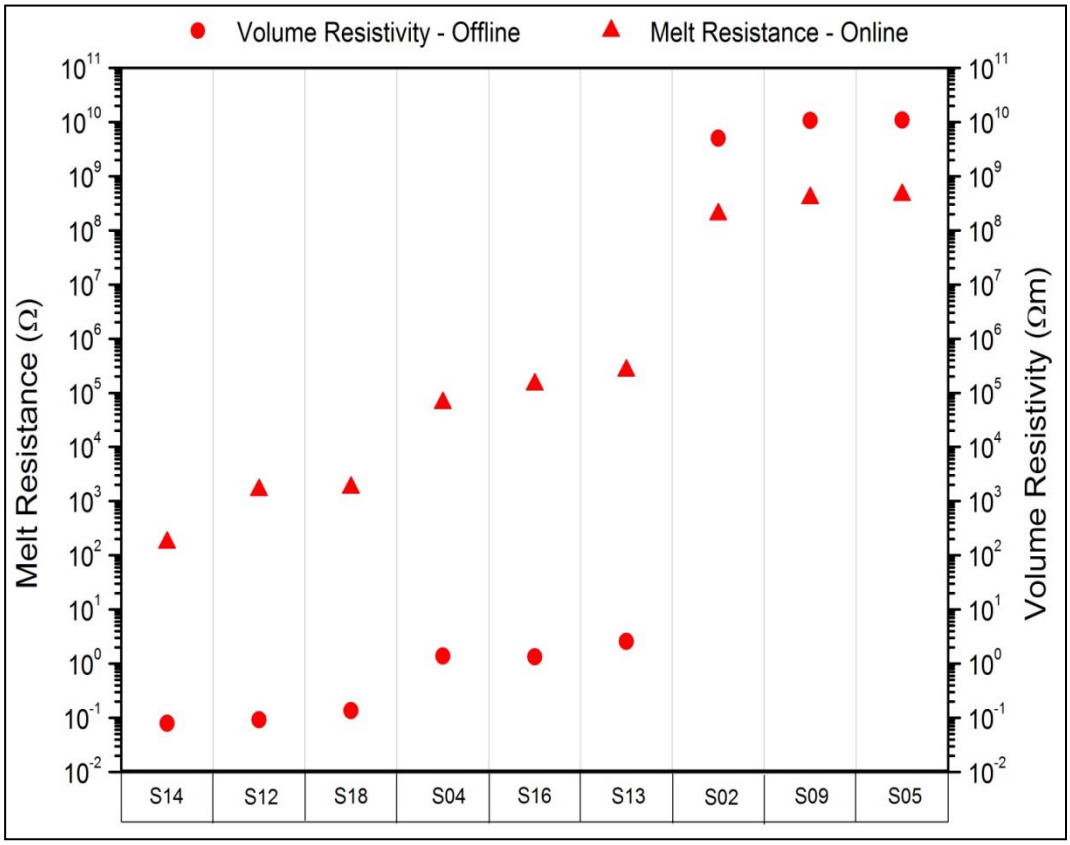

Figure 17. Online and offline electrical measurements – Correlation

4.1.4 Design of Experiments - Analysis

The summary of fit for SME and the A_f which were chosen to be the responses of the employed process parameters is presented in Figure 18. R2 is a measure of how well the model fits the data, Q2 gives a measure of how well the model predicts new data, model validity gives a measure of lack of fit and reproducibility gives variation of the response at the center points compared to the total variation of the response.

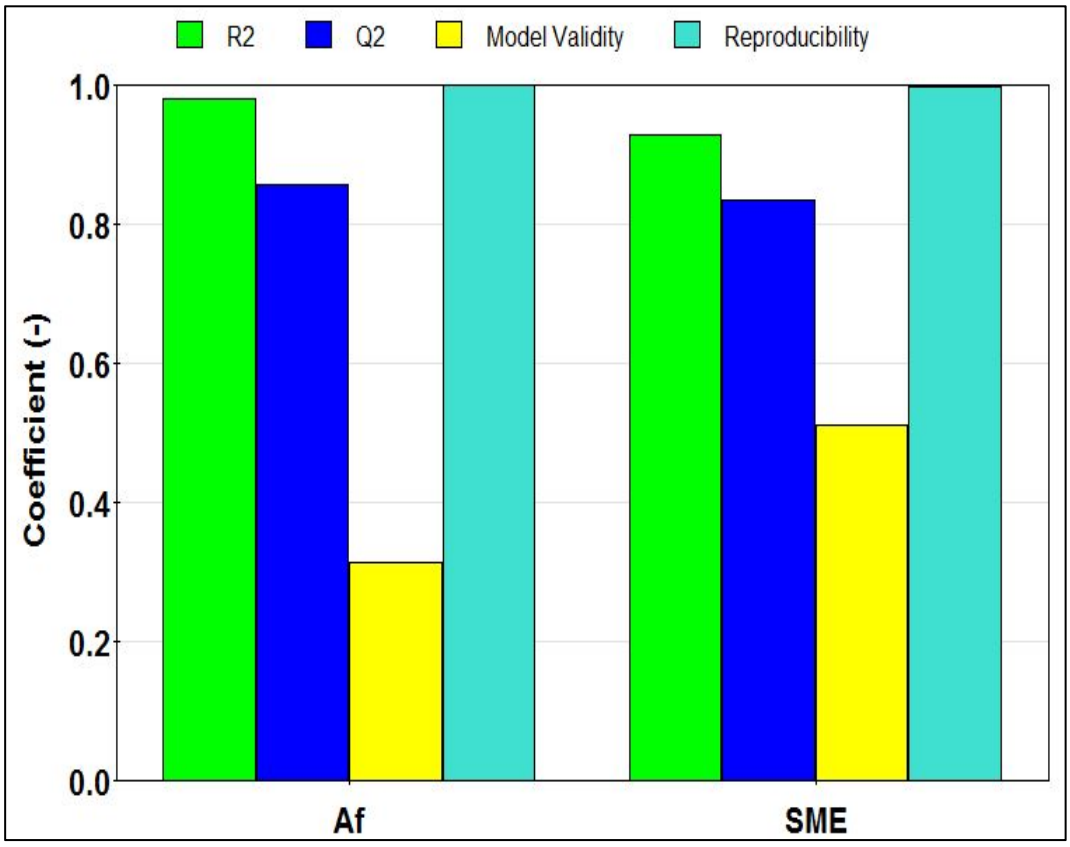

Figure 18. Summary of DoE fit for SME and A_f

Excellent measures of R2 and Q2 for both SME and A_f indicates that the data fits the model very well and this model could significantly predict new data. As the model validity in both cases is greater than 0.25, the model has no lack of fit or in other words the model error is in same range as the pure error. As excellent R2 and Q2 are visible with a reproducibility factor of 1, the lack of fit is considered to be highly artificial. This is why not so high values of model validity are observed. With the model fitting the experimental data well, the outcomes of this experiment could be used to effectively predict the SME and A_f values as a function of the 4 design factors in other operating regimes within the upper and lower limits of the conducted experiment (Figure 19). This could potentially serve as a guideline for future experiments on the same extrusion line with the same material combination to tailor the electrical properties of the composite.

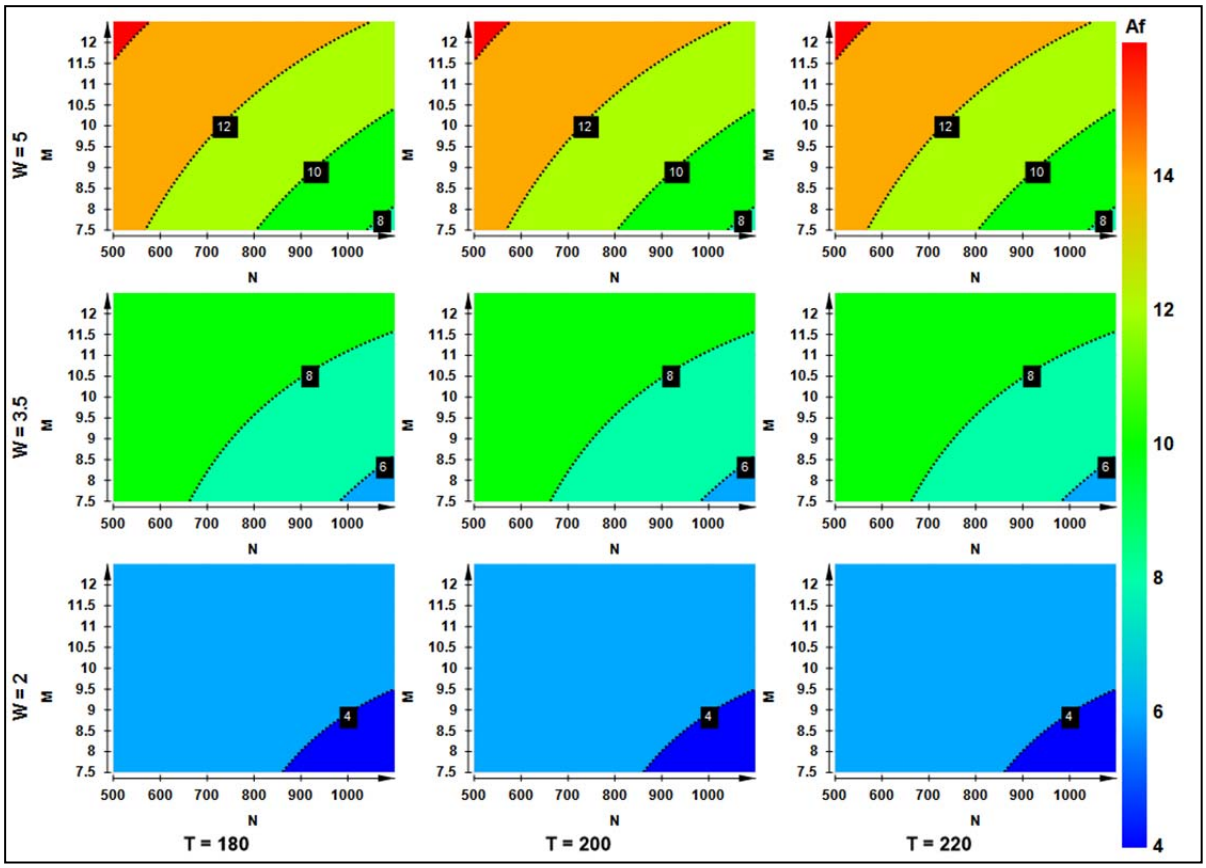

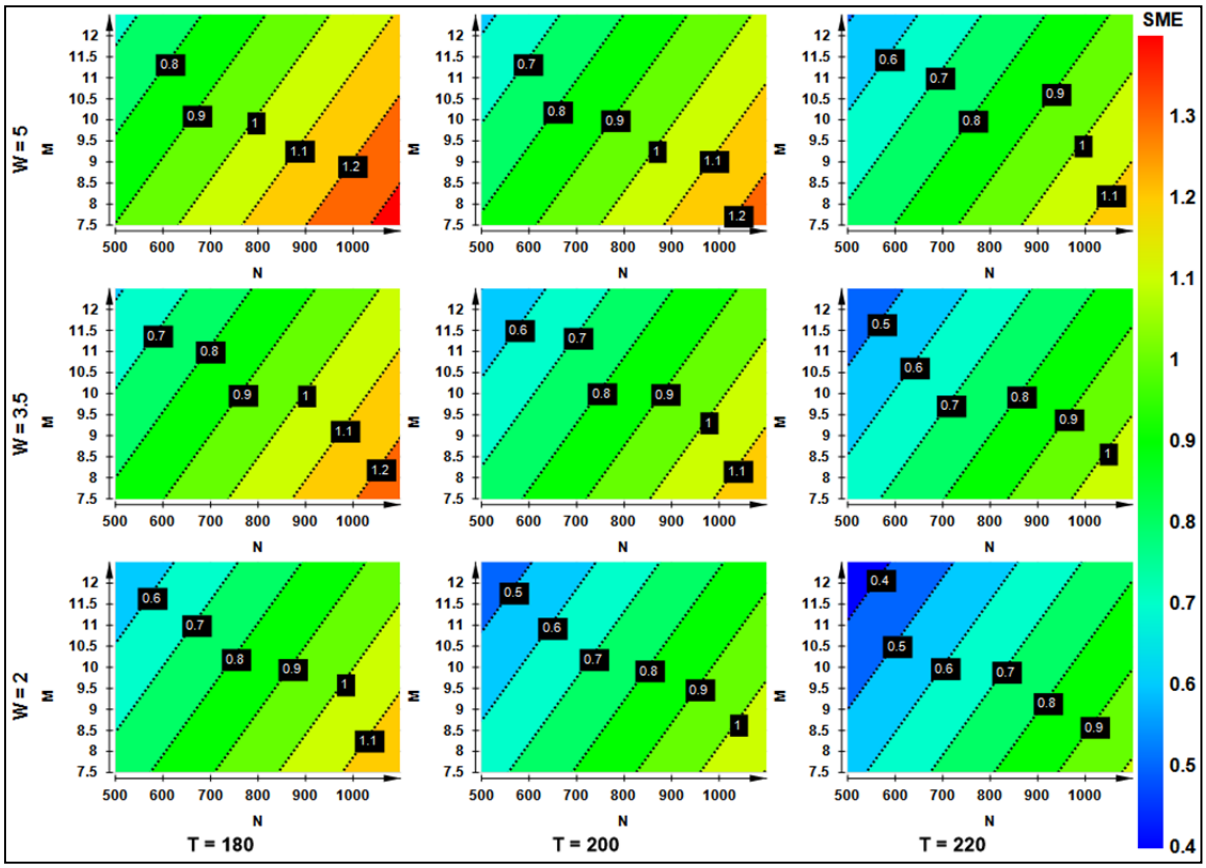

Figure 19. DoE predictions for SME

The co-efficient plot in Figure 20 illustrates the effect of participating design factors on the level of response. The size of the coefficient represents the change in the response when a factor is varied from its minimum to maximum (or 0 to 1 in coded units), while the other factors are kept at their average. It is observed that the increase in speed (N) from 500 to 1100 rpm had the single largest effect in causing a reduction of A_f, while the increase in MWCNT content (W) significantly contributed to higher A_f as expected. Lower throughputs (M) are beneficial for better dispersion quality owing to increased local residence time of the melt. The extruder barrel temperature (T) had no significant effect on A_f and the interaction factors show little influence in affecting the A_f. On the other hand, the increase in speed had the single largest effect in increasing the SME while higher throughputs and barrel temperature had lowered the SME.

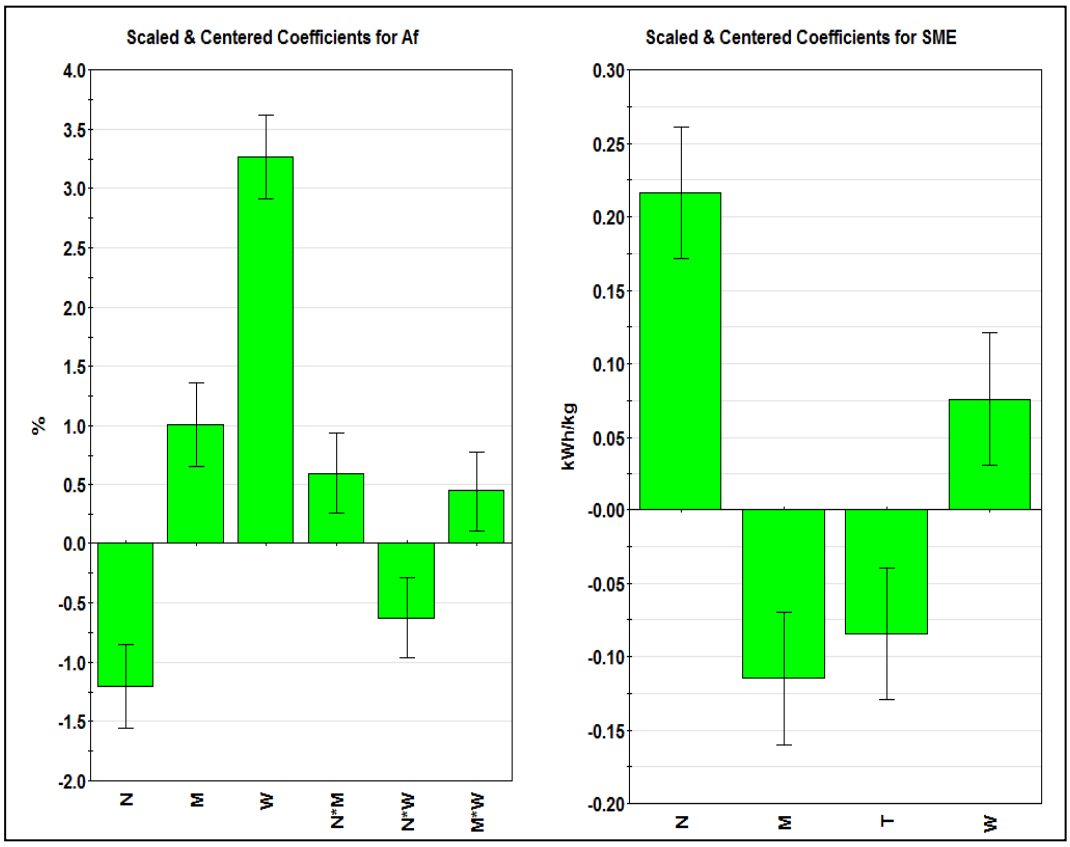

Figure 20. Co-efficient plots showing the influence of process parameters on SME and A_f

4.1.5 Screening Experiment – Snapshot

At 2 wt.% MWCNT incorporations, higher screw speeds and lower throughputs are primarily responsible for creating good filler dispersions in PP. The substantial increase in the SME while processing with these conditions has contributed to a considerable reduction in the A_f. Although the A_f is significantly decreased at these processing conditions on 5 wt.% MWCNT filler loading, no significant variation in the electrical resistivity of the composites are noticeable as the percolation threshold has already been achieved. Online process monitoring approach show promise and DoE approach has helped in identifying the extent of influence of the process conditions to achieve good filler dispersions.

4.2 Mainstream Experiment (ME)

Screw design plays a vital part in the extrusion of CNT based composites due to the shear it generates and the influence it has on the local residence time of the melt. Optimizing a screw configuration for a desired experiment is time consuming and hence a more economical approach would be to study the influence of the screw design in the desired working region.

Though it is very complicated to predict what would be an ideal screw design, knowledge could be derived from a trial like the screening experiment. The magnitude of SME required to disperse the MWCNT agglomerates, the resulting dispersion morphologies and volume resistivities of the composites in screening exercise served as an effective tool for designing the screw configuration for the samples in the mainstream exercise (Figure 11). For the samples in this case study, “Aggressive Screw” design refers to a screw design with more kneading elements with increased lead angles in order to impart higher SMEs as compared to the “Standard Screw” design adopted for SE. The “Soft Screw” configuration is designed to impart lower SMEs as compared to the “Standard Screw” by reducing the lead angle of a few of the kneading blocks. The measured melt resistances of the composites in mainstream experimental scheme are presented in Figure 21. It is interesting to note all the samples show resistances less than 10^9 Ω. Correlating this image to Figure 16 from the SE, it is seen that all the composites processed under the ME exhibited electrical conductivity except the E02 sample which was processed with a throughput of 12.5 kg/h. This shows the valuable contribution of employing an online process monitoring tool during processing.

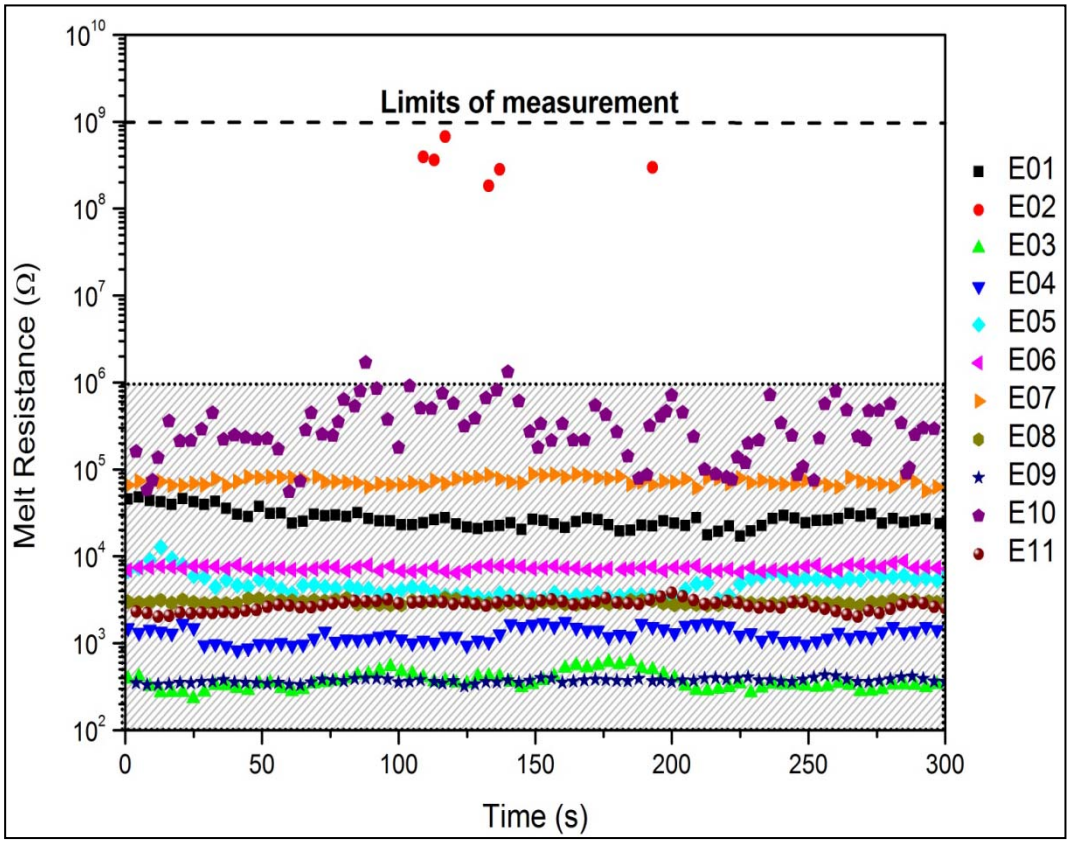

Figure 21. Observations of melt resistance for composites processed in ME

Influence of Screw Configuration on Volume Resistivity of the Composites

The variation in the screw design seems to have a considerable impact on the volume resistivity of the composites at lower MWCNT loadings, especially at higher throughputs. The effect of different screw designs on resistivity of the extruded composite strands can be seen from the data in Figure 22. Reference samples from screening experiments have also been plotted for relative comparisons. The volume resistivities of the composites E02 (SME-0.67 kWh/kg, A_f-6 %), S09 (SME-0.75 kWh/kg, A_f-5.8 %) and E07 (SME-0.77 kWh/kg, A_f-5.4 %) processed at 12.5 kg/h with a soft, standard and aggressive screw profiles respectively decrease in the mentioned order correlating well with the SME inputs and A_f. Although, the volume resistivity of composites E06 (containing 2 wt.% MWCNT and processed with an aggressive screw at 7.5 kg/h) and E07 (containing 2 wt.% MWCNT and processed with an aggressive screw at 12.5 kg/h) are not very different; the latter processed at a higher throughput is advantageous from perspective of an industrial production. The kneading blocks with lead angle 90° which give the maximum local shear is also a zone where no melt transportation theoretically occurs. The local residence time of the melt in these zones of increased lead angles of the kneading blocks is also higher, which is the case with the "Aggressive screw" as compared to the "Standard Screw". This would thereby enhance the overall SME input of the process and also comparatively increase the residence time of the melt in the extruder leading to better CNT dispersion and hence lower volume resistivity. The scenario is reversed whilst employing a "Soft Screw" wherein the quality of dispersion is comparatively poor as compared to the "Standard Screw".

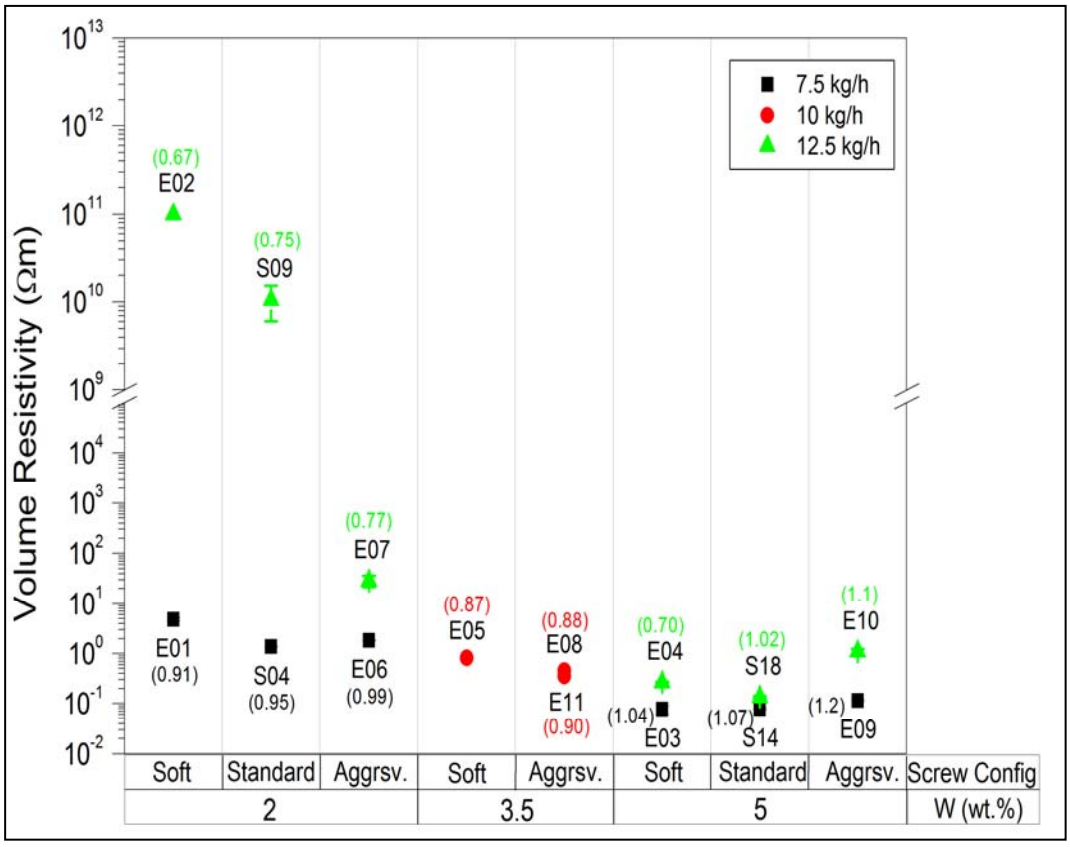

Figure 22. Influence of screw configuration on volume resistivity with respective SMEs

At lower throughputs and at higher MWCNT loadings the influence of screw configuration on the volume resistivity is low. There exists a certain threshold beyond which the enhancement in MWCNT dispersion quality is impossible as the shear stresses due to processing cannot overcome the inherent agglomerate strength of the MWCNTs. Hence, the level of dispersion and the volume resistivity could not be enhanced by varying the screw configuration.

It was interesting to observe that composites S04 and E06 (both containing 2 wt.% MWCNT) show very similar electrical properties in spite of them being processed with two different screw configurations at 7.5 kg/h. But, when these composites were processed at 12.5 kg/h (samples S09 and E07) close to 8 orders of lower resistivity is observed on E07. This finding highlights the importance of throughput consideration and shows that the most aggressive screw design (resulting in higher SME) is not mandatory to obtain better electrical properties of the composites. Processing with higher SMEs by employing the aggressive screw design could also potentially result in dispersed CNTs with reduced aspect ratio [55]. Figure 23 is a compilation of melt resistance (measured during both screening and the mainstream experiments) and volume resistivities of the strand (on which melt resistance measurements were possible).

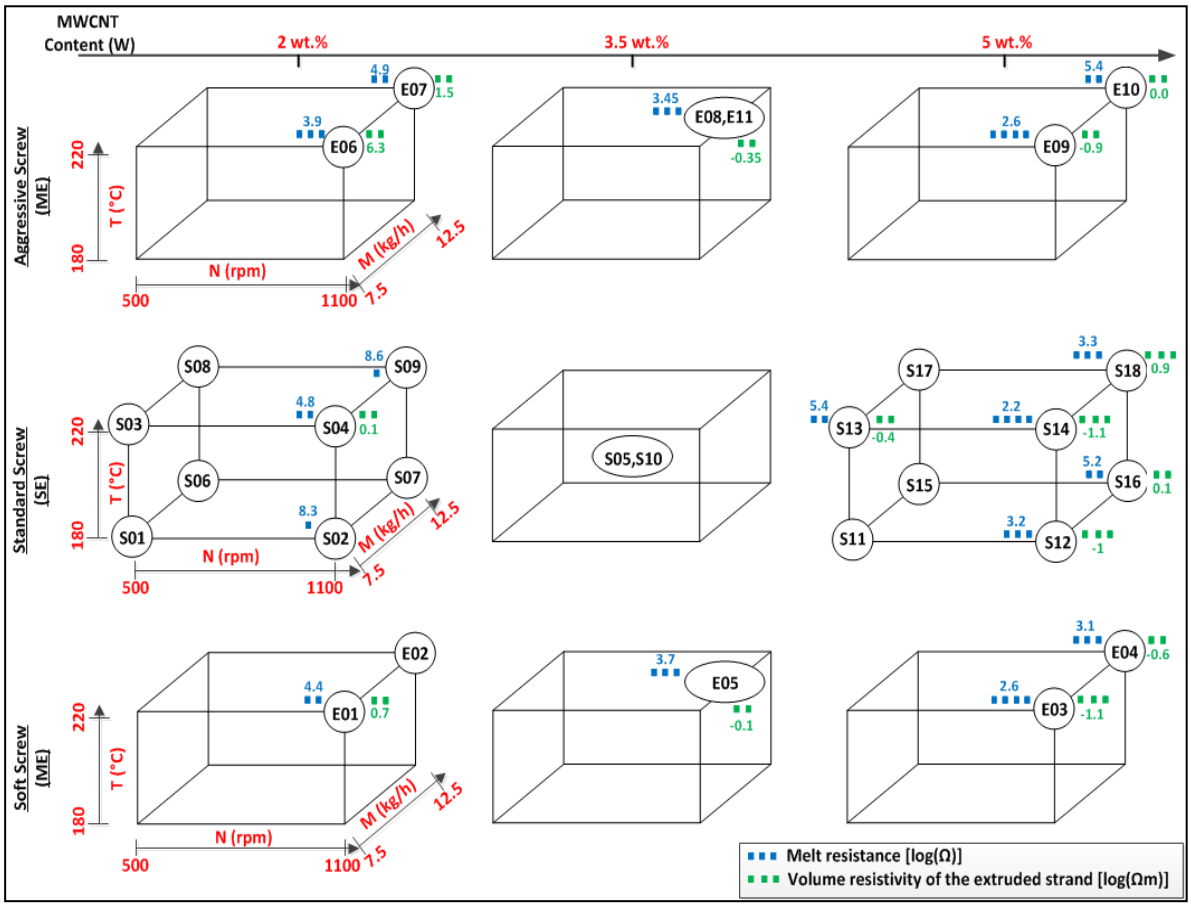

Figure 23. Summary of observed electrical properties from SE and ME

4.3 Effect of CNT Feeding Positions on Composite Properties

In the screening and the mainstream experiments the MWCNTs were fed along with PP in the main feeding port of the extruder. From literature evidences presented in Section 2.3.3, it was understood that the feeding the MWCNTs onto the polymer melt by employing a side feeder (Refer Figure 7) could facilitate better infiltration of the MWCNT agglomerates by the polymer melt, consequently enhancing the quality of MWCNT dispersion. This theory holds true when the used MWCNT have loosely entangled agglomerate fractions with a low agglomerate strength. However, the extent of dispersion would also be strongly dependant on the other compounding parameters specifically in a matrix like PP which presents poor compatibility with CNT.

The process conditions for the experiment with the side feed was kept identical to those adopted for the S04 sample (containing 2 wt.% MWCNT and processed at 1100 rpm, 7.5 kg/h, 220 °C) from the screening experiment which showed the best electrical properties. This will now on be referred to as “MF” (as the MWCNTs were fed through the main hopper) while the composite processed with a side feed will be noted as “SF” in the discussion. The extruded composites were thereafter injection molded for mechanical and electrical property measurements and also compression molded for electrical measurements.

The representative optical micrographs of the composites processed with MF and SF are presented in Figure 24. Increasing count of visible & larger MWCNT agglomerates were characteristic features of the composite processed with MF. The A_f of the composites processed with the side feed was 15% lower than that of the composites processed with the main feed indicating an improvement in the quality of dispersion. Although the overall residence time and the shear experienced by the MWCNT fed with the side feed would be lower (compared to feeding with a main feed), the principal characteristics governing agglomerate dispersion namely wetting and melt infiltration are efficiently satisfied. In this case, the contribution to enhancement of dispersion by agglomerate erosion could be higher compared to feeding with the main feed. As the agglomerate strength of the NC 7000 agglomerates is lower, SF approach would also ensure a comparatively lower extent of CNT aspect ratio reduction. The electrical and the mechanical properties of the PP-2 wt.% MWCNT composite processed with the mainfeed and side feed approaches are presented in Table 3.

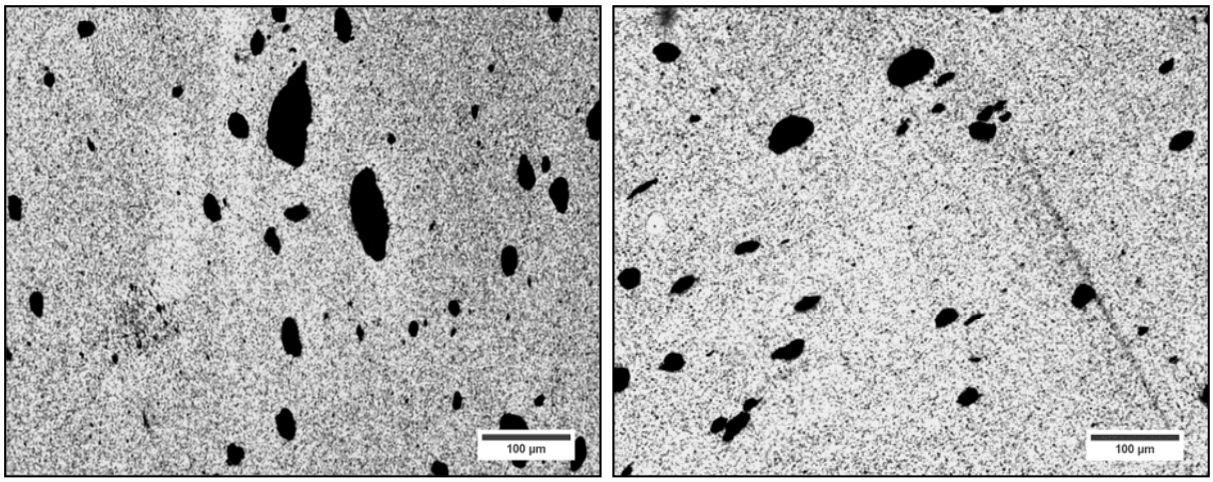

PP-2 wt.% MWCNT (MF), A_f-3.6 % **PP-2 wt.% MWCNT (SF), A_f-3.05 %**

Figure 24. Representative optical micrographs MF & SF processed composites

The melt resistance of the composite processed with SF configuration is one order lower in magnitude compared to that of the MF sample. No significant differences are observed on the volume resistivities of the extruded strand and the compression molded bar, which is expected of a composite having already passed the limits of electrical percolation. However, they were close to 15 orders in magnitude lower than that of pure PP which presents a resistivity of 10^{15} Ωm, indicating that the composites have electrically percolated.

The volume resistivity of the injection molded composites are close to three orders in magnitude higher than those observed on the compression molded composites, attributive to the formation of an insulative skin [5] due to a high temperature difference between the cold mold and the hot melt, potential reduction in CNT aspect ratio due to process shear and during its passage through the die [5], and orientation of the fillers [5,90] along the direction of flow resulting in a disturbance to the 3-D network of the CNT.

Table 3. Effect of MF and SF processing on the properties of PP-MWCNT composites

		MF	**SF**
Electrical Properties	Melt Resistance (Ω)	6.54 x 10^4	5.30 x 10^3
	Vol. Resistivity – Extruded Strand (Ωm)	1.34	0.71
	Vol. Resistivity – Compressed bar (Ωm)	1.88	0.33
	Vol. Resistivity – Injected bar (Ωm)	4.12 x 10^4	3.37 x 10^3
Mechanical Properties	Elastic Modulus, E (MPa)	862 ± 12	879 ± 13
	Tensile Strength, σ_{max} (MPa)	23.4 ± 0.1	23.4 ± 0.1
	Strain at σ_{max} (%)	11.2 ± 0.2	11.5 ± 0.3
	Notched Impact Strength, I_{notch} (kJ/m^2)	4.96 ± 0.2	5.4 ± 0.1

As the MWCNTs inherently possess higher elastic modulus than PP (E=696 MPa), the increase of modulus in the composite is evident on their incorporation into PP. The MF and the SF composites showed an elastic modulus of 862 MPa and 879 MPa respectively which is 24 % and 26 % higher than that of PP. The development of a strong interface which was not expected in a PP-MWCNT composite owing to a poor compatibility between PP and MWCNTs led to a minimal increase in the strength of the composites. Only a 10% increase in the tensile strength in the composites as compared to pure PP (σ_{max}=21.1 MPa) was observed with both MF and SF processing. The improvement in MWCNT dispersion with SF processing is substantially visible on the notched impact strength of the composites. The composites processed with MF and SF show an impact strength of 4.96 kJ/m^2 and 5.4 kJ/m^2 respectively, an increase of 17 % and 31 % compared to pure PP (I_{notch}=4.1 kJ/m^2). CNT agglomerate fractions which could act as active stress concentrators are obviously reduced with SF processing and results in better impact properties of the composite.

4.4 Synopsis

PP-MWCNT composites were processed on a large scale compounder with variations in extruder process parameters, screw configuration and filler feeding positions to identify the best processing conditions to achieve optimum MWCNT dispersion in PP. The significant conclusions of these experiments can be summarized as follows.

- Higher screw speeds have the most significant influence in creating substantially improved MWCNT dispersion in PP owing to higher shear stresses arising from increased SME input.
- Lower throughputs also result in better MWCNT dispersion due to enhanced residence times, and their contribution is valuable at higher processing speeds.
- Lower melt viscosity favors enhanced MWCNT dispersion quality.
- Higher SME by employing an aggressive screw configuration helps in achieving good electrical properties at an increased throughput.
- Employing a DoE approach results in the creation of a polymer-CNT processing database which could serve in designing future trials.
- Measurement of melt resistance online acts as a valuable tool for optimizing the process parameters in addition to being an efficient aid for quality control.
- Feeding the MWCNT into the polymer melt by employing a side feed results in better MWCNT dispersion and consequently better electrical and mechanical properties of the composite.
- Injection molding of the extruded composites results in higher electrical volume resistivities compared to those achieved with compression molding.

Understanding the mechanism of CNT dispersion during compounding is a key to effectively designing the process parameters. This would eventually lead to improved macroscopic properties of the composites at lower filler loadings as was observed in the results from this Chapter.

5. Influence of Peroxide Addition on the Properties of PP-MWCNT Composites

The synopsis of Chapter 4 suggests that optimizing the process parameters facilitates the achievement of good composite electrical conductivities at lower MWCNT concentrations. However, there is a potential limitation on the extent to which the production processes could be tailored to enhance the quality of MWCNT dispersion in a polyolefin like PP. Innovative approaches are thus necessary to further increase the scope of MWCNT filled polyolefins as competitive materials to existing fillers.

The electrical and mechanical property enhancements have been shown to be strongly hindered by inabilities to create a good CNT dispersion in polyolefins, and hence higher filler percolation thresholds as compared to those in more polar thermoplastics are a typical characteristic of these composites [67,83,91]. Physical or chemical modification of CNT is a strategy to adapt the CNT surface properties to those of the matrix polymers or to create reactive bonds, respectively. The former is shown to aid good dispersion for low electrical percolation and high electrical conductivities [92,93], while the latter is expected to result in enhanced mechanical behavior [94,95]. In situ polymerization of polyolefins in presence of CNT is possible [96], but does not present a method which can be economically performed. Hence any effort to tailor dispersion should come from a functionality of the polyolefinic matrix, a modification of CNT to reduce its surface energy and be compatible with polyolefins, or from the aid of dispersing and stabilizing additives. The latter seems more practical and hence this directs our attention towards looking at a potential additive during processing to improve the dispersion quality of MWCNTs.

The thermal decomposition of peroxides results in the release of free radicals which on abstracting hydrogen from the polymer backbone generates ternary macroradicals. The unstable macroradicals undergo a β -scission reaction in order to stabilize themselves in the process reducing the molecular weight of the polymer and therein reducing the viscosity/ increasing the melt flow rate (MFR). It is with this principle by which the molecular weight of PP resulting from the polymerization with a Ziegler-Natta catalyst is narrowed for a wider product portfolio. Oxygen radicals that would be left in the peroxide on removal of the carbon dioxide would combine with the hydrogen abstracted site of the PP to form ether linkages leading to enhanced PP polarity. Also, double bonds formed on PP on the β-scission reaction enhance their functionality to be used for further reactions [97]. Peroxides have also reported to act as side-wall functionalizing agents for SWCNTs [98].

This chapter deals with the study of the effect of peroxide addition during the processing of PP with MWCNTs in a twin-screw extruder and the observed effects on macroscopic properties of injection and compression molded composites. The effect of peroxide as a processing additive for MWCNT filled PP composites is elaborated with focus on the morphological, rheological, mechanical, electrical, and thermal properties of the composites. Composites without the addition of peroxides were also investigated as a reference. Some of

the extruded composites were also diluted in a small scale melt mixer to produce composites with lower MWCNT loadings. The list of composites prepared along with their extrusion parameters and the conditions for their subsequent dilution is presented in Table 4. The "Standard Screw" design from Chapter 4 with a side feed for CNTs at the L/D = 16 position was slightly modified by using a "shell" element immediately following the side feed position (Appendix C). This was employed to enhance the residence time of the melt by around 30 % to ensure that no unreacted peroxides remain in the composite after extrusion.

Electrical properties were measured on injection molded and compression molded bars produced from the extruded composites while mechanical testing was carried out on injection molded test specimens. The composites diluted with the melt mixer were compression molded under varying molding conditions for the evaluation of electrical percolation threshold and to study the influence of compression molding parameters on the electrical properties.

Table 4. Nomenclature of the composites along with the extrusion and melt mixing parameters

Sample	Twin-screw extrusion				Melt mixing (Dilution step)	
	wt. % MWCNT	wt. % Peroxide	Screw Speed (rpm)	Temp. (°C), Throughput (kg/h)	wt. % MWCNT	Temp (°C), Mixing Speed (rpm)
PP	-	-	500	220, 7.5		
PP-Px	-	1	500	220, 7.5		
C2-1100	2	-	1100	220, 7.5	1, 0.8, 0.6, 0.4, 0.2	220, 100
C2-500	2	-	500	220, 7.5	1, 0.8, 0.6, 0.4, 0.2	220, 100
C1-500-Px	1	1	500	220, 7.5	0.8, 0.6, 0.4, 0.2	220, 100
C2-500-Px	2	1	500	220, 7.5		

5.1 Nanocomposite Morphology

The optical micrographs of the composites with their respective SME and A_f are presented in Figure 25 (a-d). From Figure 25 (a & b) it is seen that higher screw speeds promote better macro dispersion as a result of higher SME inputs, identical to observations from Chapter 4. The A_f of composites processed at 500 rpm decreased significantly from 8.28 % to 3.05 % with the increase in screw speed to 1100 rpm. The decrease in A_f attributes to an increase in the content of individualized MWCNT or smaller agglomerates below the resolution of the optical microscope. Owing to the poor compatibility between PP and MWCNT, increased SME input is required to impart higher shear stresses leading to better dispersion quality.

The composites processed with peroxides showed an approximately three-fold reduction in A_f compared to those processed without peroxides under identical processing conditions (Figure 25 (a & d)). The agglomerate count and the areas of individual agglomerates were at

least five-fold larger in composites processed at 500 rpm without peroxide addition. Although Figure 25 (b & d) show very similar levels of dispersion, the SME input for the sample with peroxide loading produced at only 500 rpm was more than two times lower than the one without peroxide (produced at 1100 rpm) pointing out to a significant reduction in energy costs. Also, higher shear stresses at higher SME inputs could lead to a more pronounced reduction in the aspect ratio of CNT [55,67] which could be detrimental to the foreseen macroscopic properties for composites processed without peroxide addition.

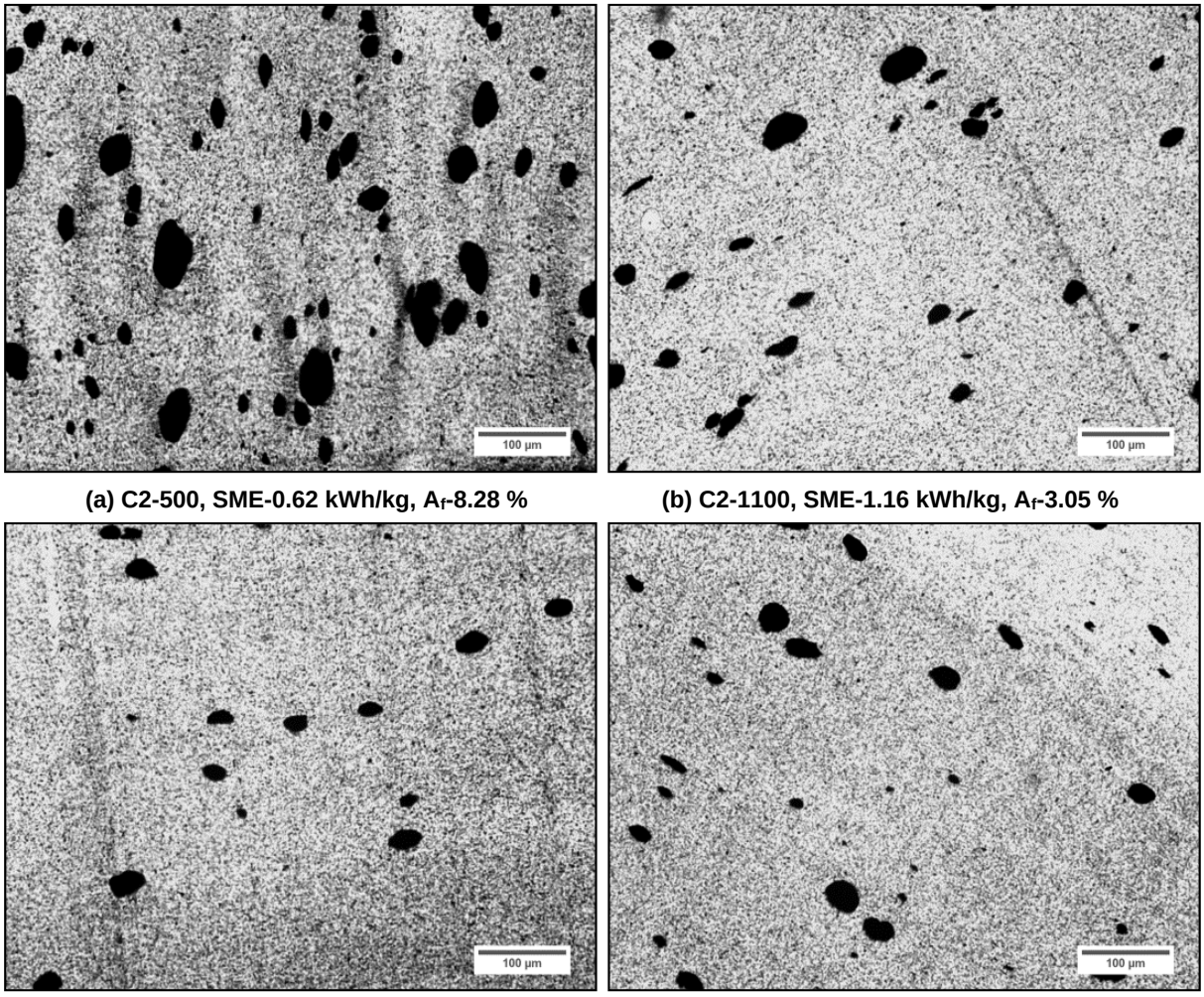

(a) C2-500, SME-0.62 kWh/kg, A_f-8.28 % **(b) C2-1100, SME-1.16 kWh/kg, A_f-3.05 %**

(c) C1-500-Px, SME-0.47 kWh/kg, A_f-2.5 % **(d) C2-500-Px, SME-0.53 kWh/kg, A_f-2.9 %**

Figure 25. Optical micrographs of the composites along with corresponding SME and A_f

The peroxide addition was principally intended to reduce the viscosity of the PP melt to facilitate better infiltration of the polymer melt into MWCNT agglomerates so as to lower the inherent strength of the primary agglomerates, but other effects could simultaneously occur. Firstly, the peroxide addition leading the chain breakage of the PP can increase the amount of functional groups and thus the PP polarity, leading to a better compatibility between the modified PP and the CNT. The evaluation of surface tension data from contact angle measurements indicate the lowering of the surface tension from 26.8 mN/m on pure PP to 21.8 mN/m on peroxide modified PP (PP-Px) with a 360 % enhancement in the polar contribution in the latter. The addition of peroxides to PP resulted in a decrease the contact

angle of water from 102° to 97° and an increase in the contact angle of diiodo-methane (non-polar solvent) from 62° on pure PP to 72° on peroxide modified PP. The decrease in the contact angle of a polar solvent and its increase on interaction with a non-polar solvent indicates an enhancement in the hydrophilic nature of PP on modification with peroxides. Although the contact angle between 0° to 90° on the solid-liquid interface results in better wetting, the decrease in the hydrophobicity of PP on peroxide modification seems to show a good potential to present enhanced compatibility with MWCNT (which are reported to be more compatible with polar polymers in the absence of a rigid structural backbone).

In the present work PP-Px was fed through the main port of the extruder, while the CNTs were fed at the L/D = 16 position changing the complexion of the experiment compared to that in literature where only a simple addition of peroxides to functionalize SWCNTs was dealt with [98]. Hence, it has to be understood that the whole of the added peroxide would not be available to react with the CNTs as some part of it would have already reacted with PP in the initial zones of the extruder. However, a certain portion of the added peroxide would react with the CNT creating functional sites on them as would be discussed by in situ and offline Raman investigation on PP-Px-MWCNT composites in Chapter 6. This approach was successfully demonstrated earlier in one other experiment carried out on MWCNT filled PS composites where Raman spectroscopy was used as a tool for understanding polymer-CNT interactions [99].

5.2 Melt Rheological Characterization

A decrease in the storage modulus (G') and complex viscosity (η*) of PP as shown in Figure 26 can be taken as an indirect measure of the extent of the decrease in its molecular weight on peroxide addition. The rheological behavior at lower frequencies is indicative of the contribution of the filler to the composite's behavior and in general is considered as a measure of the extent of interaction between the polymer and the filler. It can also be used as a tool for understanding the quality of dispersion when the content of MWCNTs is kept constant and nanotube length does not change. Rheological properties at high frequencies are dominated by the polymer as increased shear rates tend to orient the CNT, consequently resulting in lower intra-CNT and polymer-CNT interactions.

In the lower frequency regime of Figure 26, a significant reduction in the dependence of G' on frequency is an indication that all the composites with 1 and 2 wt.% MWCNT are above their rheological percolation threshold. A pseudo-like network is expected to be formed by the MWCNTs at this instance. The loss in storage modulus due to peroxide addition onto PP (by about one order of magnitude) is substantially compensated by the addition of MWCNT to PP-Px. Substantially enhanced CNT dispersion due to peroxide addition as was observed from Figure 25 (c & d) has resulted in the enhanced exposure area of MWCNTs for interaction with PP resulting in increased G' of the composites. In addition, a possibly lower CNT shortening due to the lower matrix viscosity [67], upon peroxide addition may also have contributed to the high storage modulus values.

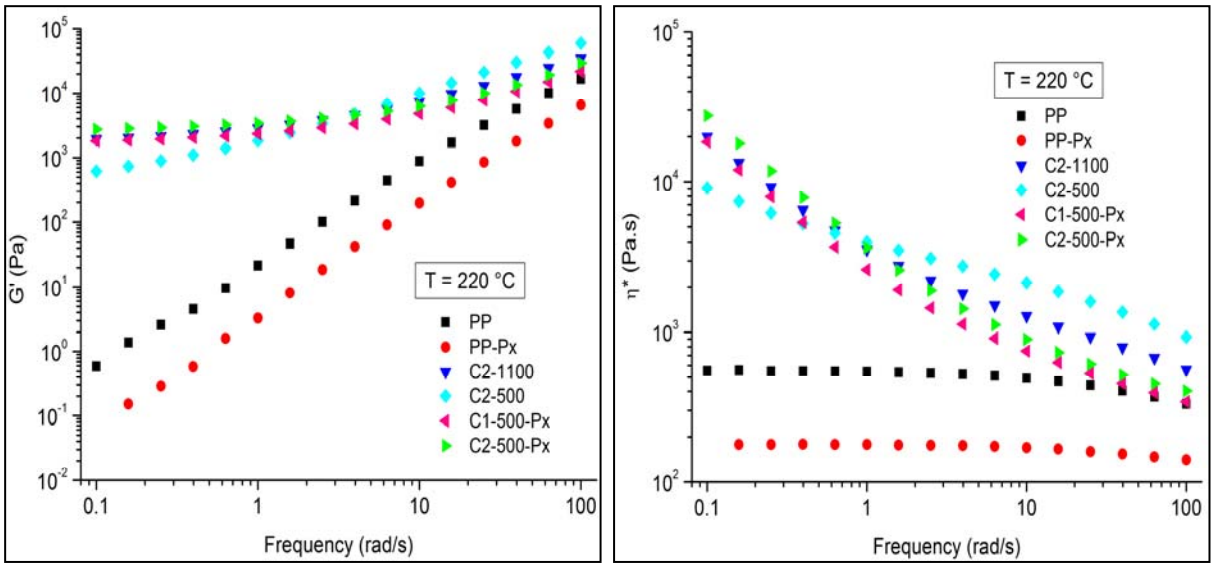

Figure 26. Dependence of G' and η* of the extrudate on frequency

The complex viscosity curve of PP and PP-Px reveals a characteristic viscoelastic behavior with a Newtonian plateau at low frequencies and evidences of shear thinning with increasing frequencies. However, the viscosity of PP is thrice as higher than PP-Px. With the addition of the MWCNTs, there is a significant increase in the viscosity of PP. Although peroxide addition resulted in decreased viscosity of PP, the addition of CNTs to PP-Px has resulted in a substantial increase in the viscosity of the composites at the lower frequencies. The enhanced surface area of the CNTs in the composites containing peroxides provides more sites for interaction with the polymer leading to enhanced viscosity. There is very little difference in the viscosities of C1-500-Px compared to C2-1100 even though the latter has two times the loading of CNT.

For composites with better dispersed and supposedly less shortened (longer) MWCNTs, there is an increase in the concentration of CNT oriented by shear. This, in addition to contribution of enhanced frictional forces due to increased surface area presented for the polymer-filler interaction results in enhanced shear thinning behavior. Parallel plate rheology observations have shown to be dependent on the temperature used for the frequency sweep [100], but measurements carried out at 180, 200, 220 and 240 °C differed very little in magnitude and hence are not presented here.

5.3 Electrical Properties of the Nanocomposites

The observed volume resistivities of the nanocomposites processed by injection molding (mold temperature of 30 °C) and compression molding (composites processed at a melt temperature of 220 °C and holding time of 4 min) is presented in Figure 27. Pure PP and PP-Px show a volume resistivity of around 10^{15} Ωm. The resistivities of injection molded samples of the composites C2-500 and C2-1100 are 1.21 x 10^5 and 3.70 x 10^3 Ωm, respectively. The decrease in the electrical resistivity of these composites by close to 10-12 orders of magnitude indicates that both of these composites are electrically percolated. Considering

the fact that both the composites were processed with identical injection molding parameters, the two reasons that could be attributed to the variation in the resistivity are the primary agglomerate dispersion quality resulting from the extrusion step and possibly different nanotube shortening. The electrical results clearly show that better dispersion for composites processed with 1100 rpm enhanced the efficiency of conductive network formation compared to composites processed at 500 rpm. In spite of higher shear stresses at 1100 rpm which could have led to a more severe reduction in the aspect ratio of the MWCNT in these samples, the contribution of primary MWCNT dispersion seems to be dominant. The volume resistivity of the peroxide containing composite with 1 wt.% (C1-500-Px) which stands at 1.71 x 10^4 Ωm is not very different in magnitude to that of the composite with 2 wt.% MWCNT processed without peroxide at 1100 rpm. This further affirms the argument of having excellent dispersion qualities from the primary processing step. The composite C2-500-Px shows 350 times lower resistivity than its counterpart (C2-500) processed without peroxide. The shear stresses created during the injection molding step were shown in literature to result in the orientation of the filler along the direction of the flow [5,90]. Additionally, the uneven cooling of the part especially at their exterior due to the high temperature difference between the melt and the walls of the mold can freeze this CNT orientation and contribute to a isolative surface skin [5], increasing the bulk resistivity of the composites. The aforementioned reasons contribute to the observed lower volume through-plane conductivities of the injection molded composite as compared to the compression molded samples. The latter of the reasons was verified by employing a mold temperature of 60 °C in the injection molding process which resulted in one order lower magnitude of electrical resistivity on the C2-1100, C1-500-Px and C2-500-Px compared to those obtained while employing a mold temperature of 30 °C.

Compression molding of extruded composite granules under constant press conditions shows volume resistivity of about 1 Ωm, orders of magnitudes lower than those observed on the injection molded samples. Very little differences are noticeable when taking into account the differences in dispersion from the extrusion processing step and the concentration of MWCNTs in the composite. Compression molding facilitates the nanoscale re-agglomeration of the previously dispersed CNT [101]. Due to the relatively long residence time at high temperatures and the absence of orientation by shear flow, the tube-tube distance attains its least minimum with sufficient holding time at the imparted pressure. Thus, a favorable environment is created for the intrinsic CNT attractive forces like the van der Waals and the Brownian forces for the formation of a conductive pathway by the combination of individualized nanotubes and their agglomerates.

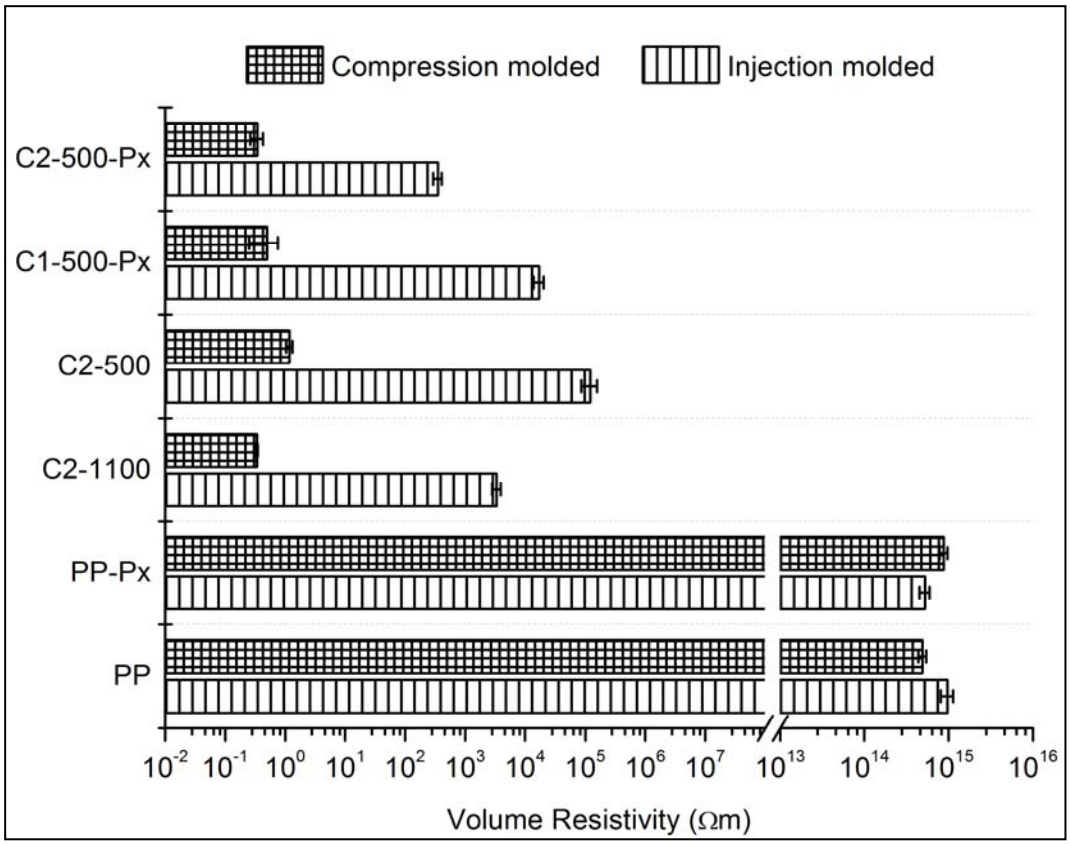

Figure 27. Volume resistivities of injection molded and compression molded composites

Electrical volume resistivities of some of the composites diluted using the Thermo Haake mixer are presented in Figure 28 along with the resistivities of the masterbatches (compression molded bars from the extrusion step) from which they were diluted. An electrical percolation threshold of around 0.4 wt.% MWCNT is evident irrespective of the extrusion parameters, peroxide incorporation, and compression molding conditions. Although well dispersed composites exhibit lower resistivities, the differences in the resistivity of the composites diminish with increase in MWCNT concentration. At lower MWCNT loadings, the temperature of molding had a significant influence on the composite's resistivity. The sample C2-500 with the worst CNT dispersion (refer to Figure 25) shows percolation at 0.4 wt. % MWCNT only when pressed at the higher molding temperature of 240 °C. This difference between the pressing temperatures was not visible for to C2-1100 and C1-500-Px which show better dispersed filler morphologies. When comparing resistivities of composites processed at 220 °C at two different holding times of 2 and 4 min in the final stage, the higher holding time results in lower resistivities owing to the enhanced time interval available for the CNT re-agglomeration process on the nanoscale. The resistivity of the C0.4-500-Px sample (240 °C and 4 min) which is 12.2 Ωm reaches it is lowest at this MWCNT loading and this value is comparable to electrical resistivities achievable on CNT filled thermosetting matrices [102].

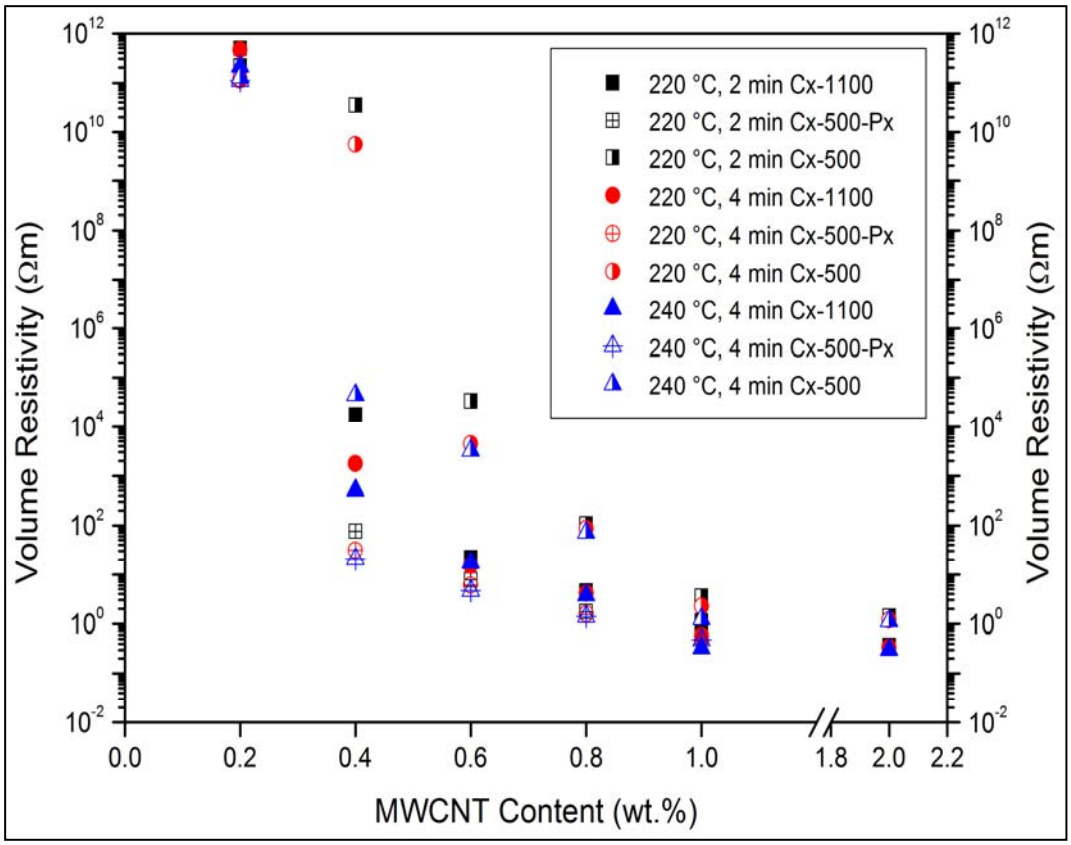

Figure 28. Influence of compression molding parameters on resistivity. “x”: wt.% in x-axis

5.4 Mechanical Performance of the Nanocomposites

The mechanical reinforcement by CNTs is governed by the effective surface area or the interface between the polymer and CNT available for the load transfer. The reinforcement is a direct function of the CNT content, the dispersion state of the CNT in the matrix and the interactions between the surface of the CNT and the polymer matrix. As the as-received CNTs did not have any surface functionalization beside the small content of functional groups originating from the synthesis process, the selected mechanical properties namely elastic modulus, tensile strength and notched impact strength presented in Figure 29 should be a function of the MWCNT loading and their state of dispersion.

The stress-strain curve of PP indicates a yield point and a cold drawing behavior with increasing strain. The samples did not break even at a maximum strain of 70 % (measurements were stopped at this stage as the tensile strength was reduced to less than 50 % of its maximum; failure strain (ε_{break}) however was around 700 %). Thus, the tensile strength is identical with the stress at yield. PP and PP-Px do not show differences in the stress-strain behavior. Looking at the specific properties derived from the stress-strain curves, the modulus of PP (700 MPa) did not change on peroxide addition. The addition of 2 wt.% MWCNT using screw speeds of 1100 rpm and 500 rpm increased the modulus of PP by 25 % and 20 %, respectively. Peroxide addition did not significantly affect the modulus of composites with 1 wt.% and 2 wt.% MWCNT. The tensile strength of pure PP and PP-Px of 21.2 MPa is enhanced after MWCNT addition by 10 % irrespective of the extrusion screw

speed, CNT content and peroxide addition. The strain at maximum strength is 13 % for all the composites and is neither influenced by the peroxide, nor by the CNT addition.

Concerning the notched impact strength, the addition of 2 wt.% MWCNT at a screw speed of 1100 rpm and 500 rpm augmented the value of PP by 28 % and 41 %, respectively. Although better filler dispersion is found at higher processing speeds, the presence of a loosely packed higher agglomerate fraction in the composite with poor dispersion has inhibited crack propagation more effectively resulting in better impact behavior. Lower CNT shortening at the lower extrusion speed seems to have dominated the effect of improved CNT dispersion in leading to better impact properties. PP-Px showed a 14 % lower impact strength compared to PP. This decrease is also reflected in the impact property of C2-500-Px which is close to 38% lower than that of C2-500. However, the impact property of this composite is still higher than that of pure PP. The C1-500-Px composite shows higher impact strength than C2-500-Px which could be due to the presence of relatively higher amount of agglomerated CNT with possibly higher CNT shortening at increased CNT loading. The lowering of the impact strength of the peroxide modified PP and its composites compared to those without peroxide addition could be due to the shorter polymer chains in the former.

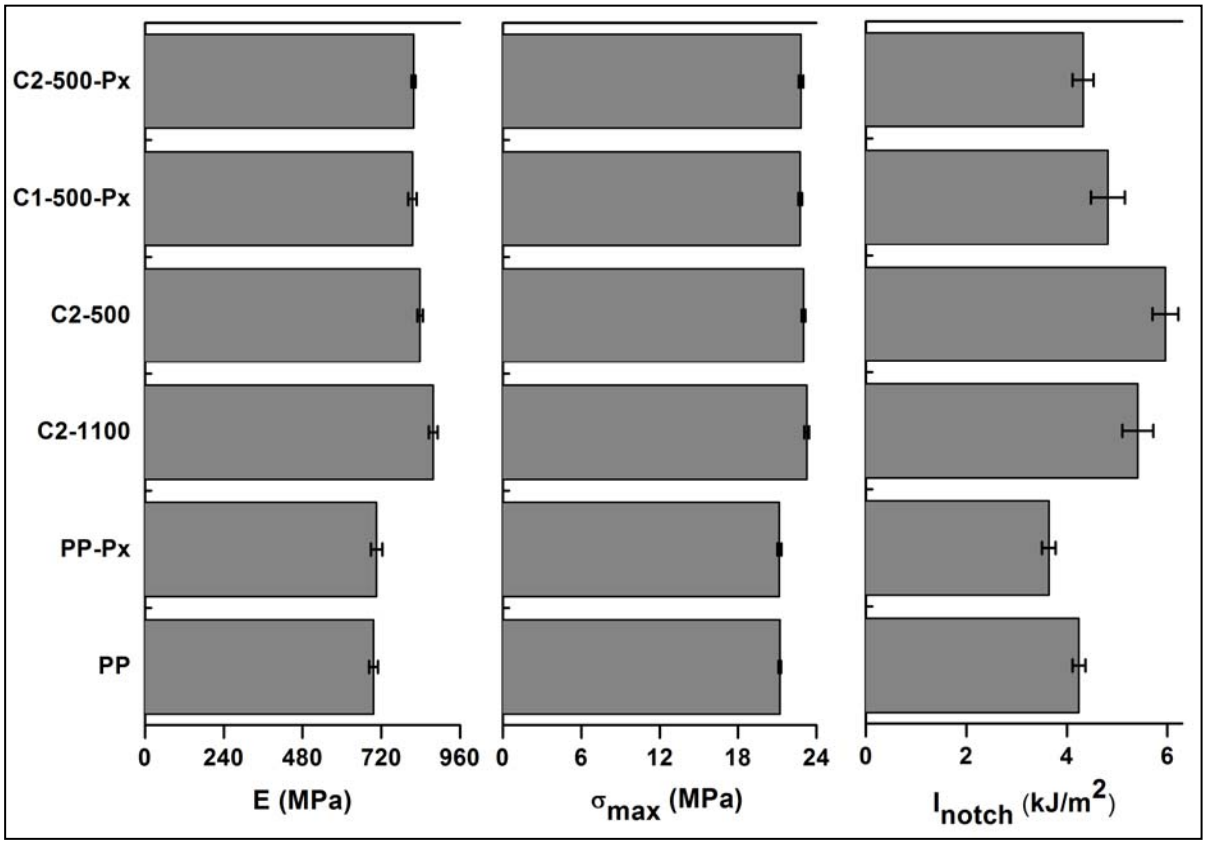

Figure 29. E, σ_{max} and I_{notch} of the injection molded composites

DSC data of the composites along with the reference samples is given in Table 5. Enhancement in crystallinity on MWCNT addition to PP has been reported earlier, principally due to the ability of CNTs to act as nucleating agents in semi-crystalline matrices [103], and this is evident by enhanced T_c for all the composites. The addition of peroxides to PP

resulted in a slight lowering of the crystallinity (X_c) of PP from 34.6 % to 33.4 % which may be a result of the reduced M_w of PP. On the other hand the addition of 2 wt.% MWCNT to PP results in an X_c of 38.8 % and 37.1 % respectively at processing speeds of 1100 rpm and 500 rpm. The enhanced crystallinity on the C2-1100 composite over the C2-500 composite is primarily due to the enhanced MWCNT dispersion in the former due to improved filler dispersion. On the other hand, composites C1-500-Px (X_c=32 %) and C2-500-Px (X_c=31.5 %) show decreasing crystallinity compared to PP-Px. In spite of significantly better MWCNT dispersion in these composites, the lower crystallinity of the composite indicates that the mechanical properties of the composites may have been strongly influenced by the structural integrity of the CNTs which seemingly has been lost by peroxide induced functionalization on its side walls. Decreased crystallinity and lower modulus of composites with improved dispersion on functionalization has also been reported earlier [104,105].

Table 5. DSC and DMA observations (at 1 Hz) of the composites

	T_m (°C)	ΔH_m (J/g)	X_c (%)*	T_c (°C)	~T_g (°C)
PP	140.30	72.30	34.6	98.1	4
PP-Px	138.60	69.1	33.4	98.3	4
C2-1100	146.40	79.40	38.8	112	2
C2-500	144.70	76.00	37.1	109	2
C1-500-Px	144.90	66.20	32	108.3	2
C2-500-Px	145.40	65.40	31.5	108.2	2

The step intensity at glass transition (T_g) was difficult to be evaluated with the DSC measurements, and hence Dynamic Mechanical Analysis (DMA) was carried out. T_g measured at the point of inflexion of the loss curve of the loss tangent (Tan δ) curve at a frequency of 1 Hz is presented in Appendix D. The T_g of PP at 4 °C did not change on peroxide addition, but all the composites presented a T_g about 2 °C lower than the reference irrespective of the CNT content and the level of filler dispersion. The T_g was shifted up by 2 °C and 5 °C respectively for all the samples at DMA frequencies of 10 Hz and 100 Hz respectively. It must be noted that there exists a variation in the T_g measured by the DSC and the DMA approaches due to the latter being conducted at a frequency 2-3 orders higher in magnitude than the former.

The addition of peroxides resulted in improved MWCNT dispersion morphology, but the speculation that their incorporation might negatively affect the mechanical properties seems to be true. The lower viscosity of the PP-Px melt and the enhanced hydrophilicity could have aided betterment in dispersion, but functionalization may have resulted in the loss of structural integrity of the CNTs. Also, it can be argued that the dispersion is still not good enough to take complete advantage of the reinforcing potential of CNTs. This has been the case with literatures published with CNT reinforcements in different matrices [62,82,87].

5.5 Thermal Stability of the Nanocomposites

The onset (T_o) and maximum temperature of degradation (T_{max}) of pure PP are at 269 °C and 312 °C, respectively (data extracted from the plot in Figure 30). The addition of peroxides lowers these temperatures to 258 °C and 302 °C respectively, indicative of the reduction in the molecular weight of PP.

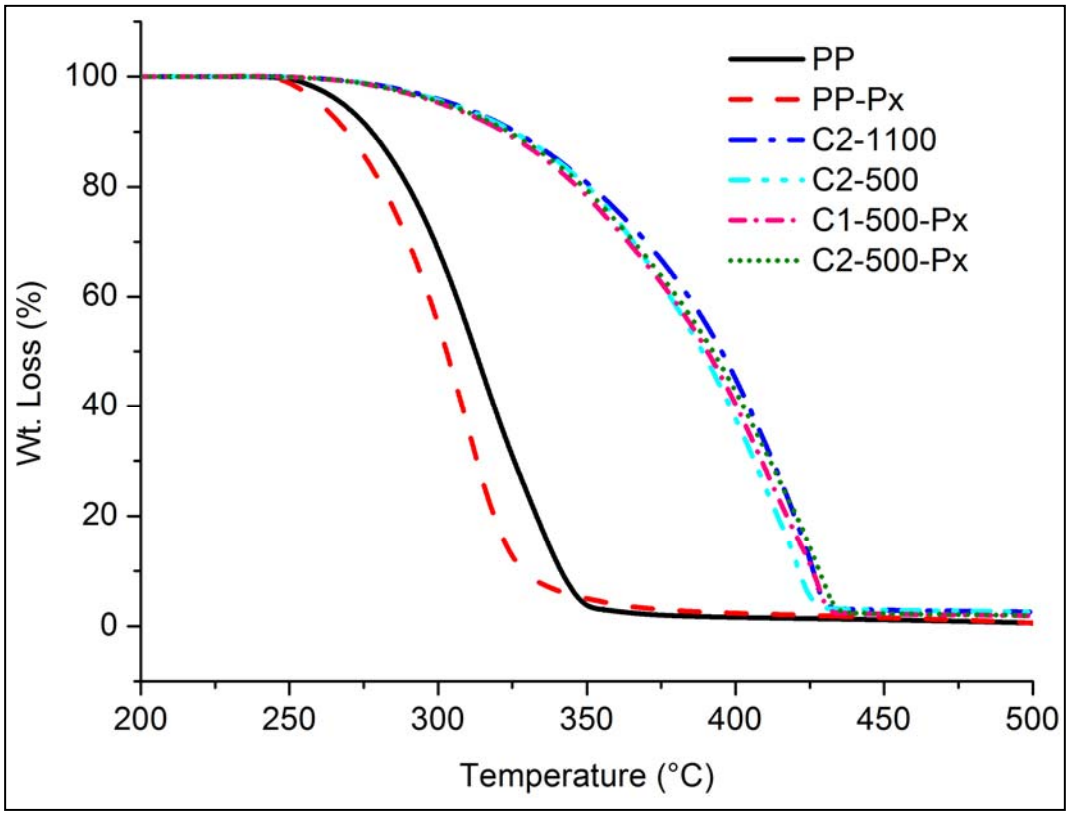

Figure 30. Thermal stability of the composites

The addition of 2 wt.% MWCNT using 1100 rpm extrusion screw speed enhances the onset and maximum temperature of degradation of the composites by 40 °C and 85 °C respectively. When using 500 rpm, slightly lower increases are observed. The composites with peroxide C1-500-Px and C2-500-Px show similar degradation temperatures as the C2-1100. This relative increase to the corresponding parent PPs (PP and PP-Px) can be explained by the fact that an increase in the surface area of the dispersed CNT increases their radical scavenging efficiency by intercepting the free radicals released during the oxidation of PP owing to their high electron affinity of about 2.65 eV [106]. The rate of degradation decreases, as well as dispersed CNTs present a higher degree of impediment to the molecular mobility of the polymer chains. As a consequence, there is very little difference in the thermal stability enhancement between the C1-500-Px and the C2-1100 composites having similar dispersion state even though the wt.% of MWCNTs is lower in the former.

5.6 Synopsis

The addition of peroxide was shown to play a crucial role in enhancing the dispersion quality of MWCNTs in PP which can be mainly attributed to the decreasing viscosity of the PP matrix, enhancement in the polarity of PP, and the functionalization of CNTs. These result in an SME reduction of more than two times for the processing of PP-2 wt.% MWCNT composite. Melt rheological observations on the composites show a substantial improvement in the storage modulus and complex viscosity of the composites with peroxides, strongly compensating for their loss on peroxide incorporation to pure PP.

Electrical conductivity of compression molded composites is at least 4 orders in magnitude higher than those observed with injection molding due to the principal variation in the way the conductive network evolves in each of these processes. The MWCNT filled PP composites percolate electrically around 0.4 wt.% filler content as measured after diluting the extruded granules using a small-scale mixer. This percolation concentration is however strongly dependent on the state of dispersion in the starting masterbatch and on the compression molding parameters.

Concerning the mechanical properties, the modulus of PP as measured in tensile tests improves with MWCNT incorporation by 28-41 % whereas the improvement in tensile strength is about 10 %. Peroxide addition does not alter the tensile strength of the composites, but present slightly reduced modulus as compared to their counterparts without peroxide, even if PP and PP-Px showed the same values. Although, the addition of peroxides resulted in lower impact properties of the composites, the notched impact strength of all the composites was better than that of PP. One may have expected improved mechanical characteristics due to the much better CNT dispersion in PP on peroxide addition, but the shorter polymer chains on peroxide addition and possible creation of defects on CNT sidewalls due to functionalization compromise on the benefits of improved CNT dispersion.

The thermal stability of the composites is substantially enhanced by the addition of peroxides with better CNT dispersion resulting in enhanced filler surface area for accepting the free radicals from the oxidative degradation of PP.

In summary, it was shown that in situ addition of peroxides during melt mixing of PP with pristine MWCNTs results in improvement in filler dispersion and corresponding electrical and thermal properties of injection molded samples without significant deterioration of mechanical properties. The properties achieved with PP-1 wt.% MWCNT on peroxide addition at much lower SMEs are not very different from those achieved with PP-2 wt.% MWCNT without peroxides indicating savings on both material and processing costs. In addition to enhanced product economics, the fact these results were achieved without any pre-treatment of the CNTs in a commercially viable process adds to the significance of this investigation.

6. Peroxides as In situ Functionalizing Additive for MWCNT in PP-MWCNT Composites

The results of Chapter 5 shows that the addition of peroxides resulted in significant lowering of the melt viscosity and enhancement in the hydrophilicity of PP which contributed towards enhanced MWCNT dispersion due to better wetting and infiltration of the MWCNT agglomerates by the polymer melt. The prospects of MWCNT functionalization was also speculated based on literature evidences. In addition it was found that the crystallinity and modulus of the composites with peroxides was lower than that of the parent PP-Px contrary to expected beliefs (of enhanced crystallinity of the semi-crystalline PP with CNT addition) which mandates understanding if reactive functionalization of CNTs really occur during composite processing. To understand this, Raman spectroscopy measurements were carried out both online during melt mixing and offline on the extruded composites and would be the focus of discussion in this Chapter.

Raman spectroscopy has been widely used to characterize the type of CNTs [107], determine the defect concentration of CNTs especially on functionalization [108], evaluate the Young's modulus of the CNTs [109], understand orientation of CNTs in polymers [110] etc. Raman spectroscopy has also been reported to be used to understand polymer-CNT interactions by tracking the CNT signature peak shifts due to applied loads on both compression and tension on polymer-CNT composites, particularly on SWCNT based composites [111,112], and thermoset based matrices [112]. The sensitivity and the viability of this measurement approach to understand thermoplastic polymer-MWCNT interactions however need more understanding owing to many contradictory reports in literature which will be underlined during the course of the discussion.

In this experiment, PP-Px and the MWCNTs were fed together onto the inlet port of the melt mixer and were mixed at two different screw speeds of 70 rpm and 120 rpm at a constant cylinder temperature of 220 °C for 12 minutes. 1 and 2 wt.% of MWCNTs were taken for investigations. Pure PP, PP-Px and PP-MWCNT composites were also processed as reference. Refer to Section 3.3.8 for the approach. The addition of peroxides as a reactive functionalizing agent for MWCNT during the processing of MWCNT incorporated PP composites is investigated with Raman spectroscopy both in the melt and on the extruded composite. In addition to this, an attempt has been made to understand the polymer-MWCNT interactions by correlating both online and offline analysis.

6.1 Morphology of the Composites

The representative optical micrographs of PP-MWCNT and PP-Px-MWCNT composites[1] are presented in Figure 31. Higher agglomerate size fractions owing to lower shear rates are

[1] The extrudates were pressed into 15 µm thick films at 160 ºC for 1 minute using a *High Temperature Constant Thickness Film Maker* Specac. The temperature was controlled by *4000 Series High Stability Temperature Controller* Specac and the films were investigated using a Leica DMRX Microscope to get transmission optical micrographs.

typical features of PP-1 wt % MWCNT composite processed at 70 rpm (C1-70) compared to those processed at 120 rpm (C1-120). Increased MWCNT loading resulted in increased agglomerate content and larger agglomerate size fractions. The incorporation of 1 wt. % MWCNT to PP-Px at 70 rpm (C1-70-Px) and 120 rpm (C1-120-Px) results in enhanced quality of MWCNT dispersion in the polymer host irrespective of the processing speed. As discussed in the previous Chapter, better PP melt infiltration into the CNT agglomerates and better wetting of the CNT agglomerates as a result of lowered surface tension of PP-Px could be attributed as reasons for enhanced MWCNT dispersion quality. PP-Px incorporated with 2 wt.% MWCNT (C2-Px) shows a good quality of CNT dispersion but presents increased agglomerate fractions as compared to C1-Px principally owing to increased MWCNT content.

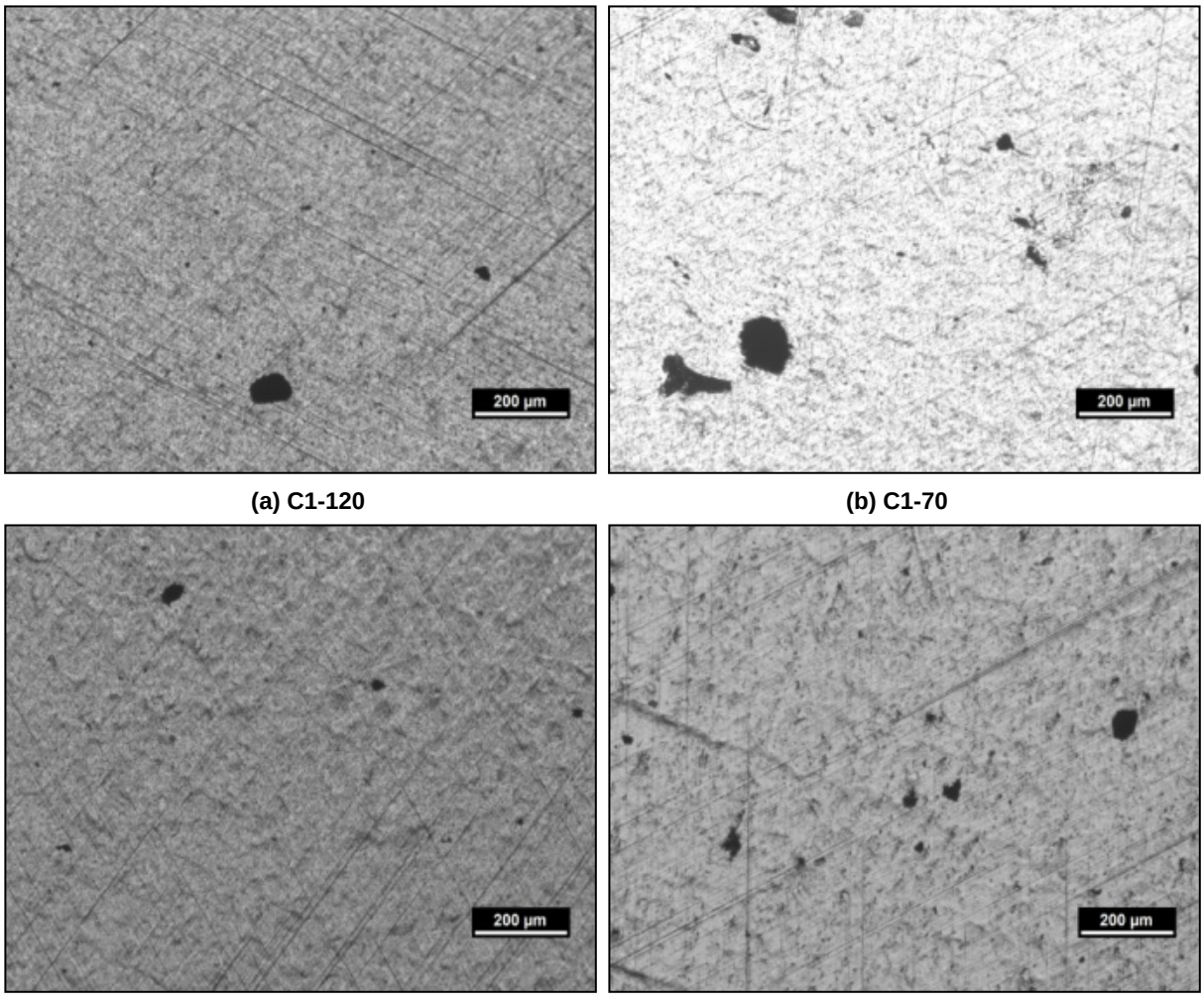

(a) C1-120 **(b) C1-70**

(c) C1-120-Px **(d) C2-120-Px**

Figure 31. Optical micrograph of the nanocomposites

6.2 Raman Spectra Analysis

Three characteristic peaks are observed from the Raman spectra of MWCNT. The peak at around 1300 cm^{-1} (D-peak) is activated by the presence of disorders in the graphitic structure while the peak at around 1600 cm^{-1} (G-peak) results from the in-plane C-C vibration. The peak at around 2700 cm^{-1} (G*-peak) is the secondary overtone of the D-peak (not used for

discussion in this work). The purity or structural integrity of CNTs is higher when the ratio of the intensity of the D-peak to that of the G-peak (or I_D/I_G) is lower. Zhao and Wagner report that polymer-CNT interactions are reflected as changes in the position or as a change in the full width at half maximum (FWHM) of the characteristic D and G peaks of CNT [113]. The peak positions and the FWHM of the CNT peaks of the as-received MWCNT and the composites measured offline, respectively are listed in Table 6 and Table 7.

Table 6. D and G peak positions of MWCNTs in the as-received form and in the composites

	Peak Position (cm^{-1})	
	D	**G**
As-received MWCNT	1311 ± 1	1605
C1-120	1312 ± 1	1603 ± 2
C1-70	1312 ± 2	1603 ± 1
C2-120	1313 ± 1	1602 ± 1
C1-120-Px	1312 ± 1	1601 ± 1
C1-70-Px	1313 ± 2	1602 ± 2
C2-120-Px	1313 ± 2	1601 ± 2

Table 7. FWHM of the D and G peaks of MWCNTs in the as-received form and in the composites

	FWHM (cm^{-1})	
	D	**G**
As-received MWCNT	55 ± 0.4	45 ± 0.6
C1-120	63 ± 0.5	54 ± 0.2
C1-70	61 ± 0.3	53 ± 0.1
C2-120	65 ± 0.4	57 ± 0.3
C1-120-Px	66 ± 0.2	57 ± 0.2
C1-70-Px	64 ± 0.5	55 ± 0.4
C2-120-Px	69 ± 0.5	59 ± 0.3

The D-peak and the G-peak positions of MWCNT at 1311 cm^{-1} and 1605 cm^{-1} respectively did not change considerably when MWCNTs were incorporated into PP. Although the quality of dispersion was significantly different for the composites processed with and without peroxides, peak shifts as evidence of varying dispersion levels could not be observed. Also

in an earlier work on PS and MWCNT no changes in the MWCNT peak position as a function of MWCNT dispersion and loading fraction were found [55,99]. In contrast, Bokobza and Zhang report a higher wavenumber shift of the peaks of the MWCNT when they were dispersed by ultrasonication in a solvent and incorporated into styrene-butadiene rubber (SBR) [114]. They regarded this as a measure of lesser inter-tube interactions. McClory et al. show a higher wavenumber shift of 24 cm^{-1} of the G-peak when MWCNT were incorporated into high impact PS (HIPS) by melt mixing, irrespective of the MWCNT content and the state of dispersion. They attributed this to the compressive stresses induced on the MWCNT due to the melt solidification of HIPS [8]. Srivastava et al. show in MWCNT/PS composite films prepared by solution mixing that with increase in MWCNT concentrations the D, G and G* peak of MWCNT shifted to lower wavenumbers [115]. The G peak of composites with 8 wt.% and 10 wt.% CNT shifted to 14–18 cm^{-1} lower wavenumbers compared to the composite with 6 wt.%. They claim this as the effect of interfacial interaction. As three different literature reports found three contrasting observations it is difficult to attribute peak position variations to one single factor. Hence, the changes in the position of the characteristic CNT peaks would have to be a strong function of the polymer host, MWCNT type and content, level of dispersion of MWCNT in the host matrix, interfacial interaction between the polymer and the filler, laser intensity and wavelength and exposure time. However, the individual contribution of each of these factors in affecting the peak shift is impossible to ascertain.

The MWCNT peak positions measured in the composite melt also did not indicate any change with increasing residence time, in spite of enhancement in the dispersion quality of the fillers (measured as the reduction in the intensity of the characteristic δ-CH_2 (δ-bending) peak of PP, refer to Figure 32). As the Raman spectral intensity of MWCNT is much stronger than PP, the intensity of the other PP peaks is too small in the composite spectra to be discussed. Hence, the peak at 1460 cm^{-1} which showed the highest intensity of all the PP signatures is monitored here.

The FWHM of both the D and the G peaks of MWCNT at 55 cm^{-1} and 46 cm^{-1} respectively increase to 63 cm^{-1} and 54 cm^{-1} respectively on the C1-120 composite. It is further increased to 65 cm^{-1} and 57 cm^{-1} respectively on the C2-120 composite indicating that enhanced MWCNT concentrations results in enhanced FWHM of the characteristics peaks of the CNT. This could also be the reason for the C1-70 composite showing lower FWHM than the C1-120 composite as the enhanced surface area of the better dispersed CNTs in the latter present enhanced active concentration of the CNTs to laser intensity. The addition of peroxides results in much higher FWHM values of the CNT peaks in the composites due to better CNT dispersion morphologies. It was also noticed that the FHWM of all of these composite melts was increasing as a function of enhanced mixing time, but the FWHM of the melt at the end of mixing process after 12 min becomes the same as measured on the solid extruded strand indicating that melt solidification had no role on the variation of FWHM of the composites. Hence, it can be summarized that that variation in FWHM of the MWCNT is dependent on the MWCNT content, the extent of dispersion and the level of polymer-CNT

interaction. Comparisons with literature were not possible as the variation of FWHM was not considered in [8,114,115].

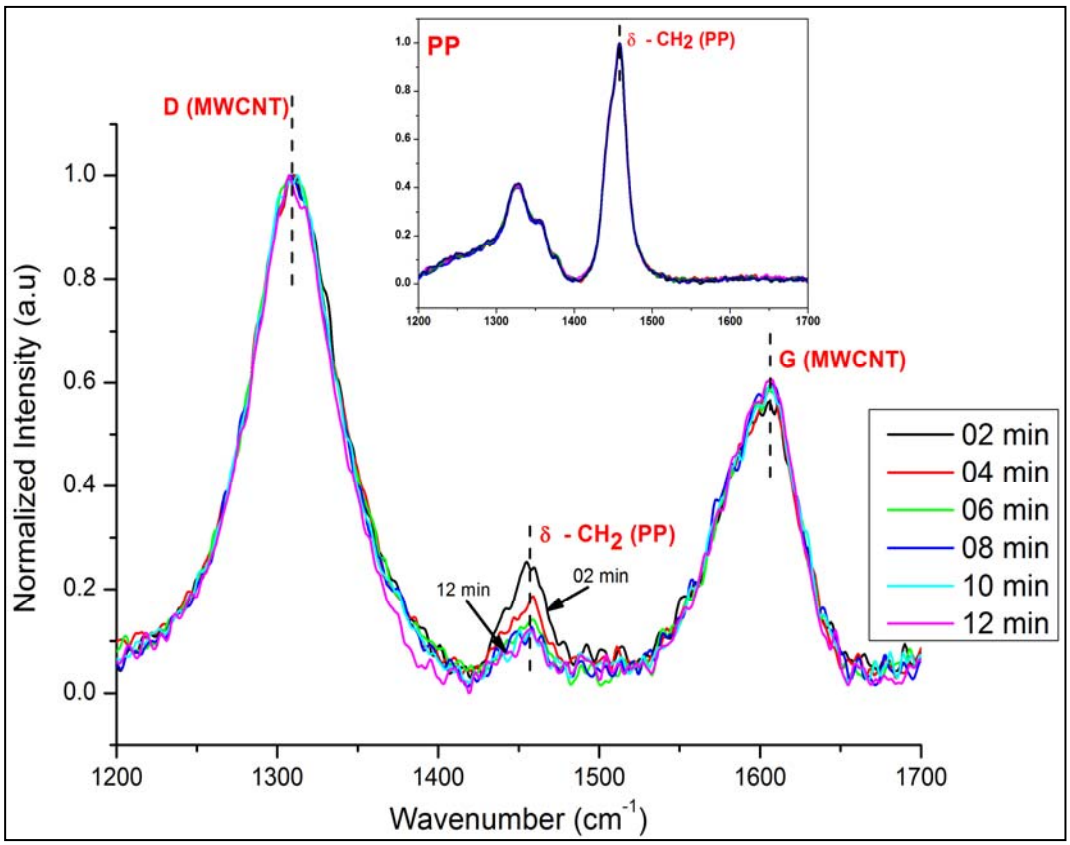

Figure 32. Online Raman Spectra of C1-120 composite. Inset - Online spectra of pure PP

The defect concentration (impurities, disorders etc.) of the MWCNTs as measured on the composite strands is presented in Table 8. The I_D/I_G of as-received MWCNT increases from 1.42 to 1.54 in C1-120 composite. The shear due to the melt mixing could have resulted in nanotube breakage resulting in a loss of the aspect ratio which could have induced an increased CNT defect concentration. The I_D/I_G of C1-120-Px composite is 1.59 which is even higher than its counterpart processed without peroxides. Hence, this increase in the I_D/I_G ratio for the composites containing peroxides processed similar to those composites without peroxides can be attributed to the functionalization of CNTs in the melt.

It was interesting to observe that composites processed with lower mixing speeds showed more defects than those processed at higher mixing speeds in spite of the former experiencing lower magnitude of shear stresses. The increase in the dispersion quality at increased rates of shear would have presented enhanced surface area of the CNT to the intense laser radiation induced by the Raman measurements. Raman measurement effects have been shown to purify the CNT resulting in lower I_D/I_G ratios in pure MWCNT as well as its composites with SBR in the work of Bokobza and Zhang [114]. Similar effects are also observed in Figure 32 which shows the spectra of C1-120 composite. With increase in the residence time in the mixer the intensity of the G band increases indicating purification of the CNT due to prolonged exposure to laser radiation. CNT shortening during melt mixing was

found to lead to lower MWCNT defects as shown on composite of PC with MWCNT by Krause et al. [116], which could have been due to breaking of the nanotubes at the defect sites resulting in purer CNTs. This aspect cannot be excluded in these experiments as the purity of the CNTs in the composites processed at 120 rpm seems to be higher than in those processed at 70 rpm.

Table 8. Defect concentration of MWCNTs in the as-received form and in the composites

	I_D/I_G
As-received MWCNT	1.42 ± 0.03
C1-120	1.54 ± 0.02
C1-70	1.59 ± 0.01
C2-120	1.62 ± 0.01
C1-120-Px	1.59 ± 0.02
C1-70-Px	1.65 ± 0.02
C2-120-Px	1.72 ± 0.02

From Figure 32 it is also seen that the intensity of the δ-CH_2 peak of PP decreases with increase in the mixing time. The increase in the amount of dispersed CNTs with time presents an enhanced surface area available for the PP to interact with the CNTs, resulting in the domination of the CNT signal over that of PP. The inset of Figure 32 shows the Raman spectra of pure PP measured similar to that of the composite. No change was observed in the intensity of the PP peaks as a function of time and hence polymer degradation is not expected to play a role in decreasing the intensity of the δ-CH_2 peak in the composite. Hence, the observed decrease in the intensity of δ-CH_2 peak could be attributed to the combined effect of filler dispersion and polymer-CNT interaction.

The influences of the processing speed and MWCNT content on the Raman spectra of the composites processed with and without peroxides are presented in Figures 33 and 34. At the same MWCNT loading, the intensity of the δ-CH_2 peak of PP is lower for composites processed with peroxides indicating that dispersion and polymer-CNT interactions are facilitated by the addition of peroxides. However, the I_D/I_G ratio for the MWCNT is higher for composites with peroxides (due to functionalization of the CNTs discussed earlier) which could negatively affect mechanical properties of the composites. The enhanced CNT dispersion as seen from Figure 31 (a&b) results in the increased absorption of incident laser radiation in the composites processed at higher screw speeds. Hence, the polymer signature of the composites (containing 1 wt.% CNT) processed with 120 rpm is weaker than those of the composites processed with 70 rpm (Figure 33). It is also logical that the intensity of the

polymer signal would weaken on increased filler loading fraction at similar processing conditions (Figure 34).

It can hence be summarized from these findings that peroxide addition results in better dispersion of the MWCNTs, but at the same time results in increased CNT defects as a result of functionalization. This confirms that the slight lowering of structural properties and crystallinity of the composites with peroxides in section 5.4 is a result of the loss in the structural integrity of the CNTs on functionalization with peroxides.

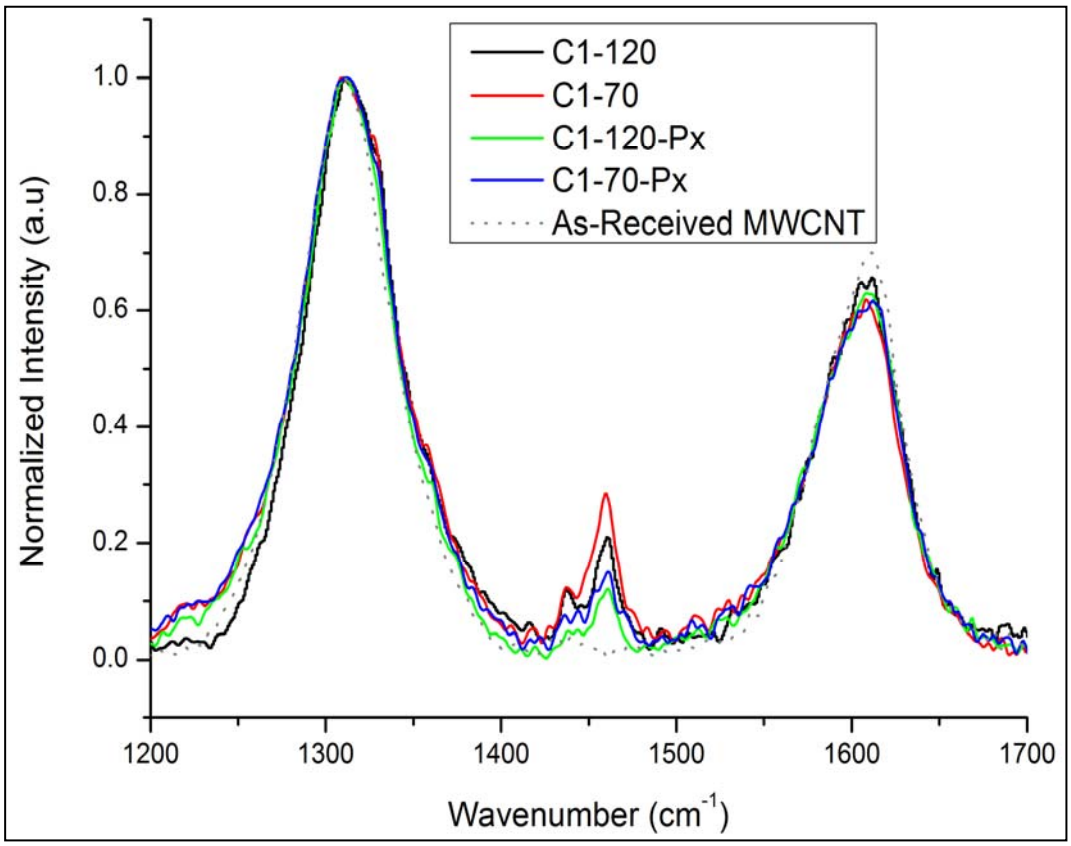

Figure 33. Variation in the offline spectra of composites as a function of processing speed.

6.3 Measurement of Electrical Volume Resistivity

The electrical volume resistivity of compression molded PP was reduced from 10^{15} to 10^{1} Ωm on 1 wt. %MWCNT addition irrespective of the processing speed in the melt mixer indicating that the composite has electrically percolated. Composites with peroxides show one order of magnitude lower volume resistivity than those without peroxides which principally arises due to enhanced filler dispersion in peroxide modified PP. The increase in the MWCNT content to 2 wt.% results in a volume resistivity of 10^{-1} Ωm and the effect of peroxide addition is not dominant at this loading.

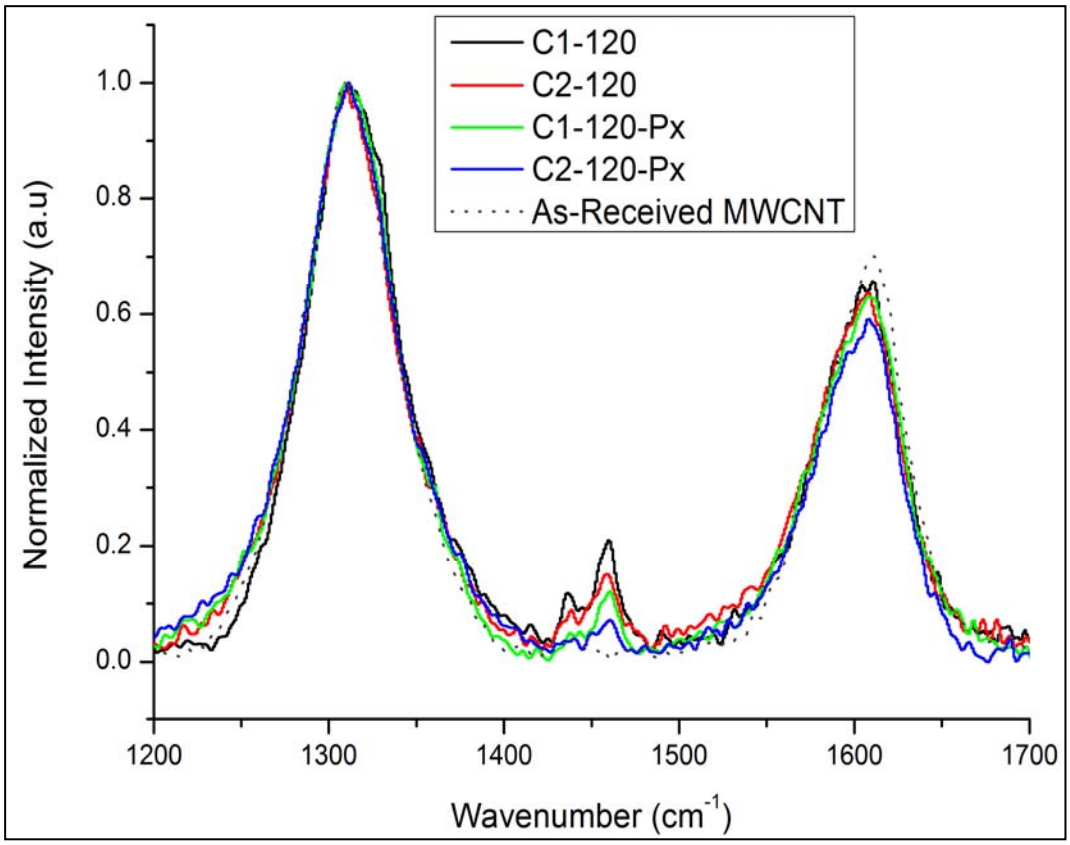

Figure 34. Variation in the offline spectra of composites as a function of MWCNT loading

6.4 Synopsis

The incorporation of peroxide into PP resulted in an improvement in the quality of MWCNT dispersion in PP based composites with 1 and 2 wt.% MWCNT. Raman spectroscopy of MWCNT and its composites showed no peak shifts as a function of MWCNT content or the level of dispersion. The addition of peroxide lowers the intensity of the δ-CH_2 peak of PP in the composite spectra indicating an enhancement in dispersion. The lowered intensity of the G-band with respect to the D-band in the composites containing peroxide compared to those without peroxide confirm peroxide initiated functionalization on the side walls of MWCNTs. This has played a strong role in enhancing the FWHM of the composites containing peroxide compared to its pristine counterpart due to improved polymer-CNT interaction and enhanced CNT dispersion quality in PP. The electrical resistivity achieved with peroxide modified PP-1 wt.% MWCNT composites is at least one order of magnitude lower than composites without peroxide addition.

Summarizing observations from Chapters 5 and 6, it is seen that the peroxide addition results in significant improvements in the quality of MWCNT dispersion in leading to substantially enhanced improved electrical properties of the composites. On the contrary, the functionalization of the side walls of the CNTs by peroxides results in increased defect density therein affecting the structural characteristics of the as-received MWCNTs. This has resulted in slightly lowered mechanical properties of the composite containing peroxides.

7. A Multi-functional Composite with PP, MWCNT and Short Glass Fibers

The results from Chapters 4, 5, and 6 show that excellent qualities of MWCNT dispersion can be achieved in a PP matrix by the optimization of process parameters and by the usage of peroxides as a functional additive. This has led to substantially improved electrical properties of the composites at very low CNT concentration. It was also seen that the mechanical properties of the composites were not considerably enhanced in spite of achieving a very good MWCNT dispersion quality in PP. The inability to develop good mechanical properties of the composites with MWCNTs in spite of achieving excellent CNT dispersions in different thermoplastic matrices in literature was discussed earlier in the state of art. Hence, an alternate strategy would have to be to employ more economical glass fibers as secondary fillers to take advantage of their well-established structural characteristics in the final part properties. Glass fibers are also attractive as they render themselves to be processed with conventional composite processing approaches.

Glass fiber filled PP has exerted its potential in the automotive industry owing to the significant mechanical reinforcements at competitive economics. In this chapter, the principal objective is to evaluate the morphology and the extent to which each of these fillers would contribute to the enhancement in the properties of the bi-filler composite.

Short glass fibers were incorporated into both pristine and peroxide modified PP-MWCNT masterbatches via twin-screw extrusion in view of developing a multifunctional composite taking advantage of the mechanical reinforcing capabilities of glass fibers and the ability of CNT to enhance electrical and thermal properties of the composites. The production of a bi-filler composite of PP with MWCNTs and glass fibers by twin-screw extrusion and their subsequent processing with injection and compression molding are presented with discussions on the morphology, rheology, electrical, mechanical, and thermal properties of the composites. The screw configuration for the production of the PP-MWCNT and (PP-Px) masterbatches was identical to that employed in Chapter 5 while the screw configuration listed in Appendix E was employed for the glass fiber addition to the previously processed masterbatches. A list of processed composites is presented in Table 9.

7.1 Morphology of the Composites

The representative optical micrographs of the MWCNT incorporated PP composites along with the SME and A_f are presented in Figure 35. The C2.5 composite processed at 1100 rpm shows an A_f of 3.5 % which is 17 % higher than that of the C2.5-Px composite eventhough the former was processed with more than twice the SME than the latter. The composite C1.5-Px also shows very good filler dispersion with a very low A_f of 2.6 %. The addition of peroxides have been shown to reduce the viscosity and enhance the polarity of PP (in Chapter 5) and also induce surface functionalities on MWCNTs (in Chapter 6) resulting in better dispersions on both C1.5-Px ad C2.5-Px.

Table 9. List of processed composites and their compounding parameters

Nomenclature	Peroxide (wt.%)	MWCNT (wt.%)	Glass fiber (wt.%)	Principal Masterbatch	N (rpm), M (kg/h)
PP					500, 7.5
C2.5		2.5			1100, 7.5
G10			10		360, 20
G20			20		360, 20
C2.5-G10			10	C2.5	360, 20
C2.5-G20			20	C2.5	360, 20
PP-Px	1				500, 7.5
C1.5-Px	1	1.5			500, 7.5
C2.5-Px	1	2.5			500, 7.5
G10-Px	1		10		360, 20
G20-Px	1		20		360, 20
C1.5-G10-Px	1		10	C1.5-Px	360, 20
C1.5-G20-Px	1		20	C1.5-Px	360, 20
C2.5-G10-Px	1		10	C2.5-Px	360, 20
C2.5-G20-Px	1		20	C2.5-Px	360, 20

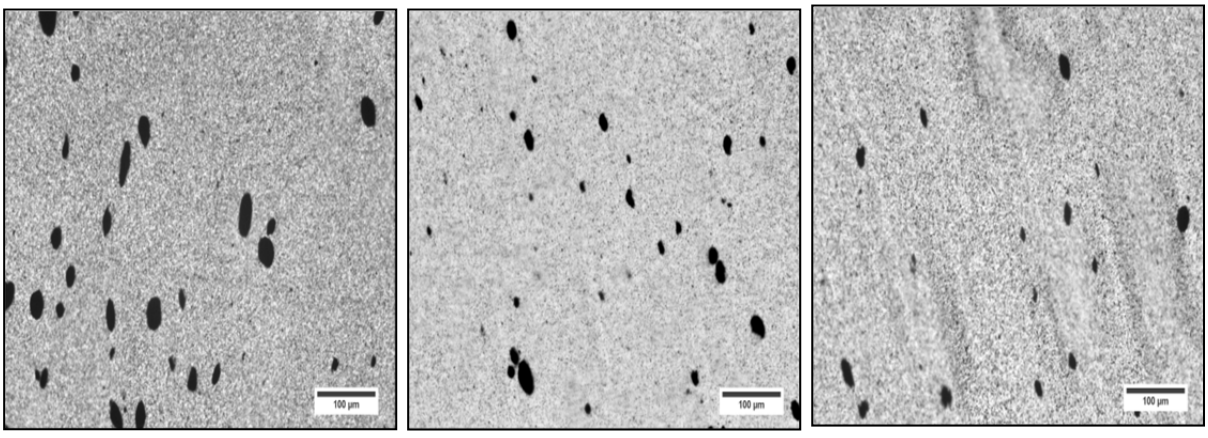

C2.5, SME-1.2 kWh/kg
A_f-3.5 %

C2.5-Px, SME-0.55 kWh/kg
A_f-3.0 %

C1.5-Px, SME-0.48 kWh/kg
A_f-2.6 %

Figure 35. Optical micrographs of the composites containing MWCNT

Representative SEM morphologies of the glass fiber incorporated PP-MWCNT composites are presented in Figure 36. The glass fibers exhibit good interfacial adhesion with the host matrix owing to the compatible sizing on the fiber surface (Figure 36b). Fiber shortening due to extrusion and the injection molding processes cannot be ruled out. Also, the glass fibers seem to be preferentially oriented in the direction of the injection. Highly agglomerated MWCNT morphologies are characteristic of the C2.5-G10 composite (Figure 36c), while better qualities of MWCNT dispersion (with much smaller agglomerates) is envisioned in the composites incorporated with peroxides (Figure 36d). The quality of MWCNT dispersion in the bi-filler composites is expected to improve owing to its re-processing in the extruder for glass fiber addition, but it is impossible to quantify the extent of enhancement.

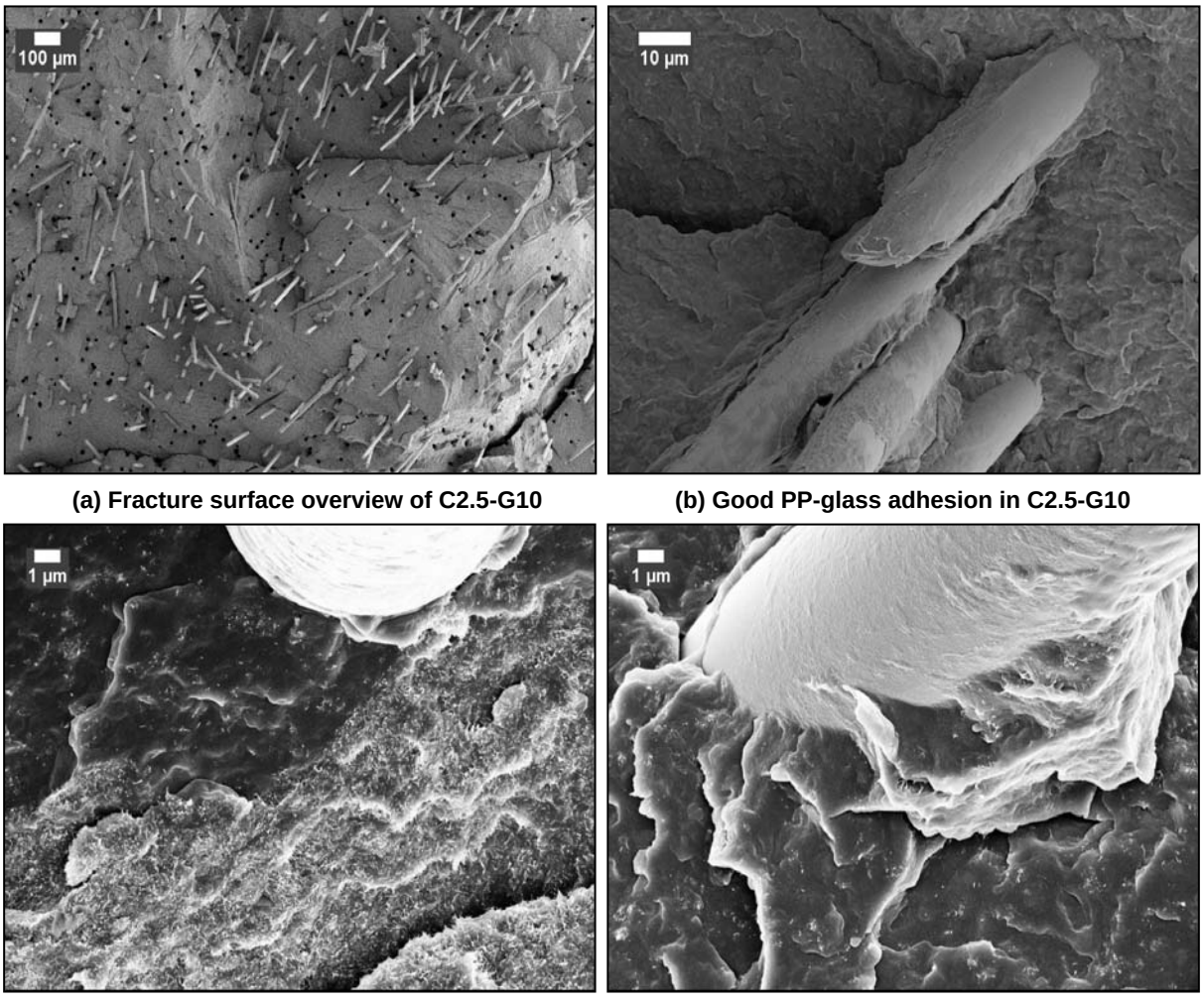

(a) Fracture surface overview of C2.5-G10 **(b) Good PP-glass adhesion in C2.5-G10**

(c) Typical morphology of C2.5-G10 **(d) Typical morphology of C2.5-G10-Px**

Figure 36. Composites containing MWCNT and short glass fibers – SEM morphology

7.2 Melt Rheological Characterization

The dependence of storage modulus (G') and complex viscosity (η*) on frequency for the different composites and their reference samples are shown in Figure 37. The G' of pure PP as expected is reduced on incorporation of peroxides. G10 and G10-Px composites present enhanced G' compared to that of their references owing to the better structural

characteristics of the glass fiber. The addition of MWCNTs considerably enhances the storage modulus of PP and PP-Px. The dependence of G' on frequency is lost at lower frequencies indicating that the composites C2.5, C2.5-Px and C1.5-Px have all rheologically percolated. The higher storage modulus of the composites with the peroxides significantly compensates for the loss of PP modulus on peroxide addition owing to better MWCNT dispersion presenting enhanced surface area for interactions with the polymer. The impact of lower SME input during processing and hence lower extent of CNT shortening for the composites with peroxides cannot be ruled out while interpreting the G' values.

The addition of short glass fibers to the PP-MWCNT and PP-Px-MWCNT masterbatches further enhances the storage modulus of the composites; however the composites without peroxide slightly outperform the composites with peroxide incorporation. The increase in the content of glass fiber addition from 10 wt.% to 20 wt.% does not have a significant impact on the storage modulus of the composites. This was observable on both the composites without (G10, G20) and with peroxide addition (G10-Px, G20-Px). The extent of G' improvement with glass fiber addition is strongly dependent on the nature of the host matrix while that for the nanofiller reinforcements is strongly dependent on the available surface area of polymer-filler interaction.

The addition of peroxide has resulted in a reduction in complex viscosity by close to 300 % at lower rates of shear indicative of the reduction in the molecular weight of the polymer on reaction with peroxides. The addition of glass fibers to PP and PP-Px resulted in an increase in η* which is characteristic feature of any filler reinforcement. The incorporation of 2.5 wt.% MWCNT to both PP and PP-Px resulted in a substantial increase in viscosity of the composites; however the level of increase in PP-Px is close to 2.2 times higher than those attained with PP. In spite of the significant viscosity reduction of PP-Px, enhanced MWCNT dispersion quality in the composites with peroxides has resulted in enhanced surface area for polymer-MWCNT interactions which has contributed to an increase in the viscosity. Shear thinning is also predominant in composites with well dispersed MWCNT morphologies at higher frequencies owing to the increased frictional forces generated by the enhanced polymer-filler and filler-filler surface interactions.

The addition of glass fibers to C2.5, C2.5-Px and C1.5-Px further increases the viscosity of the composites, and the level of glass fiber reinforcement did not have an influence on viscosity of the composites, a trend earlier observed with storage modulus. Likewise, the composites without peroxide addition showed a higher viscosity on glass addition compared to those with peroxides at the same MWCNT loading.

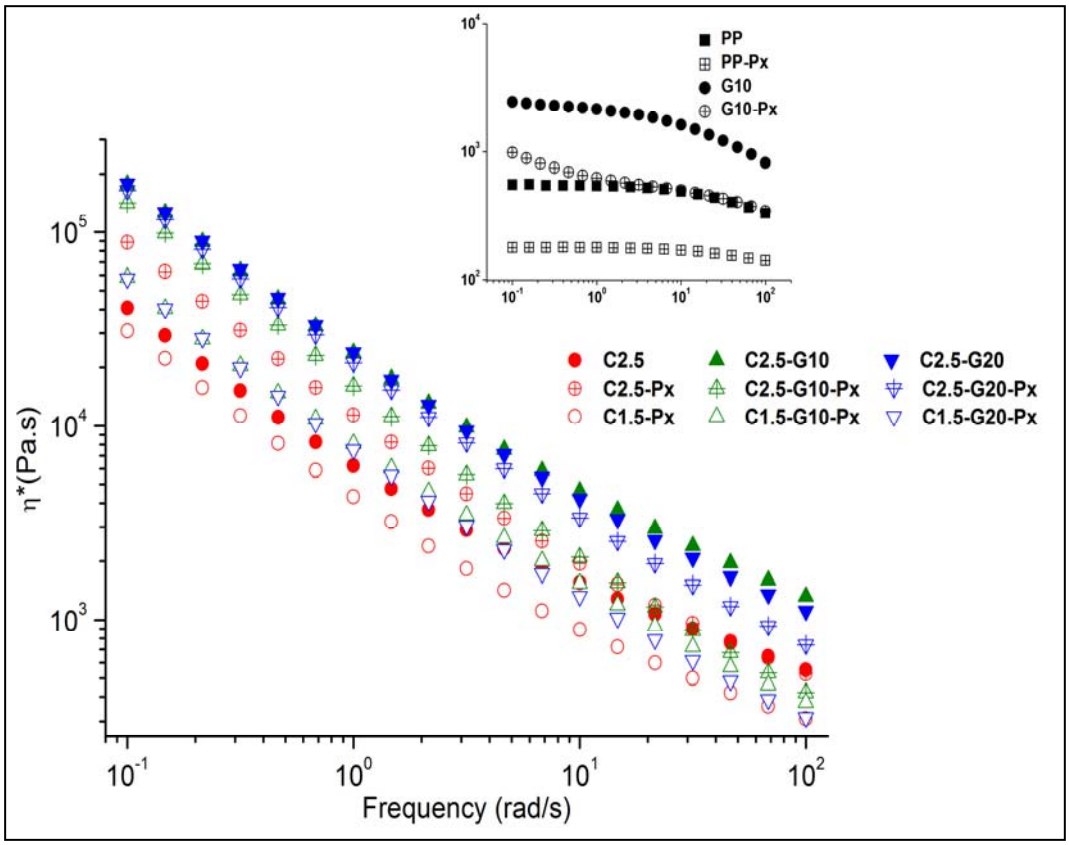

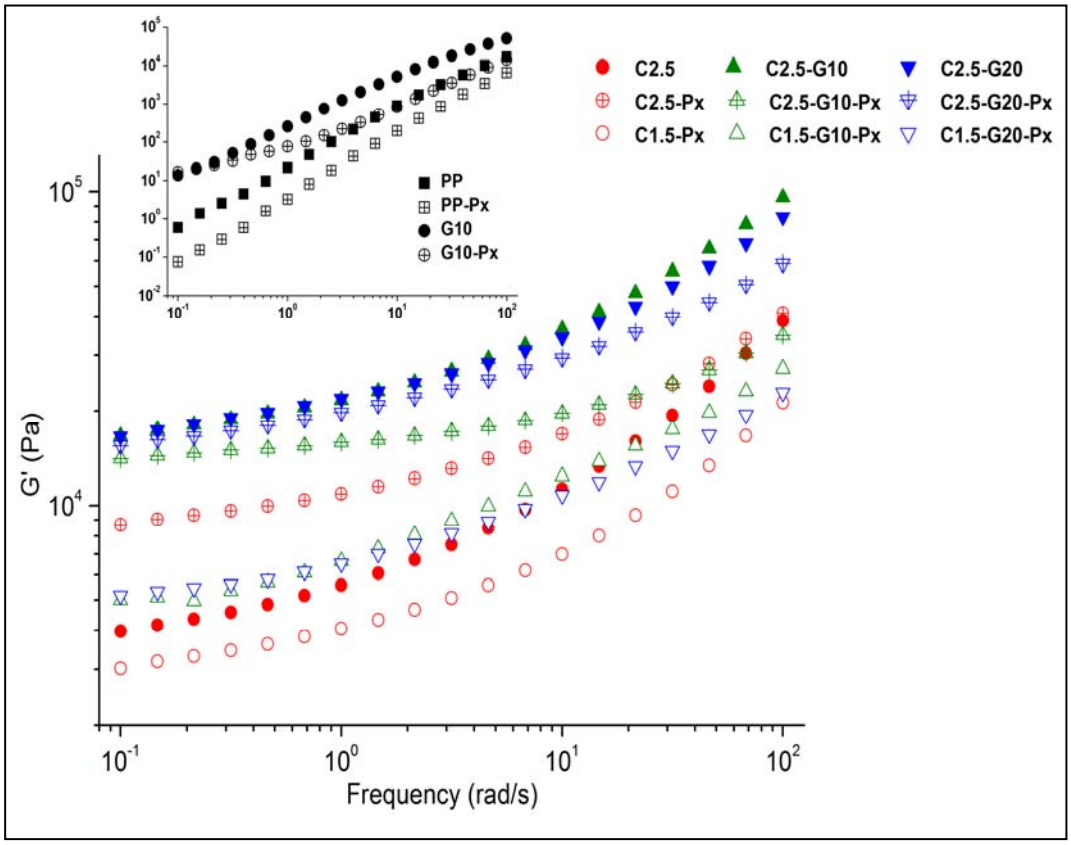

Figure 37. G' and η* of the composites with and without peroxides

7.3 Electrical Properties of the Composites

The electrical volume resistivity of the different composites measured on the extruded strands, compression molded and injection molded bars is presented in Figure 38. The electrical volume resistivity of PP and PP-Px are approximately 10^{15} Ωm as measured on samples processed by all these processes. The volume resistivities of C2.5 and C2.5-Px composites as measured on the extruded strands are 1.63 Ωm and 0.26 Ωm respectively with negligible deviation. The composites have electrically percolated and the lower resistivity of the C2.5-Px composite compared to the C2.5 composite is primarily due to the enhancement in the quality of MWCNT dispersion in the former (refer to Figure 35). The increase in the volume fraction of the MWCNT beyond the resolution of the optical microscope in the C2.5-Px composite has resulted in better conductive properties as expected.

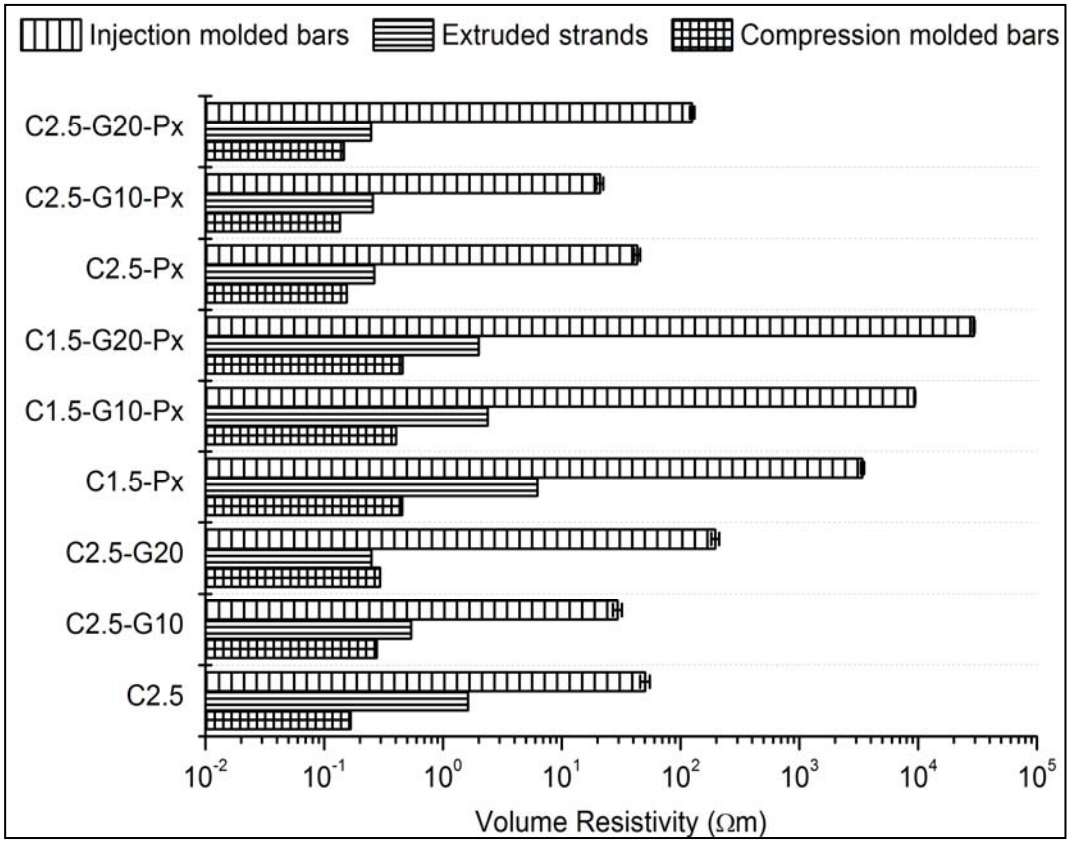

Figure 38. Electrical properties of the extruded, compressed, and injected samples

The volume resistivity of the extruded C1.5-Px composite is 6.23 Ωm and this is not very different from those observed on the C2.5 composite. The addition of 10 wt.% and 20 wt.% glass fibers to all of these composites (both with and without peroxides) has led to a lowering of the composite resistivity. The additional thermo-mechanical history on re-processing of the polymer-MWCNT masterbatch for the addition of glass fibers could have resulted in further enhancement in the quality of MWCNT dispersion contributing to the lowering of resistivity. It must be remembered that the glass fiber addition correspondingly lowers the overall CNT

weight fraction in the composite, but the ratio of the polymer to the CNT would be kept as before which is important for the formation of the percolating conductive pathway.

The injection molded composites C2.5 and C2.5-Px show a volume resistivity of 50.3 Ωm and 43.1 Ωm respectively with negligible deviation. This resistivity is clearly higher than those observed on the extruded strands even if these composites have passed limits of electrical percolation by formation of a conductive network by the interconnected CNTs. Formation of a skin-core structure, orientation of the fillers due to the secondary shear from the injection molding process, reduction in the aspect ratio of the CNT due to the shear and during the passage of the melt through the die orifice could have all resulted higher resistivity values as detailed in Chapter 4 & 5. These results also show the importance of having a good primary dispersion in the composite. The addition of 10 wt.% glass fibers to C2.5 and C2.5-Px has resulted in slightly lower resistivities of the composites, but on 20 wt.% glass fiber addition the resistivity increases. The enhancement in the level of MWCNT dispersion during re-processing of the C2.5 and the C2.5-Px masterbatches could have led to lower resistivity on 10 wt.% glass fiber addition in spite of additional effects like glass orientation along the direction of melt flow effect during the injection molding process which could have negatively affected the bulk properties. The increase in the bulk resistivity of the composites on 20 wt.% glass addition could be directed to the fact that glass fibers could play a role towards orientating the CNTs along the direction of flow (potentially losing the 3-D connections) during injection molding; due to the enhanced shear stresses in the melt. This could have had a strong influence in affecting the multiple conductive pathways. Also, the C1.5-Px composite showing a volume resistivity of 3.39×10^3 Ωm has electrically percolated but has higher resistivity compared to the C2.5-Px composite principally owing to higher filler volume fraction in the latter.

Secondary processing of the extruded composites on a compression molding machine is expected to result in better electrical properties than those observed on the injection molded composites (as elaborated previously in Chapter 5). This is evident as the volume resistivities of C2.5, C2.5-Px and C1.5-Px composites are close to two orders lower than those of their injection molded counterparts. Sufficiently large numbers of conductive pathways are expected to be formed on compression molding due to the nature of the process itself and hence the addition of glass fibers did not have a considerable effect in regulating the electrical properties of the bi-filler composites (unlike the extruded and the injection molded composites). Compression molding is not however a viable industrial approach.

7.4 Mechanical Properties of the Composites

The mechanical properties of the different composites along with their reference samples are presented in Figure 39. The modulus of PP (0.69 GPa) and PP-Px (0.69 GPa) is enhanced by 38 % and 26 % respectively on the addition of 2.5 wt.% MWCNTs, while it is significantly enhanced by 186 % and 175 % respectively on the addition of 10 wt.% of glass fibers. The addition of 20 wt.% of glass fibers further attributed to an absolute increase in the modulus of

PP and PP-Px by 394 % and 364 % respectively. The fact that the modulus of glass fibers is substantially higher than that of the CNT agglomerates attributes to the enhancement in the composite properties within the elastic limits. The rate of modulus enhancement in C1.5-Px and C2.5-Px were lower than those observed on their counterparts without peroxides in spite of identical modulus values for PP and PP-Px following explanatory trends in Chapters 5 and 6. It was interesting to note that the modulus enhancements caused by both MWCNT and glass fibers in the bi-filler composite was greater than the additive effect of their individual reinforcements on PP. The elastic modulus of PP and PP-Px were enhanced 440 % and 423 % respectively on the composite containing 2.5 wt.% MWCNT and 20 wt.% glass fibers. The properties observable on the composite 1.5 wt.% MWCNT and 10 wt.% and 20 wt.% glass was not very different from the corresponding composite with 2.5 wt.% MWCNT without peroxides.

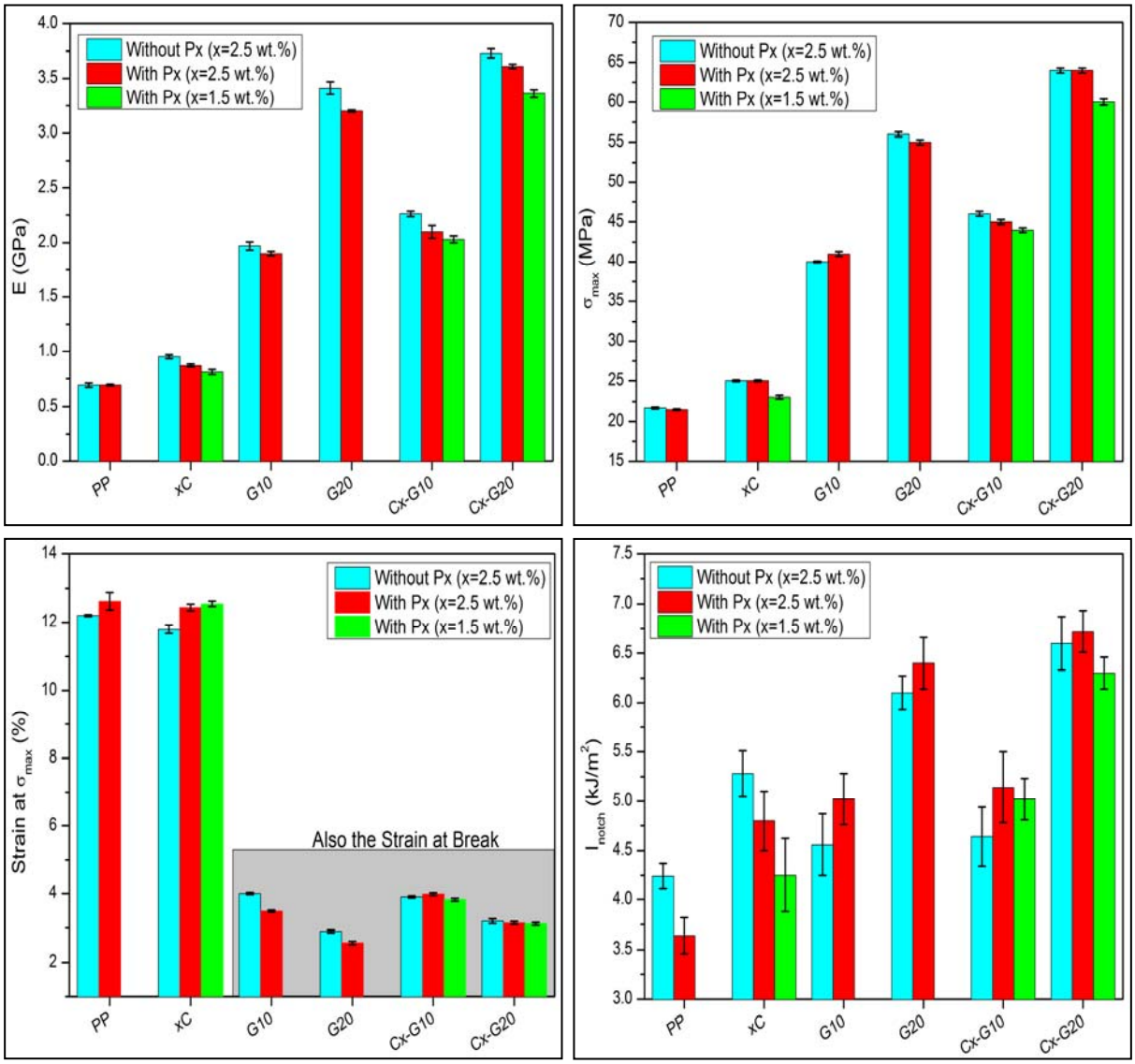

Figure 39. Mechanical properties of the processed composites

The tensile strength of PP and PP-Px are enhanced by 16 % on incorporation of 2.5 wt.% MWCNT, while 1.5 wt.% MWCNT in PP-Px resulted in an increase of 7 %. The difference in

the qualities of dispersion was not significantly expressed in the composites with and without peroxides at the same MWCNT loading. A very good interfacial adhesion between the PP host and glass fiber (Figure 36a) has contributed significantly to an 80 % and 160 % improvement in σ_{max} respectively on 10 wt.% and 20 wt.% glass fiber addition to both PP and PP-Px. The σ_{max} of the composites containing both MWCNT and glass fibers show trends similar to those observed with modulus enhancements. The tensile strength of C2.5-G20, C2.5-G20-Px, and C1.5-G20-Px are 200 %, 200 % and 180 % higher respectively compared to its pristine reference samples of PP and PP-Px and are significant numbers for employing these materials for commercial applications.

The bi-filler system in PP is composed of three interfaces namely the polymer-CNT interface, polymer-glass fiber interface and the CNT-glass interface. There is a slight probability that the enhanced CNT dispersion on re-processing of the masterbatch leads to improvements in mechanical behaviour, but this would not be significant enough as seen from the individual results on PP-CNT composites and PP-Px-CNT composites. There is no strong reason to believe why the polymer-glass fiber interface would improve in the bi-filler composite compared to what it would have been without the CNT addition. Also, the glass fiber-CNT interface would not in principal improve unless otherwise the sizing on the glass fiber is compatible with the CNT (which does not seem to be the case as CNTs could not be seen to be collected on the surface of the glass fibers). Hence, the contribution for the considerable enhancement in the structural characteristics of the bi-filler composite would have to evolve from orientation effects. It is highly probable that with increasing additions of glass, the CNTs would also be forced to be oriented along the direction of flow (due to additional shear stresses in the melt as a result of glass fiber addition) leading to enhanced unidirectional properties. This is evident from the fact that the tensile strength of PP-Px (21.5 MPa) is enhanced by 105 % and 180 % in the C1.5-G10-Px and C1.5-G20-Px composites respectively, while the increase was 91 % and 156 % respectively on the G10-Px and G20-Px composites (The observed increase in the C1.5-Px composite was only 7 %). The orientation effects as discussed here was also observed with the increase in the bulk electrical resistivity of the injection molded C2.5 and C2.5-Px composites on 20 wt.% glass fiber addition (Figure 38).

The stress-strain curves of PP and PP-Px exhibited a behaviour characteristic of a ductile material with failure not visible even after 700 % elongation. However, the measurements were stopped at 70 % strain as the design of any application would only take into account of the σ_{max}. The strain at σ_{max} of PP and PP-Px were slightly reduced by MWCNT addition. Glass fiber incorporation of 10 wt.% and 20 wt.% significantly lowered the ductility of PP and PP-Px by 205 % and 262 % and 321 % and 391 % respectively, and the fracture surface of the composites resembled a typical brittle fracture with crazed surfaces. The strain at σ_{max} also happens to be the strain at break (ε_{break}) for these composites. However, the strain at σ_{max} is slightly higher for the bi-filler composites compared to those composites containing only glass fibers. The strain at σ_{max} of the composites containing the same amount of glass

fibers and varying content of MWCNT, with and without peroxide are close to being identical indicating that the addition of glass greatly influences the brittleness of the composites.

Although the addition of peroxides lowers the notched impact strength of PP (4.24 kJ/m^2) by 16 %, the addition of 2.5 wt.% MWCNT to PP and PP-Px enhances composite toughness by 25 % and 32 % respectively. Improved CNT dispersion morphology in the C2.5-Px composite (Figure 35) resulted in better impact properties. The composite with 2.5 wt.% MWCNT loading shows higher impact properties than the composite with 1.5 wt.% MWCNT loading, pointing out that the impact properties of the composites is also dependent on CNT loading.

The notched impact strength in the bi-filler composite is dominated by the presence of the glass fibers. Fiber pullout considered as one of the main energy absorbing mechanisms resulting in enhanced toughness is significantly observable from SEM morphologies in Figure 36a. Also, a strong interface between the glass fibers and PP (seen from improvement in the tensile strength of the composites) could have resulted in the cracks being repeatedly deflected at the fiber-matrix interface contributing to better impact properties of the composites. The improvement in the notched impact strength on the increasing addition of glass fibers is higher in PP-Px compared to PP. The notched impact strength of PP-Px (3.64 kJ/m^2) was improved by 38 % and 75 % on the C1.5-G10-Px and C1.5-G20-Px composites respectively.

The observations from the mechanical properties show that the structural characteristics of the PP-MWCNT and the PP-Px-MWCNT composites have been substantially enhanced by the addition of glass fibers as secondary fillers.

7.5 Thermal Properties of the Composites

The addition of 2.5 wt.% MWCNT to PP results in the enhancement of onset (T_o) and maximum temperature of degradation (T_{max}) of PP by 31 °C and 116 °C respectively (Figure 40), very similar to those reported in Chapter 5. The addition of CNTs to PP-Px also results in considerable enhancement in the thermal stability of the composites. The incorporation of glass fibers to PP, results in an enhanced overall composite thermal stability. This is primarily due to the substitution of the overall volume fraction of the PP by 10 wt.% and 20 wt.% of glass.

The oxidative thermal stability of the bi-filler composites are lower than those of the composites containing only CNTs because the glass addition results in the reduction of the overall volume fraction of CNTs in the composites; leading to decrease in the magnitude by which free radicals could be received by the CNTs. Increasing glass addition further lowers the T_o and T_{max} of the composites. However, the thermal property of the bi-filler composites is significantly higher than the reference PP and PP-Px.

The magnitude of the increase in T_o (42 °C) and T_{max} (117 °C) while 2.5 wt.% MWCNT is incorporated into PP-Px is higher than compared to the effects observed in PP, principally

due to the enhanced surface area of MWCNTs on virtue of its better dispersion. Also the addition of only 1.5 wt.% MWCNTs to PP-Px resulted in a T_o and T_{max} of 296 °C and 419 °C which is very similar to the values observed on the C2.5 composite. The bi-filler composites with peroxides show better thermal properties but the magnitude difference in thermal properties between C1.5-G10-Px and C2.5-G10-Px is not considerable, similar to observations in Chapter 5. Increasing addition of glass fibers to C1.5-Px and C2.5-Px composites did not affect T_o even though the overall volume fraction of CNTs in these composites would have been lower, T_{max} however is decreased.

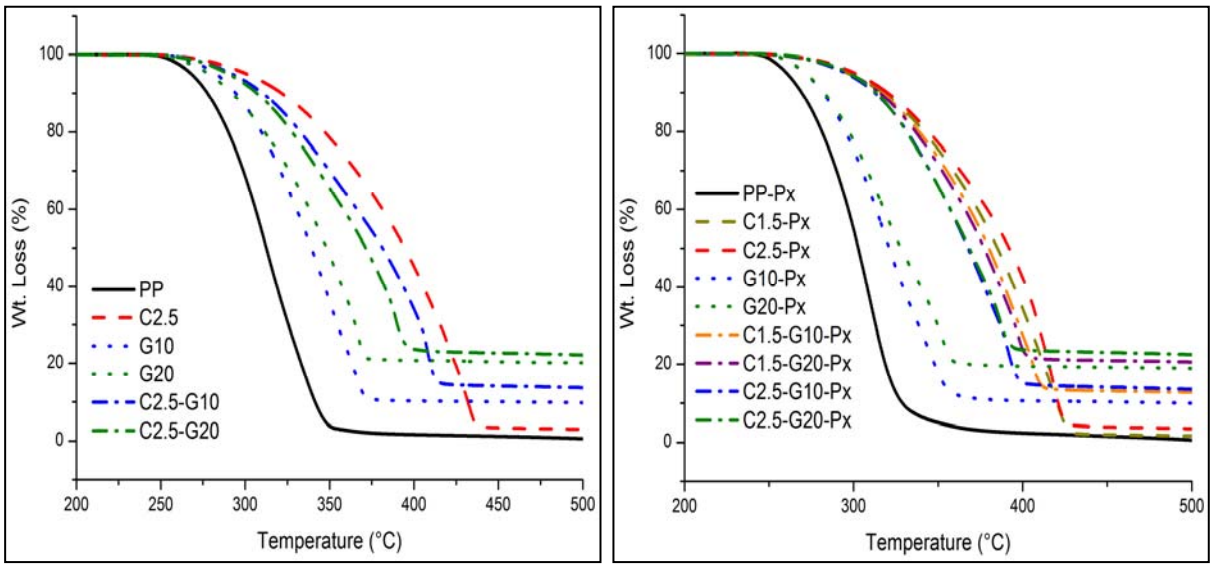

Figure 40. Thermal stability of the bi-filler composites with and without peroxides

7.6 Synopsis

A bi-filler system of MWCNT and glass fibers was successfully incorporated into PP and PP-Px via twin-screw extrusion and the composites were subjected to secondary processing via injection molding and compression molding.

SEM morphologies show a good interfacial adhesion between glass fibers and PP and morphology of less agglomerated and well dispersed MWCNT on composites with peroxides compared to its pristine counterpart. Rheological investigations show inferior storage modulus and complex viscosity for PP-Px compared to PP, but this loss is compensated by the addition of MWCNT to PP-Px. Glass fiber addition contributed to enhanced storage modulus and viscosity of both the pristine PP and PP-Px and their composites with CNTs, but increased addition of glass fibers did not have a significant impact in enhancing the storage modulus.

The re-processing of the PP-MWCNT masterbatches for glass fiber addition resulted in slightly lower electrical resistivities on extruded composites. The resistivities on the compression molded composites were almost identical, indicating the addition of glass fibers did not alter the re-agglomeration of the previously dispersed CNTs during the compression molding process. Electrical percolation was observed on all the composites with MWCNT

and the compression molded bi-filler composites present at least 2 orders lower electrical volume resistivity compared to its injection molded counterparts. Higher resistivities are noticed on injection molded composites with 20 wt.% glass fiber loadings as a result of possibly enhanced orientation of the CNTs (due to additional shear stresses in the melt due to the presence of glass fibers) and the potential formation of an isolative polymer skin. The properties observable on the peroxide incorporated composites with 1.5 wt.% MWCNT and glass fibers are not very different than those observed with composites not modified with peroxides and containing 2.5 wt.% MWCNT.

Modulus enhancements of 440 % and 423 % respectively were observed on the PP and PP-Px composite containing 2.5 wt.% MWCNT and 20 wt.% glass fibers. Also, the tensile strength increases by 200 % on an identical composition of glass fibers and MWCNT in both PP and PP-Px. The modulus and the strength of the bi-filler composites were greater than the additive effect of their individual reinforcements on PP, however with a strong compromise on the ductility of the composites. It is highly probable that with increasing additions of glass, the CNTs would also be forced to be oriented along the direction of flow due to the relatively high shear leading to enhanced unidirectional properties. Low MWCNT agglomerate fractions in the composites containing peroxides contribute to better impact properties. Also, a strong interface between the glass fibers and PP (seen from improvement in the tensile strength of the composites) could have resulted in the cracks being repeatedly deflected at the fiber-matrix interface. The notched impact strength of PP-Px (3.64 kJ/m^2) was improved by 38 % and 75 % on the C1.5-G10-Px and C1.5-G20-Px respectively.

Thermal properties of the bi-filler composites are dominated by the presence of MWCNTs owing to their tendency to act as good free radical acceptors on oxidative degradation of PP. Substantial increase in the onset and maximum temperatures of degradation were visible in the bi-filler composites compared to PP, however increasing glass fiber additions lowered the maximum temperature of degradation of the composites.

The inability of the MWCNTs to act alone as agent of structural reinforcement for PP has been compensated by the addition of more economical secondary filler in the form of short glass fibers. The fact that substantially good electrical, thermal and mechanical properties have been achieved on the composite without a strong compromise on the intrinsic characteristics of each of the participating fillers point to a potential development of a highly conductive composite with excellent structural properties, and with low processing and material costs especially on composites containing peroxides.

8. Concluding Remarks and Scope for Future Work

8.1 Conclusions

It is a pre-requisite for any filler to be effectively dispersed in the matrix to translate their inherent characteristics into improved macroscopic properties of the composites. This has exactly been the challenge with MWCNTs whose potential as functional additives for a polyolefin like PP has not been realized thus far. This is because of a wide variety of reasons ranging from the hydrophobicity of PP, incompatibility of CNTs with PP due to a high interfacial energy difference, highly entangled nature of the as-received MWCNTs, high viscosity of the thermoplastic matrix etc. Although a few attempts have been made to solve this puzzle, the observed macroscopic properties have not been quite convincing. This work was principally aimed at solving the aforementioned challenge towards the development of a good multifunctional composite with excellent electrical, thermal and mechanical properties. A pre-requisite of achieving a good CNT dispersion in PP before the addition of glass fibers for structural reinforcement also had to be addressed.

A fundamental understanding of the mechanism of CNT dispersion in thermoplastics led to the designing of trials wherein the influences of principle twin-screw compounding parameters namely screw speed, throughput, extruder barrel temperature, screw configuration, and position of the MWCNT feed were investigated. Higher screw speeds and lower throughputs contributed to a substantial reduction in the undispersed area fraction of the CNTs owing to the higher SME of processing. This led to the composites with 2 wt.% MWCNT loading exhibit similar electrical properties to those achievable on a composite containing 5 wt.% MWCNT. In a composite that had not electrically percolated, a screw configuration which could generate higher SME led to a decrease in the electrical resistivity at higher operating throughputs. Feeding of the MWCNTs into the polymer melt with a side feed resulted in better MWCNT dispersion and hence improved mechanical and electrical properties of the composite than feeding the MWCNTs with the polymer in the main feeding hopper. A novel setup to measure the resistance of the melt online was developed and used which enabled monitoring of the quality of the produced composites, in addition to serving as a tool to predicting the offline electrical properties of the composite during processing.

The incorporation of peroxides as a reactive functional additive during the processing of PP-MWCNT composites resulted in a substantial improvement in the quality of MWCNT dispersion. The A_f of a PP-2 wt.% MWCNT composite processed at a screw speed of 500 rpm was lowered from 8.28 % to 2.9 % on peroxide addition at 15 % lower SME of processing. Also this composite with peroxide showed a better CNT dispersion morphology than the PP-2 wt.% MWCNT composite (A_f=3.05 %) processed at 1100 rpm (SME more than two times than that of the composite processed with peroxides). It is thus seen that peroxide addition resulted in significantly improved MWCNT dispersion at less than half the SME required for processing without them. The lowering of the complex viscosity of PP (to about 1/3rd) and enhanced hydrophilicity of PP (the surface tension of PP was lowered to 21.8

mN/m with a 360 % improvement in the polar component) would have resulted in better melt infiltration and wetting of the CNT agglomerates respectively leading to enhanced quality of filler dispersion. In situ Raman spectroscopy observation during processing show increased I_D/I_G ratio of the characteristic CNT peaks on peroxide addition pointing to reactive functionalization of CNT by peroxides, leading to better CNT dispersion and possible structural damage to the CNTs. Melt rheology data indicated significant enhancement in storage modulus and the complex viscosity of the composites with CNT addition to peroxide modified PP owing to increased CNT surface area for polymer-CNT interactions. As a consequence of enhanced CNT dispersion, the electrical percolation threshold of the composites occurs around 0.4 wt.% MWCNT loading and the magnitude is comparable to results achieved on thermoset-CNT composites. It is also observed that the state of primary dispersion from the compounding process is crucial for achieving good macroscopic properties on secondary processing by injection and compression molding. The electrical properties of the injection molded composites however were around four to five orders of magnitude lower than the compression molded composites. Although, the mechanical properties of PP improved slightly upon MWCNT addition, the properties of the composites with peroxides were slightly lower than those without peroxides. The possible structural damage to the CNTs affecting their ability to nucleate PP's crystallinity and lowering of the degree of crystallization of the composites with peroxide compared to PP stands out as a possible cause for the aforementioned. The thermal stability of PP was decreased on peroxide addition as expected, but the addition of CNT compensates for this decrease as the thermal stability of PP-1 wt.% MWCNT composite with peroxides was not very different than that of PP-2 wt.% MWCNT composite without peroxide. The onset and maximum temperature of degradation PP-1 wt.% MWCNT composite with peroxide was close to 40 °C and 85 °C respectively greater than reference PP. The increase in CNT surface area on improved filler dispersion enhances their radical scavenging efficiency resulting in better thermal properties.

The addition of short glass fibers as secondary fillers to the PP-MWCNT composite resulted in a substantial increase in the structural properties. Modulus and tensile strength of the composites containing 2.5 wt.% carbon nanotube and 20 wt.% short glass fiber were enhanced by 440 % and 200 % respectively compared to pure PP, significantly higher than the 38 % and 16 % increase caused on the addition of only 2.5 wt.% carbon nanotubes. Bi-filler composites with peroxides showed similar observations. The modulus and the strength of the bi-filler composites were greater than the additive effect of their individual reinforcements on PP, however with a strong compromise on the ductility of the composites. The impact property of the bi-filler composite was considerably high, due to effective crack deflections from the strong PP-glass fiber interface. The electrical properties of the bi-filler composites generated by a conductive pathway of the dispersed CNTs in the matrix were not negatively affected by the addition of glass fibers, although a minimal increase in the resistivity was observed particularly on injection molded composites. CNT orientation due to increased glass fiber addition is suspected as a possible cause for enhanced mechanical

characteristics and increased bulk resistivity on the bi-filler composites. The enhanced thermal stability of the bi-filler composites was primarily due to the presence of CNTs, with increasing glass fiber addition negatively affecting the temperature of maximum weight loss. A bi-filler composite with excellent electrical, mechanical and thermal properties resulted out of these experiments.

The ability to accomplish excellent MWCNT dispersion qualities by the use of peroxide as a reactive functional additive for both PP and MWCNT eliminated the usage of extremely expensive functionalized carbon nanotubes to produce similar composites. Peroxide addition resulted in significant savings in both material and energy costs. Excellent electrical properties were achievable with extremely low MWCNT concentrations, and the addition of more economic short glass fibers as secondary fillers imparted the desired structural characteristics to the composites. A multifunctional composite with excellent electrical, structural and thermal properties with significant potential for light-weight product development has thus been developed in the framework of this dissertation.

8.2 Scope for Future Work

Addressing the following points would result in value addition for the developed multifunctional composite and hence forms the basis of recommendation for future work.

- Good EMI shielding behaviour can be expected out of these composites owing to good electrical characteristics. There exists a wide range of frequency over which these measurements could be made, and this depends on the intended purpose of the application. Measurement of these characteristics could add to the multifaceted properties of the composite.
- This study employed the use of short glass fibers as secondary fillers to PP in the PP-MWCNT composites. The usage of endless glass fibers could significantly enhance the structural characteristics of these composites owing to the increased retained length of the glass fiber in the composite. Also, an investigation on processing of these composites on an injection molding-compounder would be interesting as it would eliminate the solidification of the extruded melt prior to injection molding thereby eliminating one thermo-mechanical history on the composites.
- Injection molded foaming of PP-MWCNT composite showed promise with the retaining of the electrical characteristics of the solid composites with a 80 % weight reduction, however the bending and the tensile properties decreased by 10-12 % on the foamed composites evaluated at an equivalent property to density ratio to that of the solid composites. The addition of glass as a secondary filler has the potential to compensate this loss leading to the development of a light-weight product. Investigation on injection molded foaming of the bi-filler composites both with physical and chemical blowing agents and optimization of the injection molding parameters could be a wider scope of investigation.

References

[1] Iijima S. Helical microtubules of graphitic carbon, Nature 1991;354:56-8.

[2] Geng Y, Liu MY, Li J, Shi XM, Kim JK. Effects of surfactant treatment on mechanical and electrical properties of CNT/epoxy nanocomposites. Compos A, 2008;39:1876-83.

[3] Kasaliwal G, Göldel A, Pötschke P. Influence of processing conditions in small-scale melt mixing and compression molding on the resistivity and morphology of polycarbonate–MWNT composites. J Appl Polym Sci 2009;112:3494-509.

[4] Krause B, Pötschke P, Häussler L. Influence of small scale melt mixing conditions on electrical resistivity of carbon nanotube–polyamide composites. Compos Sci Technol 2009;69:1505-15.

[5] Villmow T, Pegel S, Pötschke P, Wagenknecht U. Influence of injection molding parameters on the electrical resistivity of polycarbonate filled with multi-walled carbon nanotubes. Compos Sci Technol 2008;68:777-89.

[6] Lellinger D, Yu DH, Ohneiser A, Skipa T, Alig I. Influence of the injection moulding conditions on the in-line measured electrical conductivity of polymer–carbon nanotube composites. Phys Status Solidi B 2008;245:2268-71.

[7] Villmow T, Kretzschmer B, Pötschke P. Influence of screw configuration, residence time, and specific mechanical energy in twin-screw extrusion of polycaprolactone/multi-walled carbon nanotube composites**.** Compos Sci Technol 2010;70:2045-55.

[8] McClory C, Pötschke P, McNally T. Influence of screw speed on electrical and rheological percolation of melt-mixed high-impact polystyrene/MWCNT nanocomposites. Macromol Mat Eng 2011;296:59-69.

[9] Coleman JN, Khan U, Blau WJ, Gun'ko YK. Small but strong: A review of the mechanical properties of carbon nanotube-polymer composites. Carbon 2006;44:1624-52.

[10] Schaefer DW, Justice RS. How nano are nanocomposites? Macromolecules 2007;40:8501-17.

[11] Srivastava R, Banerjee S, Jehnichen D, Voit B, Böhme F. In situ preparation of polyimide composites based on functionalized carbon nanotubes. Macromol Mat Eng 2009;294:96-102.

[12] Bhattacharyya AR, Pötschke P, Häussler L, Fischer D. Reactive compatibilization of melt mixed PA6/SWNT composites: mechanical properties and morphology. Macromol Chem Phys 2005;206:2084-95.

[13] Owens FJ. Properties of composites of fluorinated single-walled carbon nanotubes and polyacrylonitrile. Mater Lett 2005;59:3720-3.

[14] Saeed K, Park SJ. Preparation and properties of multiwalled carbon nanotube/polycaprolactone nanocomposites. J Appl Polym Sci 2007;104:1957-63.

[15] Yuen SM, Ma CCM, Lin YY, Kuan HC. Preparation, morphology and properties of acid and amine modified multiwalled carbon nanotube/polyimide composite. Compos Sci Technol 2007;67:2564-73.

[16] Sandler JKW, Kirk JE, Kinloch IA, Shaffer MSP, Windle AH. Ultra-low electrical percolation threshold in carbon- nanotube-epoxy composites. Polymer 2003;44:5893-9.

[17] Ebbesen TW, Ajayan PM. Large-scale synthesis of carbon nanotubes. Nature 1992;358:220-2.

[18] Ebbesen TW, Hiura H, Fujita J, Ochiai Y, Matsui S, Tanigaki K. Patterns in the bulk growth of carbon nanotubes. Chem Phys Lett 1993;209:83-90.

[19] Dresselhaus MS, Lin YM, Rabin O, Jorio A, Souza Filho AG, Pimenta MA, Saito R, Samsonidze G, Dresselhaus G. Nanowires and nanotubes. Mat Sci Eng C 2003;23:129-40.

[20] Thostenson ET, Ren Z, Chou TW. Advances in the science and technology of carbon nanotubes and their composites: a review, Compos Sci Technol 2001;31:1899-912.

[21] Carbon nanotubes: Properties and applications (Ed.: O'Connell MJ). Taylor & Francis, Boca Raton, 2006.

[22] Smalley RE, Hauge RH, Kittrell WC, Sivarajan R, Strano MS, Bachilo SM, Weisman RB. Method for separating single-walled carbon nanotubes and compositions thereof. United States Patent 7,074,310; 2006.

[23] Dresselhaus MS, Dresselhaus G, Saito R. Physics of carbon nanotubes. Carbon 1995;33:883–91.

[24] Understanding carbon nanotubes from basics to application (Eds.: Loiseau A, Launois-Bernede P, Petit P, Roche S, Salvetat JP). Springer, Berlin, 2006.

[25] Gore, Sane A. Flame Synthesis of Carbon Nanotubes, Carbon Nanotubes - Synthesis, Characterization, Applications (Ed.:Yellampalli S). http://www.intechopen.com/books/carbon-nanotubes-synthesis-characterization-applications/flame-synthesis-of-carbon-nanotubes

[26] The science and technology of carbon nanotubes (Eds.: Tanaka K, Yamabe T, Fukui K). Elsevier, Amsterdam, 1999.

[27] Carbon nanotubes: Science and applications (Ed.: Meyyappan M). Taylor and Francis, Boca Raton, 2005.

[28] Qian D, Wagner GJ, Liu WK, Yu MF, Ruoff RS. Mechanics of carbon nanotubes. Appl Mech Rev 2002;55:495–533.

[29] Che JW, Cagin T, Goddard WA. Thermal conductivity of carbon nanotubes. Nanotechnology 2000;11:65–69.

[30] Kim P, Shi L, Majumdar A. McEuen PL. Thermal transport measurements of individual multiwalled nanotubes. Phys Rev Lett 2001;87: 215502(1-4).

[31] Pop E, Mann D, Wang Q, Goodson K, Dai H. Thermal conductance of an individual single-walled carbon nanotube above room temperature. Nano Lett 2006;6:96-100.

[32] Sukhadolou AV, Ivakin EV, Ralchenko VG, Khomich AV, Vlasov AV, Popovich AF. Thermal conductivity of CVD diamond at elevated temperatures. Diamond Relat Mater 2005;14:589-93.

[33] Pantea D, Darmstadt H, Kaliaguine S, Summerchen L, Christian R. Electrical conductivity of thermal carbon blacks: Influence of surface chemistry. Carbon 2001;39:1147-58.

[34] Durkop T, Getty SA, Cobas E, Fuhrer MS. Extraordinary mobility in semiconducting carbon nanotubes. Nano Lett 2004;4:35-9.

[35] Walters DA, Casavant MJ, Qin XC, Huffman CB, Boul PJ, Ericson LM, Haroz EH, O'Connell MJ, Smith K, Colbert DT, Smalley RE. In-plane-aligned membranes of carbon nanotubes. Chem Phys Lett 2001;338:14-20.

[36] Global carbon nanotube market – industry beckons. Accessed on 1st October 2012. http://www.nanowerk.com/spotlight/spotid=23118.php

[37] Applications and benefits of multiwalled carbon nanotubes (MWCNTs). Accessed 2nd December 2012. http://www.cefic.org/Documents/Other/Benefits%20of%20Carbon%20Nanotubes.pdf

[38] Zyvex Marine Launches LRV-17 Long Range Vessel As The First Nano-Composite Manned Boat. Accessed 22nd August 2012. http://www.zyvexmarine.com/news/2012/7/18/zyvex-marine-launches-lrv-17-long-range-vessel-as-the-first.html

[39] Völkl Racquets. Accessed 2nd January 2013. http://www.tennisexpress.com/category.cfm/tennis/volkl-tennis-racquets

[40] Aldila. Accessed 14th November 2012. http://www.aldila.com/portals/12909/images/logos/aldila_2010_catalog.pdf

[41] Frost & Sullivan's study on potential market for carbon nanomaterials' applications (2011). Accessed 26th June 2012. http://www.nist.gov/cnst/upload/Valenti-NIST.pdf

[42] McEuen PL, Fuhrer MS, Park H. Single-walled carbon nanotube electronics. IEEE Trans Nanotechnol 2002;1:78-85.

[43] Dresselhaus MS, Dresselhaus G, Charlier JC, Hernández E. Electronic, thermal and mechanical properties of carbon nanotubes. Phil Trans R Soc Lond A 2004;362:2065-98.

[44] Treacy MMJ, Ebbesen TW, Gibson JM: Exceptionally high Young's modulus observed for individual carbon nanotubes. Nature 1996;381:678-80.

[45] Berber S, Kwon YK, Tománek D. Unusually high thermal conductivity of carbon nanotubes. Phys Rev Lett 2000;84:4613-6.

[46] Jou WS, Cheng HZ, Hsu CF. A carbon nanotube polymer based composite with high electromagnetic shielding. J Elec Mat 2006 ;35 :462-70.

[47] Li N, Huang Y, Du F, He X, Lin X, Gao H, Ma Y, Li F, Chen Y, Eklund PC. Electromagnetic interference (EMI) shielding of single-walled carbon nanotube epoxy composites. Nano Lett 2006;6:1141-5.

[48] Zhang T, Mubeen S, Myung NV, Deshusses MA. Recent progress in carbon nanotube-based gas sensors. Nanotechnology 2008;19:332001(14pp).

[49] Robert C, Feller JF, Castro M. Sensing skin for strain monitoring made of PC–CNT conductive polymer nanocomposite sprayed layer by Layer. Appl Mater Interfaces 2012;4:3508-16.

[50] Dervishi E, Li Z, Saini V, Sharma R, Xu Y, Mazumder MK, Biris AS, Trigwell S, Biris AR, Saini D, Lupu D. Multifunctional coatings with carbon nanotubes for electrostatic charge mitigation and with controllable surface properties. IEEE Trans Ind Appl 2009;45:1547-52.

[51] Fu X, Zhang C, Liu T, Liang R, Wang B. Carbon nanotube buckypaper to improve fire retardancy of high-temperature/high-performance polymer composites. Nanotechnology 2010;21:235701(8pp).

[52] World's first carbon nanotube reinforced polyurethane wind blades. Accessed on 15th October 2011. http://polymers.case.edu/stories/World's%20First%20PU%20CNT%20Blades.html

[53] Ravichandran J, Manoj AG, Liu J, Manna I, Carroll DL. A novel polymer nanotube composite for photovoltaic packaging applications. Nanotechnology 2008;19:085712(5pp).

[54] Zhao Y, Wei J, Vajtai R, Ajayan PM, Barrera EV. Iodine doped carbon nanotube cables exceeding specific electrical conductivity of metals. Sci Rep 2011;1:83(5pp).

[55] Sathyanarayana S, Olowojoba G, Weiss P, Caglar B, Pataki B, Mikonsaari I, Hübner C, Henning F. Compounding of MWCNT with PS in a twin-screw extruder with varying process parameters: Morphology, interfacial behaviour, thermal stability, rheology and volume resistivity. Macromol Mat Eng 2013; 298:89-105.

[56] Dyke CA, Tour JM. Covalent functionalization of single-walled carbon nanotubes for material applications. J Phys Chem A 2004;108:11151-9.

[57] Bose S, Bhattacharyya AR, Bondre AP, Kulkarni AR, Pötschke P. Rheology, electrical conductivity, and the phase behavior of cocontinuous PA6/ABS blends with MWNT: Correlating the aspect ratio of MWNT with the percolation threshold. J Polym Sci B 2008;46:1619-31.

[58] Kamaras K, Itkis ME, Hu H, Zhao B, Haddon RC. Covalent bond formation to a carbon nanotube metal. Science 2003;301:1501.

[59] Kang X, Ma W, Zhang H, Xu Z, Guo Y, Xiong Y. Vinyl-carbon nanotubes for composite polymer materials. J Appl Polym Sci 2008;110:1915-20.

[60] Padgett CW, Brenner DW. Influence of chemisorption on the thermal conductivity of single-wall carbon nanotubes. Nano Lett 2004;4:1051-3.

[61] Cohen RS, Kalisman LY, Roth EN, Rozen RY. Generic approach for dispersing single-walled carbon nanotubes: The strength of a weak interaction. Langmuir 2004;20:6085-8.

[62] Bose S, Khare RA, Moldenaers P. Assessing the strengths and weaknesses of various types of pre-treatments of carbon nanotubes on the properties of polymer/carbon nanotubes composites: A critical review. Polymer 2010;51:975-93.

[63] Safadi B, Andrews R, Grulke EA. Multiwalled carbon nanotube polymer composites: Synthesis and characterization of thin films. J Appl Polym Sci 2002;84:2660-9.

[64] Qian D, Dickey EC, Andrews R, Rantell T. Load transfer and deformation mechanisms in carbon nanotube-polystyrene composites. Appl Phys Lett 2000;76:2868(3pp).

[65] Cadek M, Coleman JN, Barron V, Hedicke K, Blau WJ. Morphological and mechanical properties of carbon-nanotube-reinforced semicrystalline and amorphous polymer composites. Appl Phys Lett 2002;81:5123(3pp).

[66] Menzer K, Krause B, Boldt R, Kretzschmar B, Weidisch R, Pötschke P. Percolation behaviour of multiwalled carbon nanotubes of altered length and primary agglomerate morphology in melt mixed isotactic polypropylene-based composites. Compos Sci Technol 2011;71:1936-43.

[67] Socher R, Krause B, Müller MT, Boldt R, Pötschke P. The influence of matrix viscosity on MWCNT dispersion and electrical properties in different thermoplastic nanocomposites. Polymer 2012;53(2):495-504.

[68] Chen L, Pang XJ, Qu MZ, Zhang QT, Wang B, Zhang BL, Yu ZL. Fabrication and characterization of polycarbonate/carbon nanotubes composites. Compos A 2006;37:1485-89.

[69] Lin TS, Cheng LY, Hsiao CC, Yang ACM. Percolated network of entangled multi-walled carbon nanotubes dispersed in polystyrene thin films through surface grafting polymerization. Mat Chem Phys 2005;94:438-43.

[70] Wu TM, Chen EC. Preparation and characterization of conductive carbon nanotube-polystyrene nanocomposites using latex technology. Comp Sci Technol 2008;68:2254-9.

[71] Vigolo B, Pénicaud A, Coulon C, Sauder C, Pailler R, Journet C, Bernier P, Poulin P. Macroscopic fibers and ribbons of oriented carbon nanotubes.Science 2000;290:1331-4.

[72] Xia H, Wang Q, Li K, Wu GH. Preparation of polypropylene/carbon nanotube composite powder with a solid-state mechanochemical pulverization process. J Appl Polym Sci 2004;93:378-86.

[73] Masuda J, Torkelson JM. Dispersion and major property enhancement in polymer/multiwall carbon nanotube nanocomposites via solid-state shear pulverization followed by melt mixing. Macromolecules 2008;41:5974-7.

[74] Sen R, Zhao B, Perea DE, Itkis ME, Hu H, Love J, Bekyarova E, Haddon RC. Preparation of single-walled carbon nanotube reinforced polystyrene and polyurethane nanofibers and membranes by electrospinning. Nano Lett 2004;4:459-64.

[75] Yuan JM, Fan ZF, Chen XH, Chen XH, Wu ZJ, He LP. Preparation of polystyrene–multiwalled carbon nanotube composites with individual-dispersed nanotubes and strong interfacial adhesion. Polymer 2009; 50:3285-91.

[76] Alig I, Pötschke P, Lellinger D, Skipa T, Pegel S, Kasaliwal GR, Villmow T. Establishment, morphology and properties of carbon nanotube networks in polymer melts. Polymer 2012;53:4-28.

[77] Datasheet Baytubes® C 150 P. Bayer Material Science AG, Leverkusen, Germany, 2009.

[78] Krause B, Mende M, Pötschke P, Petzold G. Dispersability and particle size distribution of CNTs in an aqueous surfactant dispersion as a function of ultrasonic treatment time. Carbon 2010;48:2746-54.

[79] Datasheet Nanocyl™ NC 7000. Nanocyl S.A.,Sambreville, Belgium, 2010.

[80] Mamunya Y, Boudenne A, Lebovka N, Ibos L, Candau Y, Lisunova M. Electrical and thermophysical behaviour of PVC-MWCNT nanocomposites. Compos Sci Technol 2008;68:1981-8.

[81] Castillo FY, Socher R, Krause B, Headrick R, Grady BP, Prada-Silvy R, Pötschke P. Electrical, mechanical, and glass transition behavior of polycarbonate-based nanocomposites with different multi-walled carbon nanotubes. Polymer 2011;52:3835-45.

[82] Mack C, Sathyanarayana S, Weiss P, Mikonsaari I, Hübner C, Henning F, Elsner P. Twin-screw extrusion of multi walled carbon nanotubes reinforced polycarbonate composites: Investigation of electrical and mechanical properties, IOP Conference Series: Mat Sci Eng 2012;40:012020.

[83] McNally T, Pötschke P, Halley P, Murphy M, Martin D, Bell SEJ, Brennan GP, Bein D, Lemoine P, Quinn JP. Polyethylene multiwalled carbon nanotube composites. Polymer 2005;46:8222-32.

[84] Advances in Chemical Engineering Vol.25 (Ed.: Wei J). Academic Press, San Diego, 1999.

[85] Kasaliwal GR, Göldel A, Pötschke P, Heinrich G. Influences of polymer matrix viscosity an molecular weight on MWCNT agglomerate dispersion. Polymer 2011;52:1027-36.

[86] Villmow T, Pötschke P, Pegel S, Häussler L, Kretzschmar B. Influence of twin-screw extrusion conditions on the dispersion of multi-walled carbon nanotubes in a poly(lactic acid) matrix. Polymer 2008;49:3500-9.

[87] Müller M, Krause B, Kretzschmar B, Pötschke P. Influence of feeding conditions in twin-screw extrusion of PP/MWCNT composites on electrical and mechanical properties. Compos Sci Technol 2011;71:1535-42.

[88] Clark EJ, Hoffmann JD. Regime III crystallization in polypropylene. Macromolecules 1984;17:878-85.

[89] Gau C, Kuo CY, Ko HS. Electron tunneling in carbon nanotube composites. Nanotechnology 2009;20:395705(6pp).

[90] Arjmand M, Apperley T, Okoniewski M, Sundararaj U. Comparative study of electromagnetic interference shielding properties of injection molded versus compression molded multi-walled carbon nanotube/polystyrene composites. Carbon 2012;50:5126-34.

[91] Micusik M, Omastová M, Krupa I, Prokes J, Pissis P, Logakis E, Pandis C, Pötschke P, Pionteck J. A comparative study on the electrical and mechanical behaviour of multi-walled carbon nanotube composites prepared by diluting a masterbatch with various types of polypropylenes. J. Appl Polym Sci 2009;113(4):2536-51.

[92] Bose S, Bhattacharyya AR, Kulkarni AR, Pötschke P. Electrical, rheological and morphological studies in co-continuous blends of polyamide6 and acrylonitrile-butadiene-styrene with multiwall carbon nanotubes prepared by melt blending. Compos Sci Technol 2009;69(3-4):365-72.

[93] Barrau S, Demont P, Perez E, Peigney A, Laurent C, Lacabanne C. Effect of palmitic acid on the electrical conductivity of carbon nanotubes–epoxy resin composites. Macromolecules 2003;36:9678–80.

[94] Yang BX, Pramoda KP, Xu GQ, Goh SH. Mechanical reinforcement of polyethylene using polyethylene-grafted multiwalled carbon nanotubes. Adv Funct Mater 2007;17(13):2062–9.

[95] Byrne MT, McNamee WP, Gun'ko YK. Chemical functionalization of carbon nanotubes for the mechanical reinforcement of polystyrene composites. Nanotechnology 2008;19(41):415707(4pp).

[96] Funck A, Kaminsky W. Polypropylene carbon nanotube composites by in situ polymerization. Compos Sci Technol 2007;67:906-15.

[97] Malz H, Tzoganakis C. Hydrosilylation of terminal double bonds in polypropylene through reactive processing. Polym Eng Sci 1998;38(12):1976-84.

[98] Peng H, Reverdy P, Khabashesku VN, Margrave JL. Sidewall functionalization of single-walled carbon nanotubes with organic peroxides. Chem Commun 2003; 362-3.

[99] Sathyanarayana S, Bendfeld A, Hübner C, Henning F. Online Raman spectroscopy observations during melt mixing of multiwalled carbon nanotubes with polystyrene to form composites, Proceedings of SAMPE Tech 2012, Charleston, SC, USA, Oct 22-25, 2012, Society for the Advancement of Material and Process Engineering.

[100] Pötschke P, Abdel-Goad M, Alig I, Dudkin S, Lellinger D. Rheological and dielectrical characterization of melt mixed polycarbonate-multiwalled carbon nanotube composites. Polymer 2004;45:8863–70.

[101] Pegel S, Pötschke P, Petzold G, Alig I, Dudkin SM, Lellinger D. Dispersion, agglomeration, and network formation of multiwalled carbon nanotubes in polycarbonate melts. Polymer 2008;49:974-84.

[102] Thostenson ET, Ziaee S, Chou TW. Processing and electrical properties of carbon nanotube/vinyl ester nanocomposites. Compos Sci Technol 2009;69:801-4.

[103] Valentini L, Biagiotti J, Kenny JM, Santucci S. Morphological characterization of single-walled carbon nanotubes-PP composites. Compos Sci Technol 2003;63:1149–53.

[104] Chen W, Auad ML, Williams RJJ, Nutt SR. Improving the dispersion and flexural strength of multiwalled carbon nanotubes–stiff epoxy composites through β–hydroxyester surface functionalization coupled with the anionic homopolymerization of the epoxy matrix. Eur Polym J 2006;42:2765-72.

[105] Li S, Wang S, Wang Y, Wang J, Ma J, Ziao J. Effect of acid and TETA modification on mechanical properties of MWCNTs/epoxy composites. J Mater Sci 2008;43:2653-8.

[106] Krusic PJ, Wassermann E, Keizer PN, Morton JR, Preston, KF. Radical reactions of C60. Science 1991;254(5035):1183-5.

[107] Costa S, Borowiak-Palen E, Kruszynska M, Bachmatiuk A, Kalenczuk RJ. Characterization of carbon nanotubes by Raman spectroscopy. Materials Sci-Poland 2008;26:433-41.

[108] Zhao B, Zhang L, Wang X, Yang J. Surface functionalization of vertically-aligned carbon nanotube forests by radio-frequency Ar/O2 plasma. Carbon 2012;50:2710-6.

[109] Lourie O, Wagner HD. Evaluation of Young's modulus of carbon nanotubes by micro-Raman spectroscopy. J Mater Res 1998;13:2418-22.

[110] Poulin P, Vigolo B, Launois P. Films and fibers of oriented single wall nanotubes. Carbon 2002;40:1741-9.

[111] Mu M, Osswald S, Gogotsi Y, Winey KI. An in situ Raman spectroscopy study of stress transfer between carbon nanotubes and polymer. Nanotechnology 2009;20:335703(7pp).

[112] Cooper CA, Young RJ, Halsall M. Investigation into the deformation of carbon nanotubes and their composites through the use of Raman spectroscopy. Compos A 2001;32:401-11.

[113] Zhao Q, Wagner HD. Raman spectroscopy of carbon–nanotube–based composites. Phil Trans R Soc Lond A 2004;362:2407-24.

[114] Bokobza L, Zhang J. Raman spectroscopic characterization of multiwall carbon nanotubes and of composites. eXPRESS Polym Lett 2012;6:601-8.

[115] Srivastava RK, Vemuru VSM, Zeng Y, Vatjai R, Nagarajaiah S, Ajayan PM, Srivastava A. The strain sensing and thermal-mechanical behavior of flexible multi-walled carbon nanotube/polystyrene composite films. Carbon 2011;49:3928-36.

[116] Krause B, Villmow T, Boldt R, Mende M, Petzold G, Pötsche P. Influence of dry grinding in a ball mill on the length of multiwalled carbon nanotubes and their dispersion and percolation behaviour in melt mixed polycarbonate composites. Compos Sci Technol 2011;71:1145-53.

Appendix A. Measurement of Online Melt Resistance

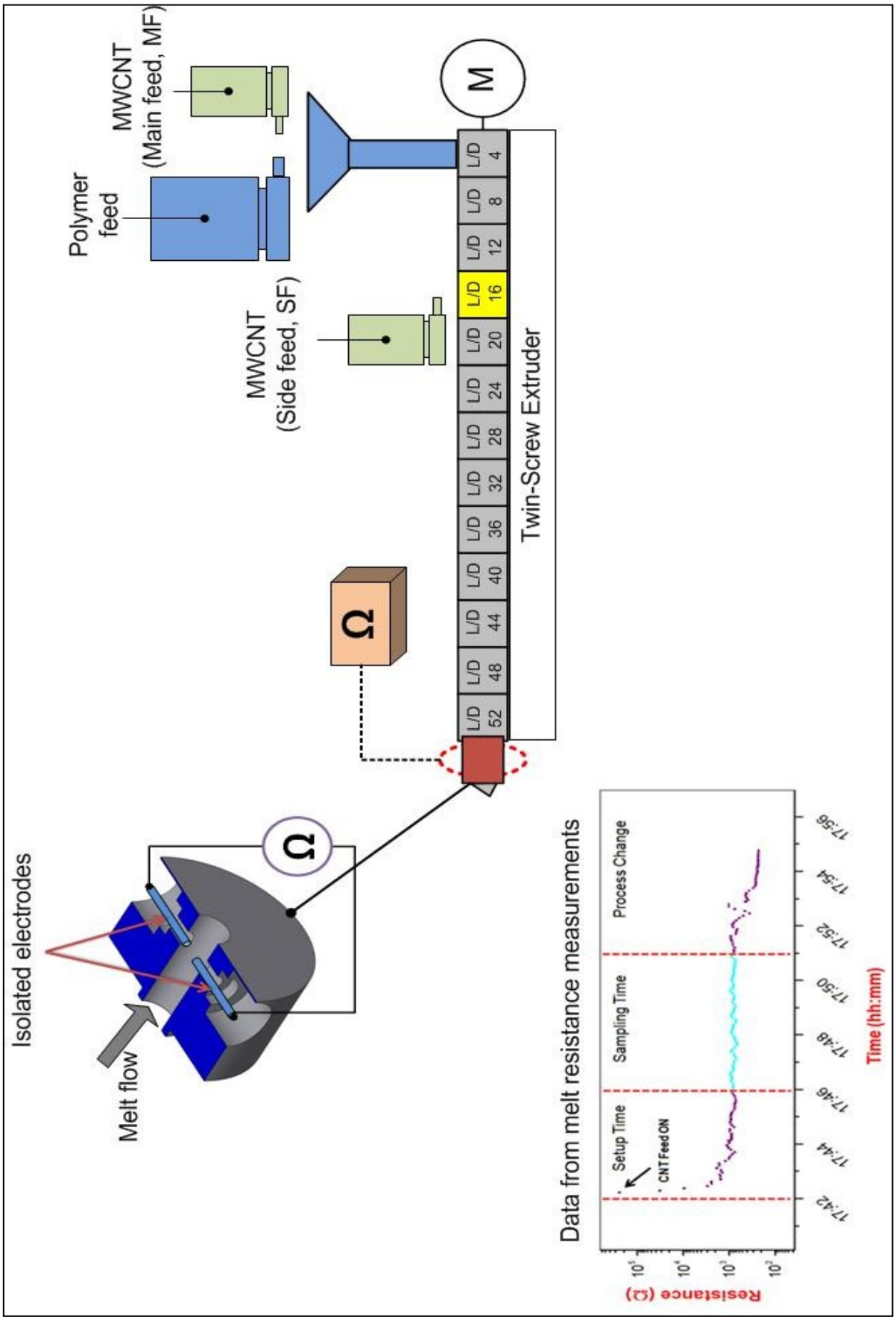

Appendix B. Description of Screw Elements

7.5.1. Schneckenbezeichnungen

GFA_2_15_30
GFA_2_15_60
GFA_2_15_90
GFA_2_20_30
GFA_2_20_60
GFA_2_20_90
GFA_2_30_30
GFA_2_30_60
GFA_2_30_90
GFA_2_40_30
GFA_2_40_60
GFA_2_40_90
GFF_2_40_90

KS1_2_10_A
KS1_2_10_M
KS1_2_10_E

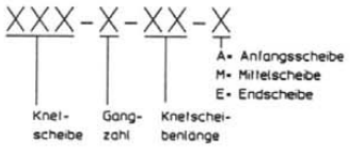

KB5_2_30_30°_RE
KB5_2_30_60°_RE
KB5_2_30_90°
KB5_2_30_30°_LI
KB5_2_30_60°_LI

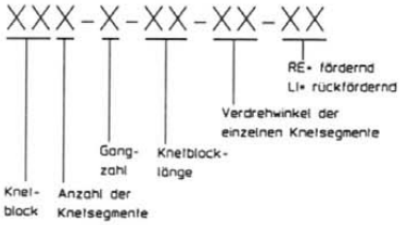

FD_1_20_90
FD_1_20_30
FD_1_30_90
FD_1_30_30
FD_2_30_90
FD_2_30_30
FD_3_45_90
FD_3_45_30
FF_1_30_30
KFD_1_30/20_90
KDD_1_30/20_90

7.5.2. Wirkungsweise von Schneckenelementen mit unterschiedlichen Steigungen

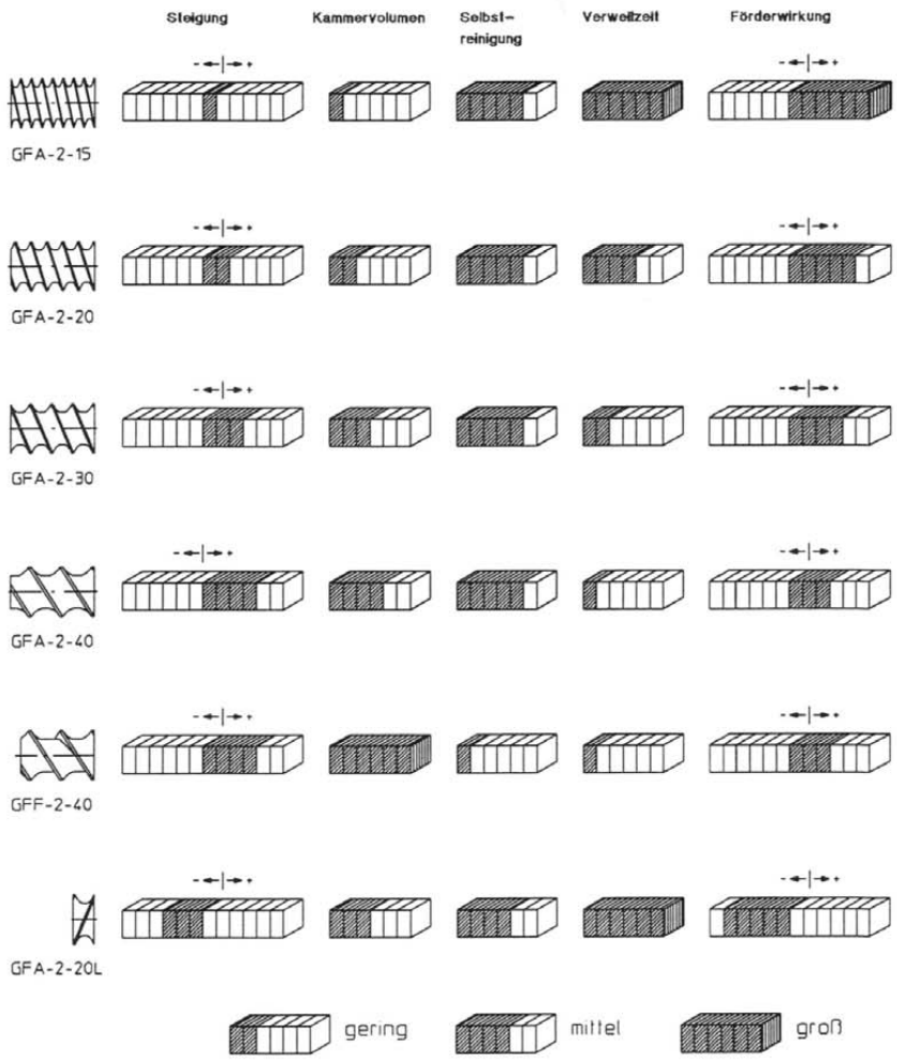

7.5.3. Wirkungsweise von Schneckenelementen und Knetscheibenkombinationen mit unterschiedlichen Versatzwinkeln der Scheiben

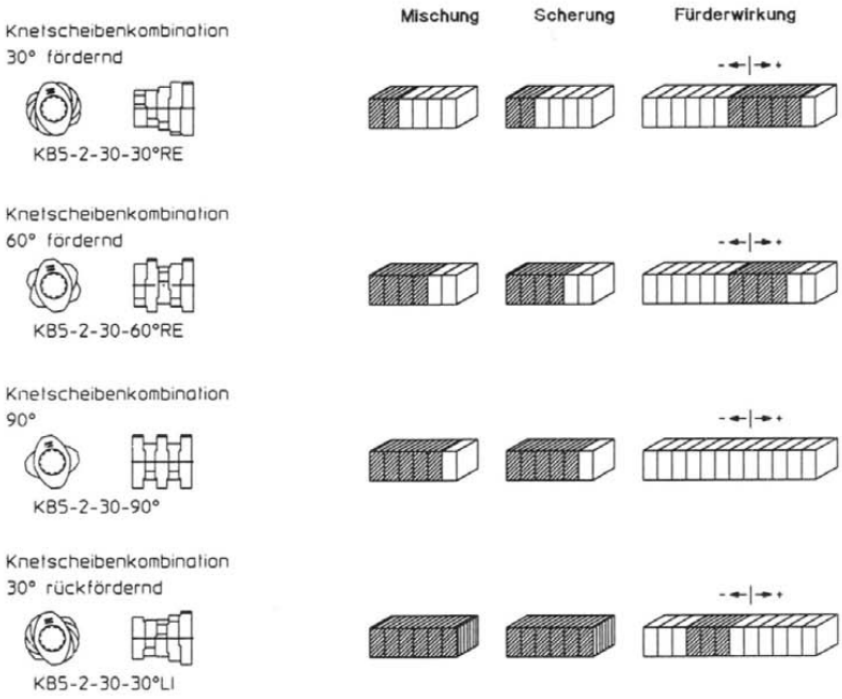

Appendix C. Screw Configuration for Peroxide Trials

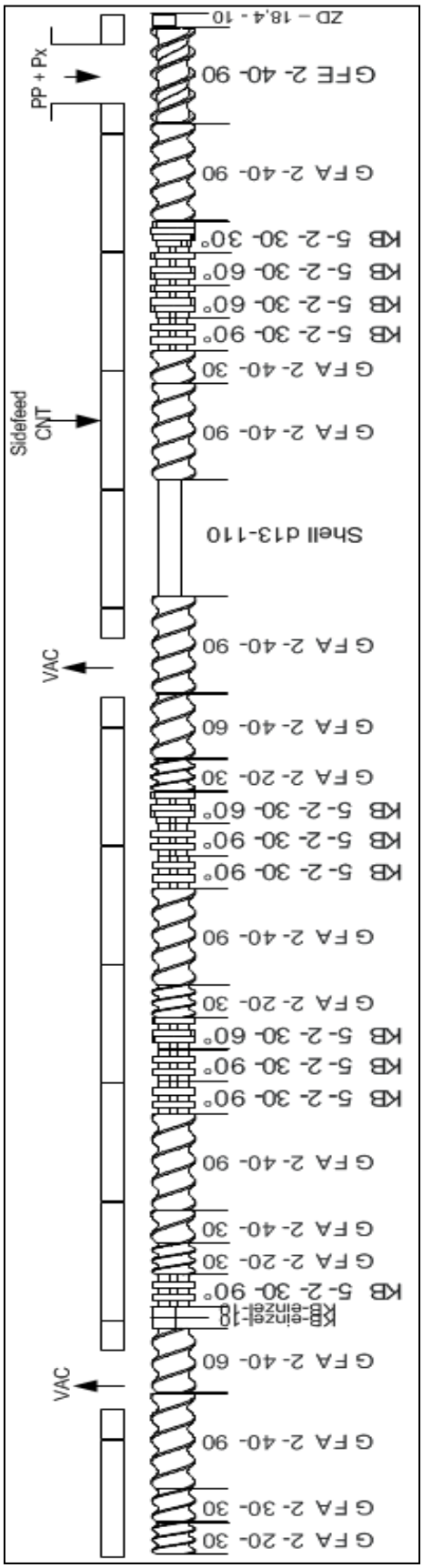

Appendix D. Loss Curve (Tan δ) of the Composites

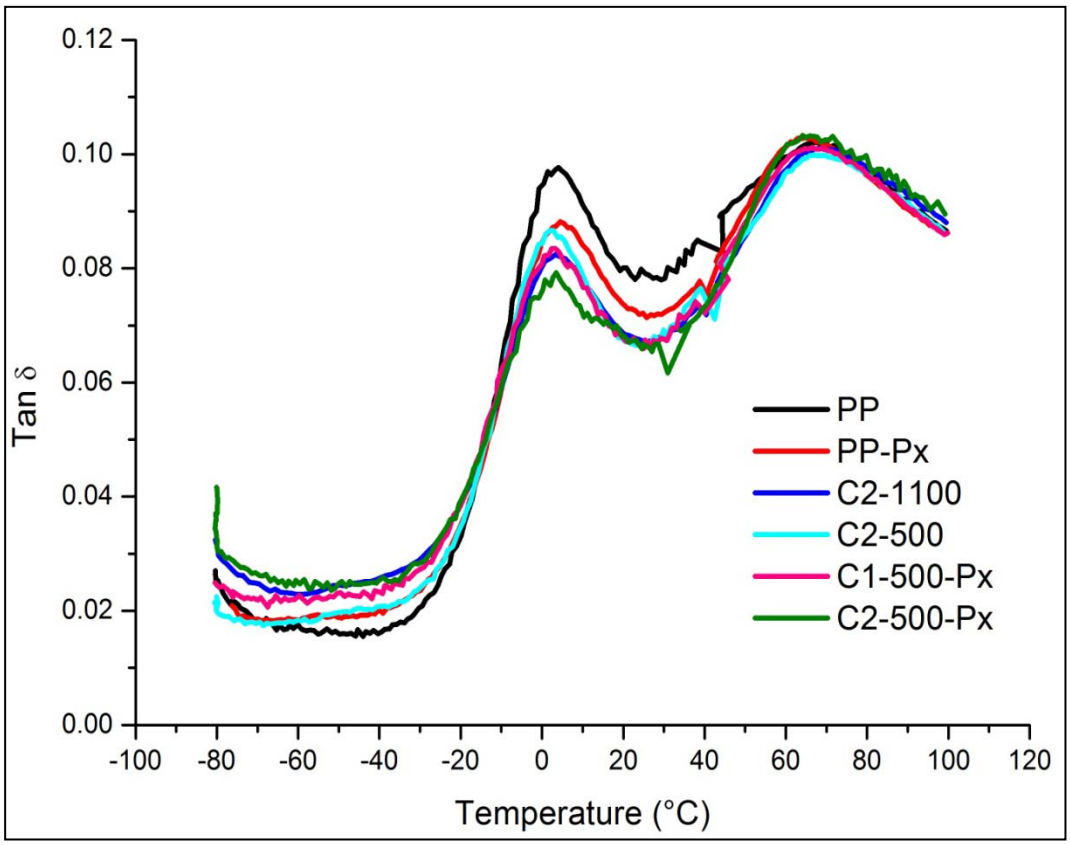

DMA was carried out in tension mode on a injection molded sample (50 x 10 x 4 mm^3) with the help of a Advanced Rheometric Expansion System from Rheometric Scientific Inc. Temperature steps of 1 °C was employed with a dynamic strain of 0.00075 at a frequency of 1 Hz.

Appendix E. Screw Configuration for Short Glass Fiber Addition

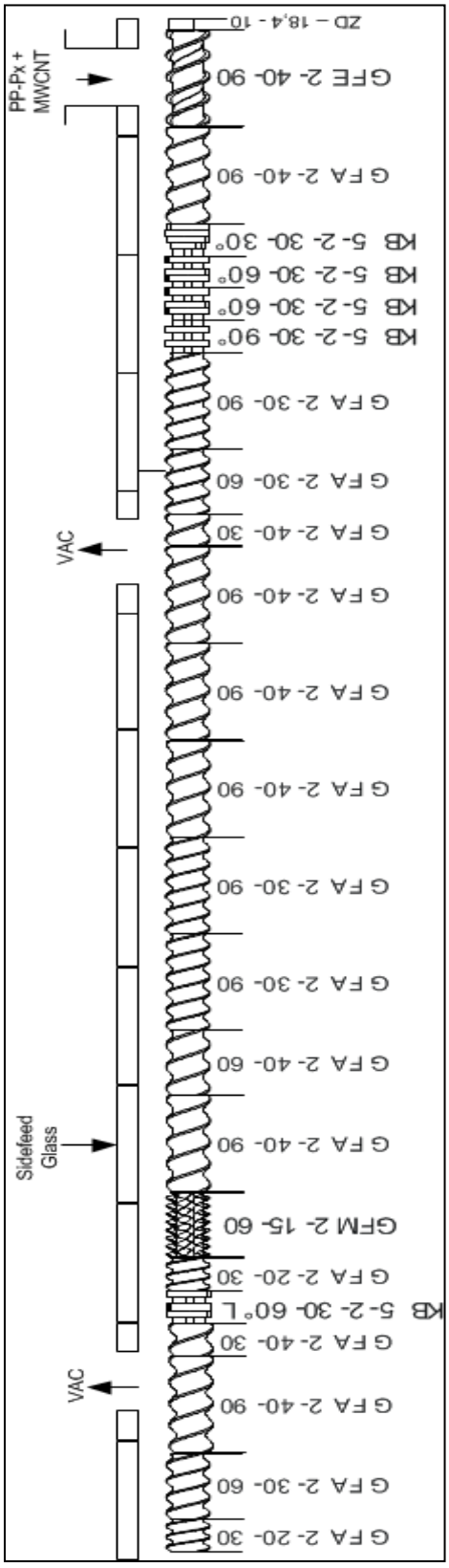

List of Publications

Peer reviewed journal articles:

[1] Shyam Sathyanarayana, Ganiu Olowojoba, Burak Caglar, Patrick Weiss, Bernadeth Pataki, Irma Mikonsaari, Christof Hübner, Frank Henning. Compounding of MWCNTs with PS in a twin-screw extruder with varying process parameters: Morphology, interfacial behavior, thermal stability, rheology and volume resistivity. *Macromolecular Materials and Engineering* 2013;298:89-105.

[2] Ganiu Olowojoba, Shyam Sathyanarayana, Burak Caglar, Bernadeth Pataki, Irma Mikonsaari, Christof Hübner, Peter Elsner. Influence of process parameters on the morphology, rheological and dielectric properties of three-roll-milled multiwalled carbon nanotube/epoxy suspensions. *Polymer* 2013;54:188-98.

[3] Shyam Sathyanarayana, Marcin Wegrzyn, Adolfo Benedito, Enrique Giménez, Christof Hübner, Frank Henning. Multiwalled carbon nanotubes incorporated miscible blend of poly(phenylenether)/polystyrene – Processing and characterization. *Express Polymer Letters* 2013;7:621-635.

[4] Shyam Sathyanarayana, Christof Hübner, Jan Diemert, Petra Pötschke, Frank Henning. Influence of peroxide addition on the morphology and properties of polypropylene - multiwalled carbon nanotube composites. *Composites Science and Technology* 2013;84:78-85.

[5] Shyam Sathyanarayana, Petra Pötschke, Ganiu Olowojoba, Patrick Weiss, Christof Hübner, Frank Henning. Conductive PP/MWCNT/Glass fiber composites with excellent structural composites. In preparation.

Peer reviewed conference proceedings:

[1] Shyam Sathyanarayana, Christof Hübner, Frank Henning. Experimental investigation of polystyrene-multiwalled carbon nanotubes (PS-MWCNT) interaction, Abstract in the Proceedings of the 5th International Conference on Nano Science and Technology (ICONSAT), Hyderabad, India, Jan 20-23 2012. Pg.129

[2] Daniel Berkowitz Zamora, Shyam Sathyanarayana, Patrick Weiss, Christof Hübner, Jan Diemert, Frank Henning, Peter Elsner. Compounding extrusion of polypropylene-carbon nanotube composites: Optimizing and economizing process with a commercial perspective – A case study, ANTEC 2012 - Proceedings of the 70th Annual Technical Conference & Exhibition, Orlando, FL, USA, April 2-4, 2012, Society of Plastics Engineers. Pg.442-447

[3] Shyam Sathyanarayana, Ganiu Olowojoba, Patrick Weiss, Christof Hübner, Frank Henning. Influence of compounding parameters on the electrical properties of polystyrene carbon nanotube nanocomposite, Proceedings of SAMPE2012, Baltimore, MD, USA, May 21-24, 2012, Society for the Advancement of Material and Process Engineering. CD-ROM Pg.1-15

[4] Christoph Mack, Shyam Sathyanarayana, Patrick Weiss, Irma Mikonsaari, Christof Hübner, Frank Henning, Peter Elsner. Twin-screw extrusion of multi walled

carbon nanotubes reinforced polycarbonate composites: Investigation of electrical and mechanical properties, IOP Conference Series: Material Science and Engineering, 2012, 40, 012020.

[5] Shyam Sathyanarayana, Anja Bendfeld, Christof Hübner, Frank Henning. Online Raman spectroscopy observations during melt mixing of multiwalled carbon nanotubes with polystyrene to form composites, Proceedings of SAMPE Tech 2012, Charleston, SC, USA, Oct 22-25, 2012, Society for the Advancement of Material and Process Engineering. CD-ROM Pg.1-9

[6] Burak Caglar, Shyam Sathyanarayana, Ganiu Olowojoba, Peter Fischer, Christof Hübner, Peter Elsner. Development of carbon nanotube based bipolar plates for vanadium redox flow batteries, Proceedings of SAMPE Tech 2012, Charleston, SC, USA, Oct 22-25, 2012, Society for the Advancement of Material and Process Engineering. CD-ROM Pg.1-13

[7] Shyam Sathyanarayana, Patrick Weiss, Christof Hübner, Jan Diemert, Frank Henning. Twin-screw compounding: Process optimization for multiwalled carbon nanotubes reinforced polypropylene composites, ANTEC Mumbai 2012 - Proceedings of the Annual Technical Conference & Exhibition, Mumbai, India, December 6-7, 2012, Society of Plastics Engineers. Pg.394-400

[8] Shyam Sathyanarayana, Marcin Wegrzyn, Patrick Weiss, Enrique Giménez, Christof Hübner, Frank Henning. Influence of glass fiber addition on the morphology and properties of PC-MWCNT composites. PPS28 - Proceedings of the 28th Annual Meeting, Pattaya, Thailand, Dec 11-15 2012, Polymer Processing Society.

[9] Ganiu Olowojoba, Shyam Sathyanarayana, Burak Caglar, Irma Mikonsaari, Christof Hübner, Peter Elsner. Rheological, dielectric and morphological properties of three-roll-milled multiwalled carbon nanotube/epoxy suspensions: influence of processing parameters, Proceedings of SEICO 13 - 34th International Conference and Forum, Paris, France, March 11-12, 2013, Society for the Advancement of Material and Process Engineering. Pg:53-60

[10] Shyam Sathyanarayana, Ganiu Olowojoba, Christof Hübner, Jan Diemert, Petra Pötschke, Frank Henning. Raman spectroscopy study on the addition of peroxides as a dispersing additive in multiwalled carbon nanotube reinforced polypropylene composites. ANTEC 2013-Proceedings of the 71st Annual Technical Conference & Exhibition, Cincinnati, OH, USA, April 21-25, Society of Plastics Engineers. Pg.566-570

[11] Ganiu Olowojoba, Shyam Sathyanarayana, Burak Caglar, Irma Mikonsaari, Christof Hübner, Peter Elsner. Influence of processing temperature, carbon nanotube agglomerate bulk density and functionalization on the dielectric and morphological properties of carbon nanotube/epoxy suspensions. PPS 29 - Proceedings of the 29th Annual Meeting, Nürnberg, Germany, July 15-19 2013, Polymer Processing Society.

Invited lectures:

[1] MWCNT filled commodity thermoplastic composites - Process optimization and understanding material systems, June 2012, Leibnitz Institute of Polymer Research, Dresden, Germany.

[2] Process optimization and development of multifunctional composites with multiwalled carbon nanotubes reinforced polypropylene, Jan 2013, Nanocyl S.A, Sambreville, Belgium.

Book chapter:

[1] Shyam Sathyanarayana, Christof Hübner. Thermoplastic nanocomposites with carbon nanotubes. To appear in: Structural Nanocompsites (Ed.: James Njuguna), 2013, Springer, Berlin.

The excellent electrical, mechanical and thermal properties along with the high specific surface area of carbon nanotubes make them a strong candidate as functional fillers for polymer matrices. However, the significant challenge in achieving a good dispersion of these nanotubes in the host polymer due to their inert chemical surface and tendency to exist as agglomerates inhibits their theoretical potential. Thermoplastic polymers, specifically olefins present a complex scenario for achieving good carbon nanotube dispersion owing to their high melt viscosity and incompatible surface energies with carbon nanotubes. Process parameter optimization and the usage of an economical reactive processing additive resulted in an extremely good carbon nanotube dispersion in polypropylene, which consequently led to excellent electrical and thermal properties of the composite at very low filler loadings. Incorporation of glass fibers as secondary fillers lead to a substantial improvement in the mechanical properties of the bi-filler composite whilst preserving the enhancements in electrical and thermal properties caused by carbon nanotube addition. This led to a multifunctional composite with excellent electrical, structural and thermal properties with significant potential for light-weight product development.

ISSN 0933-0062

Herausgeber:
Fraunhofer-Institut für Chemische Technologie ICT
Joseph-von-Fraunhofer-Straße 7
76327 Pfinztal (Berghausen)
Telefon +49 721 4640-0
Telefax +49 721 4640-111
info@ict.fraunhofer.de
www.ict.fraunhofer.de

ISBN 978-3-8396-0603-2